TU Delft

Delft University of Technology

Document Version
Final published version

Licence
Dutch Copyright Act (Article 25fa)

Citation (APA)
Krishnan, S., Adesanya, E. D., Chen, B., Djobo, J. N. Y., Huang, Y., Marsh, A. T. M., Nedeljkovic, M., Ye, G., Yliniemi, J., Yue, Z., & Bernal, S. A. (2026). Non-conventional Precursors and Activators. In G. Ye, & F. Dehn (Eds.), *Mechanical Properties of Alkali-Activated Materials: State-of-the-Art Report of the RILEM Technical Committee 294-MPA* (pp. 69-133). (RILEM State-of-the-Art Reports; Vol. 46). Springer. https://doi.org/10.1007/978-3-032-07116-3_4

Important note
To cite this publication, please use the final published version (if applicable).
Please check the document version above.

Copyright
In case the licence states “Dutch Copyright Act (Article 25fa)”, this publication was made available Green Open Access via the TU Delft Institutional Repository pursuant to Dutch Copyright Act (Article 25fa, the Taverne amendment). This provision does not affect copyright ownership.
Unless copyright is transferred by contract or statute, it remains with the copyright holder.

Sharing and reuse
Other than for strictly personal use, it is not permitted to download, forward or distribute the text or part of it, without the consent of the author(s) and/or copyright holder(s), unless the work is under an open content license such as Creative Commons.

Takedown policy
Please contact us and provide details if you believe this document breaches copyrights.
We will remove access to the work immediately and investigate your claim.

This work is downloaded from Delft University of Technology.

Non-conventional Precursors and Activators



Sreejith Krishnan, Elijah D. Adesanya, Boyu Chen, Jean Noel Yankwa Djobo, Yuyan Huang, Alastair T. M. Marsh, Marija Nedeljkovic, Guang Ye, Juho Yliniemi, Zengliang Yue, and Susan A. Bernal

Abstract Alkali-activation is a technically sound pathway to valorize industry wastes and by-products, and there has been a burgeoning interest in evaluating the potential of waste streams and/or by-products from different industries as precursors for alkali-activated materials production. In the context of sustainable construction materials, as well as other industrial systems, the use of such non-conventional precursors addresses the challenges associated with the global availability and management of such resource streams. This includes the availability of alternative valorisation routes, the life cycle implications of using waste streams, and the pragmatic issues around incorporating a wide range of precursor materials for future proof this technology. In this chapter an overview of studies utilizing alternative precursors for producing alkali-activated cements is presented, analyzing the characteristics of each resource, and identifying the links between mix design formulations and the performance of the alkali-activated materials produced with them. This in order to elucidate the existing knowledge gaps to facilitate the widespread uptake of such resources as key precursors for producing this type of cements.

S. Krishnan · Y. Huang · A. T. M. Marsh · Z. Yue · S. A. Bernal (✉)
School of Civil Engineering, University of Leeds, Leeds, UK
e-mail: sbl30@bath.ac.uk

S. Krishnan
Department of Civil and Infrastructure Engineering, Indian Institute of Technology Jodhpur, Jodhpur, India

E. D. Adesanya · J. Yliniemi
Fibre and Particle Engineering Research Unit, University of Oulu, Oulu, Finland

B. Chen · M. Nedeljkovic · G. Ye
Section Materials and Environment, Department of 3Md, Faculty of Civil Engineering and Geosciences, Delft University of Technology, Delft, The Netherlands

J. N. Y. Djobo
Local Materials Promotion Authority, MINRESI/MIPROMALO, Yaoundé, Cameroon

M. Nedeljkovic
Ministry of Infrastructure and Water Management, Utrecht, the Netherlands

S. A. Bernal
Department of Architecture and Civil Engineering, University of Bath, Bath, UK

© RILEM 2026

G. Ye and F. Dehn (eds.), *Mechanical Properties of Alkali-Activated Materials*, RILEM State-of-the-Art Reports 46, https://doi.org/10.1007/978-3-032-07116-3_4

Keywords Construction and demolition wastes · Ashes · Industrial waste and by-products · Metallurgical slags · Mine tailings · Non-kaolinitic clays · Non-conventional activators

1 Introduction

As discussed in Chap. "Conventional Precursors and Activators", alkali-activated cement and concretes have historically been produced using granulated blast furnace slags or pulverized fly ashes, which are recognized as conventional precursors. However, these resources are already largely exploited by the construction sector in the production of Portland blended cements and might become scarce in the years to come. This is a consequence of changes in the industries producing such by-products. A well-known critique of using non-conventional precursors in cementitious systems (not limited just to alkali-activated cements) is that the global volumes available are insufficient to meet a significant proportion of the demand for cementitious materials [1]. Whilst this observation is valid for an average perspective of the world, many (but not all) wastes and by-products make up substantial resource streams at the local or regional level [2]. All things considered, whilst using non-conventional precursors will not be convenient or economically feasible in all locations, such materials still have the potential to make a meaningful contribution at the regional scale—a matter of 'the right waste in the right place'.

For many by-products and wastes other valorisation routes are technically possible (even if they are not yet commercially viable). Secondary recovery is a technically feasible option in some cases, to extract particular elements or minerals [3]. This raises broader questions over whether it is more desirable to dissipate potentially valuable materials in low value applications (such as cementitious materials), rather than try and extract them for use in higher value applications [4]. Crucially, these options are not mutually exclusive. For example, zero-waste strategies for metallurgical wastes view additional recovery steps as a way to simultaneously generate additional value streams and simplify the slag chemistry before use in applications such as cement production [5, 6]. This leads to a wider observation—every industry (not just cement and concrete) is taking measures to address its carbon footprint and waste generation. In the hierarchy of waste management, preventing waste is nearly always preferable to recycling. This becomes particularly relevant when considering the viability of using novel precursors in future decades. Many current waste flows in different industries could be dramatically reduced in a technically feasible Circular Economy in future years—they will either be designed out, or re-integrated into the manufacturing processes which produced them. When considering the use of novel precursors, there is thus a need to be vigilant around the risk of designing tomorrow's solutions for yesterday's problems.

The premise of immobilising hazardous elements requires a full life cycle perspective. A motivation for valorising potentially hazardous wastes into alkali-activated materials is that they are effectively immobilised, converting what would otherwise

be a hazardous material into construction material that provides a valuable function to society. However, the question needs to be raised—is this still true if the material is crushed and recycled [4]. There is a risk of using Circular Economy aspirations as a motivation to valorise problematic wastes but then becoming 'stuck' halfway around the life cycle circle. Nevertheless, waste cementation is deemed a technically sound approach to treat hazardous waste that minimizes other environmental impacts associated with other more costly disposal routes.

Lastly, there are pragmatic questions about the commercial viability of using a broad range of feedstocks, at least in the short-to-medium term. In an idealised future world, performance-based standards will unlock the commercial viability of a wide range of different cements, made with infinite combinations of different precursors to best valorise the resources of a given area. Yet, whilst much progress has been made, it should be acknowledged that many of the barriers to adopting alkali-activated materials identified a decade ago remain to some extent, including standards [7, 8]. Beyond formal inclusion in standards, social drivers influence practitioners and their approach to risk when using novel construction solutions [4, 9]. Whilst the use of 'exotic' resources in cement production can be appealing from a researcher's point of view, enthusiasm for novelty is not always shared by practising engineers and contractors. Thus, there is a risk that promoting a broad range of precursors may dilute the effectiveness and diminish confidence in alkali-activated materials as a mainstream option (rather than an eternal alternative). If a bad experience occurs with a novel precursor alkali-activated cement, will this tarnish the reputation of alkali-activated materials?

These debates will continue in the coming years as researchers and practitioners grapple with the complex questions of how to build structures whilst minimising carbon and waste whilst not getting sued or going bankrupt in the process. Although alkali-activated materials are not a panacea for valorising all waste streams or industrial by-products, this technology offers flexibility with a genuine promise for achieving lower carbon and more circular industrial systems. In the following sections of this chapter, an overview of potential precursors and advances in understanding how best they can be used for producing alkali-activated cements is presented.

2 Construction and Demolition Wastes

Construction and Demolition Waste (CDW) is generated by the construction, maintenance, demolition and deconstruction of buildings and civil works [10]. In Europe, CDW is 25–30% of the total waste [11]. Recycling CDW into recycled concrete aggregates (RCA) is a way to reduce simultaneously the amount of waste, and consumption of natural mineral resources [12]. Table 1 provides an overview of the range of components in CDW. The average composition of CDW shows that up to 85% of the waste is concrete, ceramics and masonry, although CDW can be heterogeneous depending on the origin, and may contain large amounts of wood

Table 1 Construction and demolition waste composition from [13]

Waste category	wt.%, min–max range
Concrete and masonry	40–84
Concrete	12–40
Masonry	8–54
Asphalt	4–26
Others (mineral)	2–9
Wood	2–4
Metal	0.2–4
Gypsum	0.2–0.4
Plastics	0.1–2
Miscellaneous	2–36

and plasterboard [10]. An illustration of the CDW at the recycling plant is shown in Fig. 1.

RCA is mainly used in the construction industry to replace coarse natural aggregates in concrete [14]. The use of coarse RCA is defined by EN 206 2014 + A2 2021. The application of fine RCA as fine natural aggregates is limited in concrete mainly due to their high water absorption [14]. Besides using CDW as recycled aggregates, CDW has also been investigated as a binder for new concrete. CDW fines can be used as an alternative raw material for fillers [15–18], Portland clinker production [19–21], and as a pozzolanic additive [22]. This can partially reduce the usage of cement in the construction industry.

The physical properties and chemical composition of concrete waste fines, as reported by several authors, are presented in Tables 2 and 3, respectively. The fines in natural river sand are composed mainly of more than 93 wt.% SiO_2 and minor



Fig. 1 Photograph illustrating CDW. Courtesy of M. Nedeljkovic

CaO, Al_2O_3, MgO, K_2O, Fe_2O_3 and total sulfur expressed as SO_3 [23]. The concrete waste fines are made up mainly of SiO_2 (6–68 wt.%), CaO (8–65 wt.%), Al_2O_3 (1.5–15 wt.%) and Fe_2O_3 (0.75–10.4 wt.%). Compared to natural fines, concrete waste fines contain lower amounts of SiO_2 and higher amounts of CaO, Al_2O_3, MgO, K_2O, Fe_2O_3, and SO_3. This is due to the presence of old cement paste in concrete waste fines. The unreacted binder components such as Portland clinker, slag, fly ash and limestone filler are usually encountered in the old cement paste [23], as shown in Fig. 2. Fine CDW inorganic fraction is frequently characterised as inert due to a lack of chemical reactivity in ambient conditions [23]. Several studies investigated the alkali-activation of CDW to reveal the potential of this material. A brief overview of CDW-based alkali-activated materials will be presented in the following section.

Since CDW contains an abundant silicon-aluminium fraction (Table 3), the CDW fines may have pozzolanic activity, micro-aggregate filling and nucleation effects [31–33]. The main CDW used to synthesise alkali-activated materials are concrete waste, ceramic tiles and clay brick waste [26]. The most commonly used alkaline activator for the synthesis of CDW-based alkali-activated materials is a mixture of sodium silicate (Na_2SiO_3) with sodium hydroxide (NaOH) [26, 34]. The studies on the compressive strength of CDW-based alkali-activated materials [29, 35, 36] indicated that the optimum Na_2SiO_3/NaOH ratio is in the range of 1.0–2.0, as shown in Fig. 3.

To maximise the potential of alkali activation of CDW-based precursors, curing conditions such as steam curing, saline water, high-temperature curing, and autoclave have been reported in the literature [37–39]. The most promising results in terms of compressive strength of CWD-based alkali-activated materials development have been reported when using high-temperature curing (>60 °C) [29, 40]. Furthermore, alkaline activation of blends of CDW fines and conventional precursors (e.g. blast furnace slag, fly ashes and metakaolin) resulted in a significant increase of the compressive strengths, compared to mixtures without SCMs [37], as shown in Fig. 4. The compressive strength of CDW-based alkali-activated materials was doubled when the finer particles (190 μm) were used instead of coarser ones (400 μm). Huo et al. [36] showed that particles smaller than 125 μm could be alkali-activated due to their higher reactivity, whilst others [33, 41, 42] recommended that the particle size of CDW-based precursors should be finer than 75 μm. The compressive strength of brick and tile-based geopolymer was 49.5 MPa and 57.8 MPa, respectively [29]. The 28-days compressive strength of the ceramic waste-based geopolymer reached 71.1 MPa [43]. However, concrete waste-based alkali-activated material showed a lower compressive strength (13 MPa) [29]. A high content of SiO_2 can be found in both bricks and tiles (50–70 wt.%) with a reduced Al_2O_3 content (10–20 wt.%) [34], compared to concrete waste whose SiO_2 content varies from 6 to 68 wt.% and Al_2O_3 from 1.5 to 15 wt.% (Table 3). The high contents of silicon-aluminium components can be solubilized during the activation process and subsequently participate in forming Si–O–Al bonds [29]. Concrete waste contains a high quantity of CaO, while tiles and brick waste have low CaO content. The high oxide content of CaO in concrete waste is mostly linked to the reduction of concrete strength as it consumes

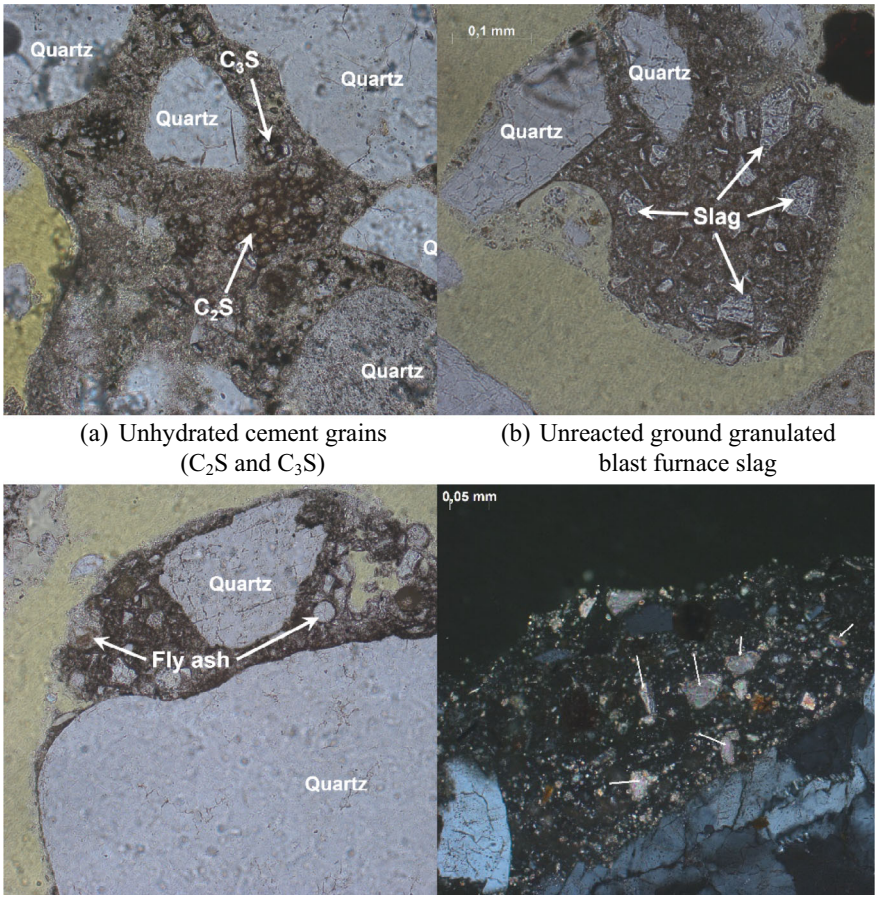
Table 2 Overview of the physical properties of CDW fines from concrete waste (<250 µm)

	Units	Nedeljkovic 2021 natural fines* [23]	Robayo-Salazar 2017 [24]	Bassani 2019 [25]	Nedeljkovic 2021 [23]	Villaquirán-Caicedo 2021 [26]	Boracherro 2022 [27]
Specific gravity	g/cm^3	2.65	–	2.64	2.48	2.71	–
Mean particle size	µm	125	24.73	–	41	25.6	19.24
Specific area	m^2/g	0.7	–	–	8.9	–	–

Table 3 Overview of the chemical composition of CDW fines from concrete waste (<250 µm) measured with X-ray fluorescence (wt.%)

Element oxides	Nedeljković 2021 natural fines [23]	Allahverdi 2013 [28]	Komnitsas 2015 [29]	Robayo-Salazar 2017 [24]	Bassani 2019 [25]	Nedeljković 2021 [23]	Villaquirán-Caicedo 2021 [26]	Tefa 2021 [30]
Na_2O	0.5	1.8	0.57	2.08	–	0.6	1.02	-
MgO	0.2	1.85	4.21	3.35	7.62	1.2	1.78	8.21
Al_2O_3	2.5	8.6	1.49	10.68	13.2	5.2	14.7	6.45
SiO_2	93.6	40.05	5.81	56.21	46.1	67.8	60.84	36.69
SO_3	0.04	–	0.82	–	4.02	0.97	–	1.14
K_2O	0.9	2.27	1.26	0.36	2.33	1.3	1.52	0.98
CaO	1.1	25.14	65.42	15.37	16.4	19.1	8.34	25.7
TiO_2	0.2	–	0.03	0.24	0.84	0.4	0.61	0.35
Fe_2O_3	0.9	10.36	0.75	10.39	8.52	3.1	5.46	3.46

* Reference [23] [1 includes physical properties and chemical composition of natural river sand fraction (<250 µm) for comparison with compositions of concrete waste fines



(a) Unhydrated cement grains (C_2S and C_3S)

(b) Unreacted ground granulated blast furnace slag

(c) Unreacted fly ash

(d) Limestone filler

Fig. 2 Microphotographs showing, **a** residual unhydrated cement grains (C_2S and C_3S) in old cement paste; **b** unreacted ground granulated blast furnace slag in old cement paste; **c** unreacted fly ash in old cement paste; **d** microphotograph showing limestone filler (indicated by white arrows) in cross polarized light [23]

a large part of NaOH solution [44]. Therefore, balancing the main elements (i.e., SiO_2, Na_2O, Al_2O_3 and CaO) is crucial for the alkali activation process of CDW.

Although studies demonstrate that CDW fines can be used in the development of alkali-activated materials, the potential to develop CDW-based alkali-activated materials at ambient temperature is still a challenge, particularly when compressive strength and appropriate fresh properties are required [32]. Moreover, research on the structural performance of CDW-based alkali-activated materials is limited. The flexural and shear behaviour of alkali-activated concrete beams with different CDW-based precursors under ambient conditions were investigated in only two studies [45, 46]. For the investigated materials, the performance of reinforced

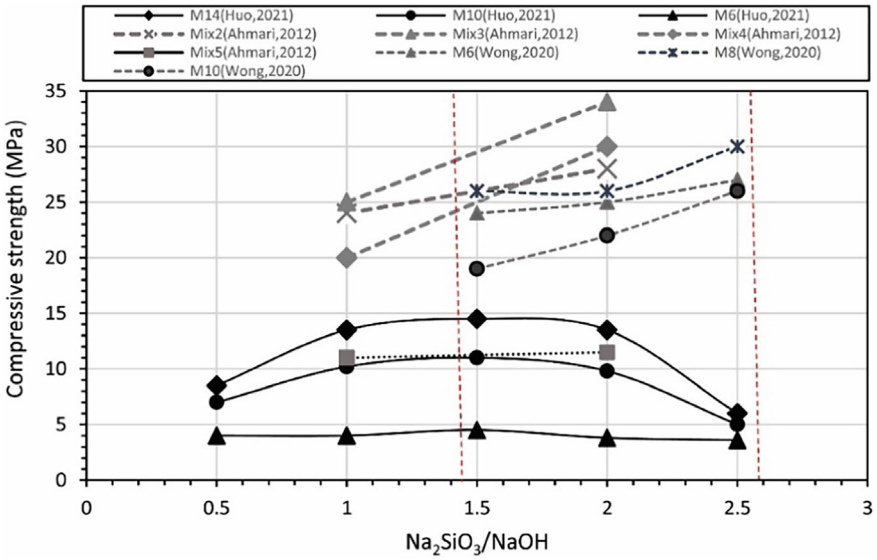


Fig. 3 Influence of sodium silicate-to-sodium hydroxide ratio on the compressive strength of CDW-based alkali-activated materials, adopted from [34]

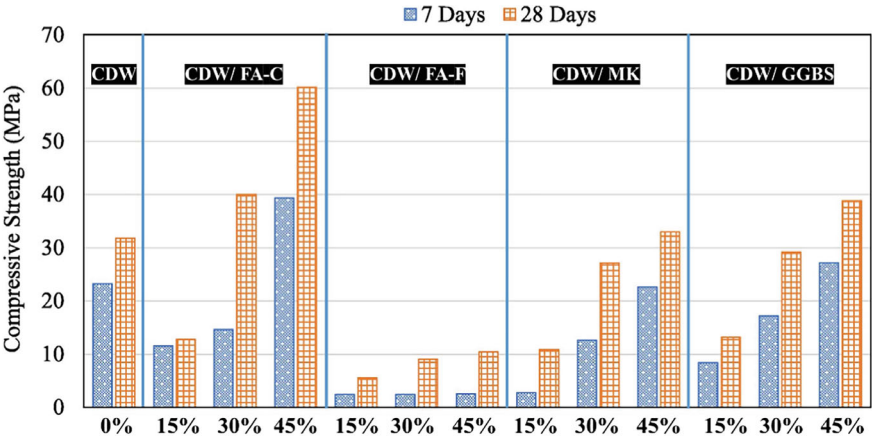


Fig. 4 Effect of the addition of supplementary cementitious materials on the compressive strength of ceramic tile waste-based alkali-activated materials. Adapted from [37]

alkali-activated concrete was similar to that of conventional reinforced concrete for flexure-dominated a/d ratios as long as the load capacity, displacement capacity, and energy dissipation capacity were considered. The percentage deviations for the listed parameters were all less than 10%.

2.1 Mineral Wool

Mineral wools are insulation materials used in buildings. In 2019, the global mineral wool consumption was 19.3 M tonnes, of which 4.9 M tonnes was consumed in China, 3.9 M tonnes in the United States, and 2 M tonnes in India [47]. The consumption of mineral wool is continuously increasing—from 2013 to 2019, the total output volume increased at an average annual rate of +1.8%. This means that when buildings are demolished after ~40 years, which is the average lifetime of a modern concrete building [48], around 20 M tonnes of mineral wool waste is generated per annum. 'Mineral wool' is a general term, but they are also referred to as synthetic vitreous fibres, man-made vitreous fibres, man-made mineral fibres, and manufactured vitreous fibres. There are several mineral wool types, such as stone wool, glass wool, slag wool, refractory ceramic mineral wool, and high-temperature mineral wool. Stone wool and glass wool are the two main types used in buildings; thus, those are most relevant when considering mineral wool waste utilization. For the remainder of this chapter, 'mineral wool' is used as a general term to describe both stone wool and glass wool. While mineral wool waste is not a significant fraction of total construction and demolition waste on a per-weight basis (<1 wt.%), it takes large volume due to its low density (20–200 kg/m^3), low stiffness, high elasticity, and poor compressibility [49, 50]. Due to these challenging properties, its utilization percentage is currently low. However, mineral wools are amorphous silicates, so they have been investigated as potential precursors for alkaline-activated materials.

Stone wool and glass wool waste compositions are presented in Table 4. Typical stone wool composition is similar to that of blast furnace slag but with lower CaO content, while glass wool depicts a typical soda-lime-glass composition. Mineral wools typically also contain phenol formaldehyde-based resin (~3 wt.% in stone wool and ~7 wt.% in glass wool), mineral oil (<1 wt.%), and other minor constituents that are added during the mineral wool manufacturing process [49, 51]. Resin can influence the hardening reactions, as discussed later in this section.

As mineral wools are fibrous (Fig. 5), they must be milled to use them as alkali-activated materials precursors. Most studies have used laboratory ball mills to reach a d_{50} particle size of 10 μm, while alternative milling methods have been investigated by Yliniemi et al. [52]. BET surface area of laboratory ball milled stone wool and glass wool have been reported to be 7241 cm^2/g and 6528 cm^2/g, respectively [53]. Table 5 summarizes the state-of-the-art research on alkali-activated mineral wools. Most studies have used elevated curing temperature to accelerate the hardening process. Some have reported unusually high flexural strength, possibly due to the undissolved fibre remnants in the binder matrix, as seen in Fig. 6.

Yliniemi et al. [54] determined the phase assemblage of stone wool and glass wool activated with typical sodium silicate and NaOH solutions. The main reaction product of stone wool was amorphous a sodium calcium aluminosilicate hydrate (C–(N)–A–S–H) gel when using either of the activators evaluated, which is broadly comparable to the gels identified in alkali-activated blast furnace slag binders. When using sodium silicate, an additional reaction product was identified – an Al-rich

Table 4 Chemical oxide composition of stone wool and glass wool samples collected from various sources around Europe

	Stone wool (N = 55)			Glass wool (N = 33)		
	Median	Min	Max	Median	Min	Max
CaO	17.9	10.0	40.1	7.8	3.0	9.9
SiO_2	42.0	39.1	54.0	63.4	57.5	68.3
Al_2O_3	16.1	7.0	24.0	3.1	1.3	5.8
Fe_2O_3	7.0	0.0	13.2	0.4	0.0	2.1
Na_2O	2.3	0.1	6.2	15.5	10.1	17.7
K_2O	1.0	0.3	3.8	0.8	0.0	2.9
MgO	9.3	2.0	14.2	2.8	0.2	4.1
SO_3	0.2	0.1	1.7	0.3	0.0	1.8
TiO_2	1.7	0.5	3.3	0.1	0.0	0.6

Data from [49]

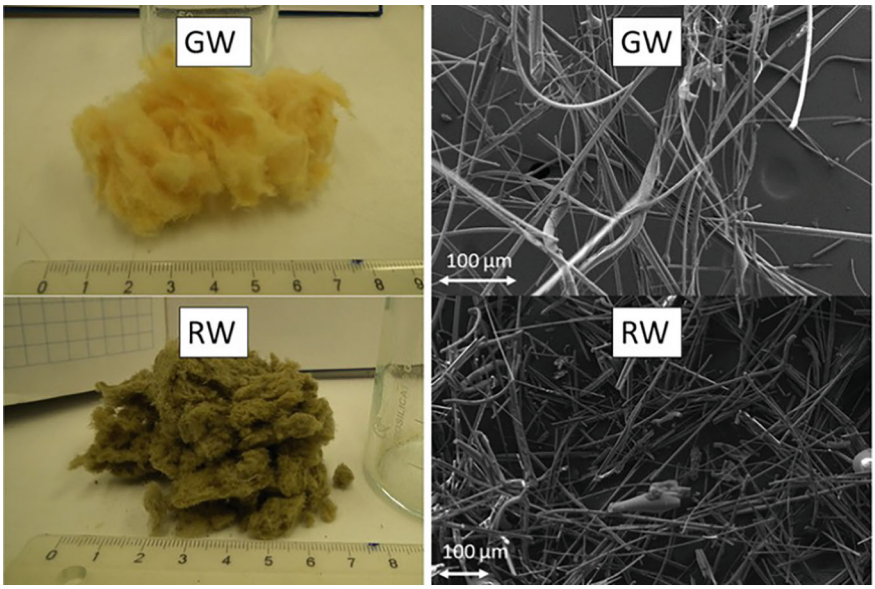


Fig. 5 Photograph of glass wool (GW) and stone wool (RW) and respective SEM images showing their fibrous nature. Image from [52]

sodium aluminosilicate hydrate (N–A–S–H) gel. When using NaOH solution as an activator, the presence of MgO in stone wool resulted in an additional Mg-rich layered double hydroxide phase formation. The main reaction product forming when using glass wool as a precursor were amorphous sodium silicate and N–(C)–(A)–S–H type gels with both activator types.

Table 5 Summary of mix designs, curing temperature, and mechanical strengths obtained for alkali-activated mineral wools

Precursor	Co-binder	Activator	Curing temp	1d compressive strength (MPa)	28d compressive strength (MPa)	Flexural strength (MPa	References
Stone wool		NaOH/sodium silicate/sodium aluminate/ Na_2CO_3	40 °C	20/27/1/0	61/38/59/1		[53]
Glass wool		NaOH/sodium silicate/sodium aluminate/ Na_2CO_3	40 °C	2/28/0/2	47/64/64/70		[53]
Stone wool	Coal fly ash	Sodium aluminate	80 °C for 48 h		13		[63]
Stone wool		Sodium aluminate	22 °C/50 °C for 4 d		28/30		[64]
Glass wool		Sodium aluminate	22/50 °C for 4 d		4/49		[64]
Stone wool production waste		NaOH	90 °C steam curing	68		13.5	[65]
Stone and glass wool	Metakaolin, foam, fibers[a]	Sodium silicate + NaOH	60 °C for 24 h		1–9	3–8	[66]
Stone wool		Potassium silicate	23 °C	15–20	36–44		[67]
Glass wool		Potassium silicate	23 °C	0	27–34		[67]
Stone wool	PVA fibers	NaOH	Hot-press for 3 h/ 60 °C for 24 h		35–40 at 60 days	7–11	[68]

(continued)

Table 5 (continued)

Precursor	Co-binder	Activator	Curing temp	1d compressive strength (MPa)	28d compressive strength (MPa)	Flexural strength (MPa	References
Stone wool		Sodium silicate/ NaOH	22/40 °C		41	15	[69]
Glass wool		Sodium silicate/ NaOH	22/40 °C		30	14	[69]
Stone wool	Metakaolin/ladle slag/glass wool	Sodium silicate + NaOH	60 °C for 24 h		75	10	[57]
Glass wool	Metakaolin/ladle slag/stone wool	Sodium silicate + NaOH	60 °C for 24 h		40	8	[57]
Stone wool		Sodium silicate/ NaOH	22 °C/40 °C for 3 d	0/40 at 3 d	34/NA	9/10 at 3 d	[70]
Glass wool		Sodium silicate/ NaOH	22/40 °C for 3 d	0/53 at 3 d	32/NA	10/15 at 3 d	[70]
Glass wool	BFS	Sodium silicate + NaOH	20 °C	40	65 at 7 d	7 at 7 d	[58]
Stone wool		NaOH	60 °C for 24 h		19		[59]
Glass wool (phenolic resin)		Sodium silicate	23/40 °C for 24 h/ 60 °C for 24 h	1/11/8	49/48/24		[55]
Glass wool (sugar resin)		Sodium silicate	23/40 °C for 24 h/ 60 °C for 24 h	2/7/5	40/58/55		[55]
Glass wool (resin free)		Sodium silicate	23/40 °C for 24 h/ 60 °C for 24 h	5/25/16	62/48/33		[55]
Stone wool		Sodium silicate + NaOH	70 °C for 2d		62	4.8	[61]

(continued)

Table 5 (continued)

Precursor	Co-binder	Activator	Curing temp	1d compressive strength (MPa)	28d compressive strength (MPa)	Flexural strength (MPa	References
Glass wool	Bauxite/Al_2O_3 powder	Sodium silicate + NaOH	70 °C for 2d		51/59	4.1/4.5	[61]
Stone wool[b]	Lime/metakaolin/ EAF slag/fly ash	Sodium silicate + NaOH	22 °C		28–56	12–15	[60]
Stone wool	H_2O_2[c]	Sodium silicate	70 °C for 3d		3–14	4–7	[56]

[a] Application was fiber-reinforced lightweight mortar; [b] Application was façade panel; [c] Application was lightweight foamed material

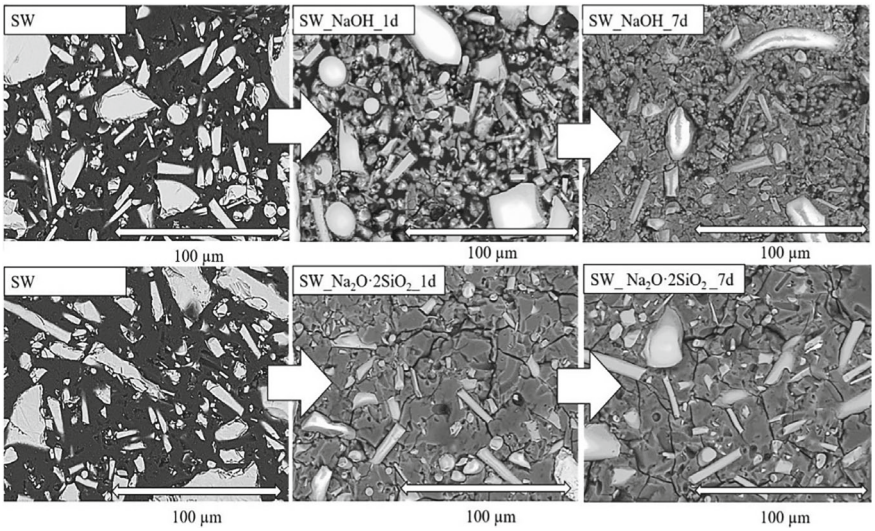


Fig. 6 Backscattered electron micrographs of the cross-section of alkali-activated stone wool. The binder matrix contains remnants of undissolved fibres. Image from [54]

The organic resin present in mineral wools can slow down hardening, and the hardened material may leach out organic components. Lemougna et al. [55] investigated the effect of phenolic and sugar-based organic resins in alkali-activated glass wool. They noted that resin decreased milling efficiency, modified rheology by increasing the liquid demand, and slowed the strength development at room temperature. Curing for 24 h at 40 °C was beneficial for one-day strength development, compared to 20 and 60 °C, independent of the presence of the resin. All the cured paste samples, with and without resin, achieved a compressive strength of more than 40 MPa at 28 days.

Nevertheless, water immersion affected the materials' strength, suggesting their suitability for dry environments or the need for suitable co-binders to increase their durability and water resistance. Pavlin et al. [56] reported that alkali-activated stone wool façade panels had low freeze–thaw durability. However, freeze–thaw resistance was excellent with lime, metakaolin, or EAF slag as co-binders. Bleeding of red-coloured liquid originating from the organic resin has also been observed [57, 58].

Sgarlata et al. [59] reported no antibacterial properties and an absence of cytotoxicity for stone wool-based AAMs. Also, concentrations of potentially toxic elements in leachates were lower than the European law limit when tested in water. Also, Pavlin et al. [60] and SŁaźniewska-Piekarczyk et al. [61] reported that leaching was below the non-hazardous waste limits except for barium for which leaching above the limit was observed. As with AAMs prepared with other precursors, the leading CO_2 contributor of the mix is the alkaline activator.

König et al. [62] investigated the suitability of stone wool and glass wool as alternative activators by dissolving them in 10 M NaOH solution with a solid mass to

solution volume ratio of 0.1–0.025 g/mL at 120 °C for 4 h or 24 h. This procedure dissolved up to 95% of Si from stone wool and 77% of Si from glass wool. However, the resulting Si concentration was much lower compared to commercial sodium silicate activators. Thus, the applicability of this process remains questionable. Nevertheless, when the prepared alternative activators were used to activate fly ash or blast furnace slag, an improvement in mechanical properties was observed when compared to the sole NaOH activator.

3 Ashes

3.1 Biomass-Derived Ashes

It is estimated that approximately 140 billion tonnes of biomass are produced globally every year, with agriculture being the main source of biomass generation. Producing energy from this residual agricultural biomass involves burning it at high temperatures, forming waste biomass-derived or agricultural ashes [71]. It is important to ensure that the biomass is burnt at the right temperatures (typically 700–900 °C) so the material present sufficient amorphous content in the ashes [71]. Several studies have highlighted the feasibility of utilizing agricultural ashes for producing alkali-activated materials [72–76]. Rice husk ash (RHA), sugarcane bagasse ash (SCBA), and palm oil fuel ash (POFA) are some examples of such agricultural ashes that have been investigated extensively to determine their suitability as precursors for alkali-activated cements production.

The microstructural and morphological characteristics of the agricultural ashes can vary depending on their origin. Rice husk ash has a microporous cellular microstructure with a high surface area, leading to increased water absorption [77]. The microstructure of sugarcane bagasse ash (SCBA) is a combination of fibrous, irregular, and spherical particles [78], while palm oil fuel ash consists of irregular particles with surface porosity [79]. The variations in the chemical compositions of the different agricultural ashes available in the literature were reported by Athira et al. [80] in their comprehensive review (Fig. 7). Often, these ashes may require additional processing before being used as a precursor. The presence of unburnt carbon due to incomplete combustion of organic fibres could harm the performance of alkali-activated concretes (e.g., workability) [80, 81]. Therefore, it would be desirable to minimize the unburnt carbon in ashes. The loss of ignition (LOI) test can be used to estimate the unburnt carbon [80], and recalcination/burning may be required to reduce the unburnt carbon content in the ashes.

In some cases, further processing of the ashes, like sieving and grinding, may be required to minimize the mean particle sizes of these ashes to ensure optimum reactivity [82, 83]. In the case of RHA, additional grinding can also help break down the cellular microstructure and reduce the water absorption. In addition to amorphous

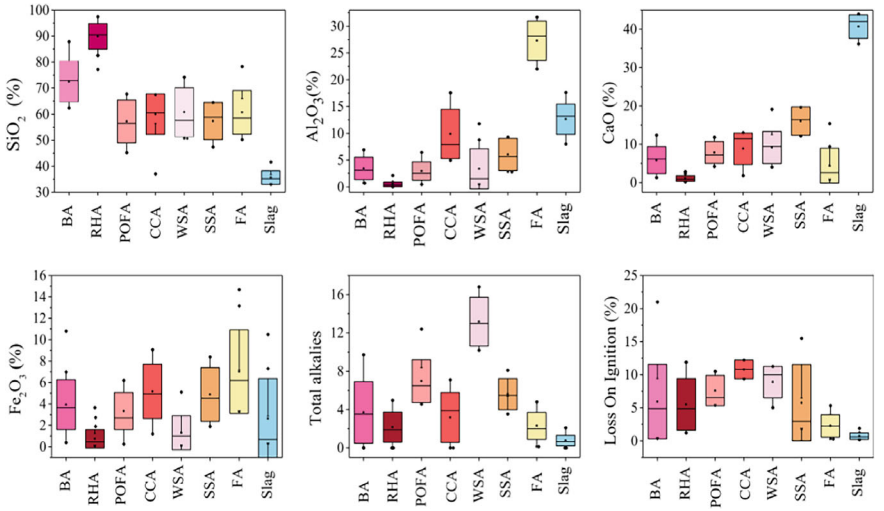


Fig. 7 The oxide compositions of biomass-derived ashes. Fig from [79]. BA—Bagasse Ash, RHA—Rice Husk Ash, POFA—Palm Oil Fuel Ash, CCA—Corn Cob Ash, WSA—Wheat Straw Ash, SSA—Sugarcane Straw Ash, FA—Fly Ash

content, crystalline phases like quartz, cristobalite and kyanite are reported in the agricultural ashes [74, 84].

While it may be possible to use agricultural ashes as a sole precursor for producing alkali-activated cements [84, 85], the more favoured approach seems to be combining these ashes with conventional precursors such as fly ash, metakaolin, or blast furnace slag due to the lower reactive Al_2O_3 content in these ashes [76, 83, 86, 87]. Rice husk ash, for example, predominantly contains SiO_2 and alkalis (>90 wt.%), with Al_2O_3 being a minor fraction (<5 wt.%), and an additional source of alumina would be required for the effective utilization of RHA as a precursor for producing alkali-activated binders. Therefore, RHA may be more valuable as an alternative activator [88–91], with only a few studies attempting to investigate its potential as a precursor [84, 92–95].

The processing temperature and fineness of the RHA can influence its reactivity. An optimum processing temperature of 690 °C and 1–5% retention on No. 325 sieve (45 μm) was recommended by Detphan et al. [95] for producing RHA suitable for alkali-activated materials applications. Hwang et al. [93] investigated the combination of RHA and FA as mineral precursors using sodium hydroxide as an activator and found that replacement levels greater than 35% affected the mechanical performance of the alkali-activated composite. Acceptable compressive strengths in the range of 28–35 MPa could be obtained in the range of substitution levels investigated. In the case of RHA-slag systems, an optimal replacement level of 10% has been suggested [96].

Castaldelli et al. [83] investigated using sugarcane bagasse ash (SCBA) as a secondary precursor by partially replacing slag up to 40% using sodium silicate

and sodium hydroxide as activators. The compressive strengths of the SCBA-slag systems were lower than the 100% slag systems. Compressive strengths in the range of 55–65 MPa were reported for the SCBA-slag systems after 270 days. Specimens cured at 20 °C showed better mechanical performance when compared to specimens cured at 60 °C. Deepika et al. [75] suggested that using a potassium-based activator improves mechanical performance in SCBA-slag systems. Their results also agree with Castaldelli et al. [83] regarding the effect of substitution levels and curing temperature on SCBA-slag mixes (Fig. 8). The reduced performance at heat curing was attributed to the loss of water, which affected the reaction of slag.

Similarly, alkali-activated binders were prepared using SCBA to partially replace fly ash as a precursor, using potassium hydroxide and potassium silicate as activators. A replacement level of 25% was observed to be ideal [97]. Yadav et al. [98] explored the alkali activation potential of SCBA-metakaolin combination with 25–75% metakaolin replacement. No specific recommendations regarding the optimal

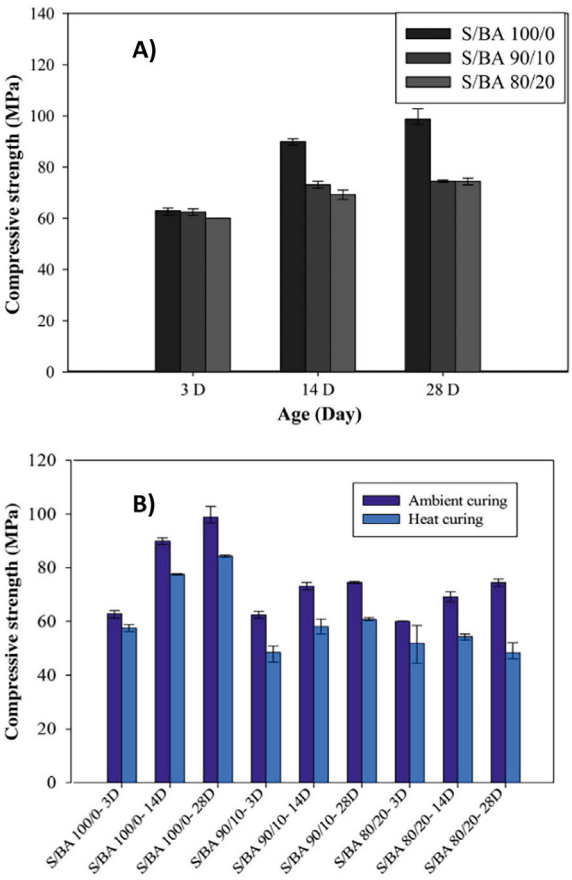


Fig. 8 **a** Effect of substitution levels on strength development in SCBA-slag mixtures. **b** Effect of curing temperature on strength development in SCBA-slag mixtures. Fig from [75]

substitution levels were made in this study. It was observed that additional calcination and grinding of the SCBA were required to increase its reactivity. The studies on palm oil fuel ash [85, 99, 100] also show positive results regarding its potential as primary and secondary precursors.

Durability characteristics like acid resistance, fire resistance, and chloride ingress are seen to improve in agricultural ash containing AAMs [80]; however, detailed long-term durability studies are required to establish the robustness of these systems. One potential barrier in using agricultural ashes appears to be the variability in its chemical composition which makes it difficult to produce a generalised guidelines for formulating the AAMs.

3.2 Paper Sludge Ash

Another ash suitable as a precursor to produce alkali-activated materials is derived from calcining paper sludge. Paper sludge is produced as a waste stream during pulp and paper production and contains organic and inorganic matter such as calcium carbonates, kaolinite, muscovite, talc, quartz, and cellulose fibres [101–103]. Nowadays, this sludge is burnt to recover the energy used in pulp and paper processes and/or municipal heating, while the burnt residues, referred to as paper sludge ash (PSA), are generated [104]. Though with different processing and pre-treatment, wastepaper sludge ash has a mineralogy and chemical composition similar to PSA and, therefore, is regarded as the same material in this section. The mineralogy and chemical composition of PSA vary and are dependent on the content of the sludge or recycled paper used. In some incinerators, wood wastes are added together with the sludge during combustion, and these inputs deviate from different plants and batches. The mineral phases in PSA can include gehlenite (Ca_2AlSiO_7), quartz (SiO_2), mayenite ($Ca_{12}Al_{14}O_{33}$), calcite ($CaCO_3$), muscovite $KAl_2(F, OH)_2$, clinochlore $(Mg_{2.5}Fe_{1.0}Mn_{0.7}Zn_{0.7})Al(Si_3Al)O_{10}(OH)_8$, free lime, and talc ($Mg_3Si_4O_{10}(OH)_2$) [103, 105, 106]. While the principal chemical composition is calcium oxide (CaO) 35–60 wt.%, silicon oxide (SiO_2) 16–35 wt.%, and aluminium oxide (Al_2O_3) 9–19 wt.% and regarded as calcio-aluminosilicate material [105, 107].

During calcination (700–800 °C), decarbonation of calcite and dehydroxylation of kaolinitic clays in the sludge result in the formation of lime and metakaolin, respectively, which influences the reactivity of PSA when used in cementitious applications. Notably, the content of kaolinitic clays in some paper sludges can be non-existent [108]. The suitability of PSA as a precursor in alkali-activated materials has been previously investigated [105, 109–112]. Due to the free lime content, which hydrates to calcium hydroxide ($Ca(OH)_2$), PSA has also been used as an alternative activator [113, 114]. Solely water-hydrating or alkali-activation of PSA has shown good binding properties [105, 106, 114]. However, PSA is frequently utilized as co-precursors with conventional precursors such as blast furnace slag (BFS) or fly ash. Whereas having a similar chemical composition as BFS and pH of 12.4, alkali-activating PSA alone was observed not to be effective as a low strength (<5 MPa) were

produced [106, 114, 115]. In contrast, combining PSA with other precursors has shown better strength. A 90-day compressive strength as high as 70 MPa has been measured by co-activating PSA with fly ash [116]. In that study, the dimensional stability was improved with the PSA increment up to 40% replacement of the fly ash having the lowest drying shrinkage. Similar observations have been reported for uncalcined paper sludge [117]. Alkali-activated blends of BFS and PSA have also shown good strength properties as mortars used in high-sulfate environments [112]. Considering the free lime content (3–11 wt.%) that might be present in PSA, potential soundness problem is one technical obstacle that should be considered during mix designs.

3.3 Municipal Solid Waste Incineration (MSWI) Bottom Ash

The amount of municipal solid waste (MSW) generated in the world is expected to reach 3.4 billion tons by 2050 [118]. Incineration of MSW at waste-to-energy plants is considered a better solution for managing MSW that is difficult to compost or recycle [119–121]. While waste incineration dramatically reduces the volume of MSW, it also generates residual by-products [122–124]. The primary residue of municipal solid waste incineration (MSWI) is the ash collected at the bottom of the incinerator, commonly known as MSWI bottom ash [125, 126]. Given the widespread adoption of waste incineration techniques around the world, the amount of MSWI bottom ash produced is also growing, highlighting the urgent need to deal with this residue [127].

The metals present in MSWI bottom ash are usually recycled [128]. Subsequently, the mineral-enriched fraction can be utilized to produce ceramics [129–134] and construction materials [135–141]. MSWI bottom ash is commonly used in some regions as aggregates to construct roads and embankments [142]. Using MSWI bottom ash as a binder material offers a higher value-added application than using it as aggregate. The utilization of MSWI bottom ash as a precursor for alkali-activated materials (AAM) holds significant promise. Incorporating MSWI bottom ash in construction has the potential to realize the large-scale application of these industrial by-products. The feasibility of using MSWI bottom ash in producing AAM has been demonstrated in previous research [128].

MSWI bottom ash collected upon discharge from the bottom of the municipal solid waste incinerator cannot be used directly as a construction material. Fresh MSWI bottom ash usually undergoes plant-scale treatments to recycle metals and reduce their leaching potential. The plant-scale treatments usually include particle size reduction, metal extraction, stabilization, cleaning, and classification (see Fig. 9) [128]. The stabilization of MSWI bottom ashes is usually realized through a weathering process, which typically lasts one to three months [143–159]. When the weathering process is included in the plant-scale treatments, the resulting mineral-enriched fraction is called weathered MSWI bottom ash. Compared with fresh MSWI bottom

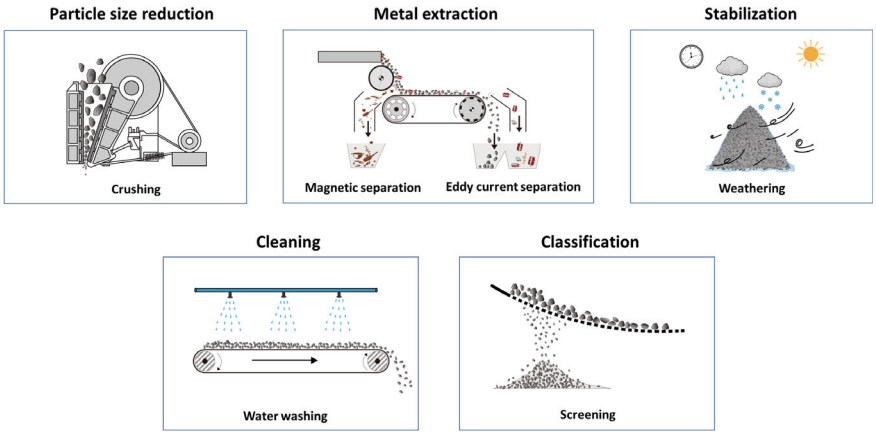


Fig. 9 Illustration of plant-scale treatments conducted on fresh MSWI bottom ash [128]

ash, weathered MSWI bottom ash is more commonly used for construction materials due to its lower leaching potential.

The compositional data of the weathered MSWI bottom ash reported in the literature is consolidated and presented in Table 6. The chemical composition of weathered MSWI bottom ash, as shown in Table 6, is comparable to a class C coal fly ash but dissimilar to that of granulated blast furnace slag [128, 160, 161]. The main components of weathered MSWI bottom ash are SiO_2, CaO, Al_2O_3, and Fe_2O_3. These four components together account for over 60% of the total weight of weathered MSWI bottom ash. The SiO_2 content in weathered MSWI bottom ash ranges from 10.2 to 59.3 wt.%, while the CaO content is 13.6–48.1 wt.%. The weight percentage of Al_2O_3 changes from 4.2 to 16.3. The weathered MSWI bottom ash usually contains 1.3–20.2 wt.% Fe_2O_3. The heavy metals and soluble salts found in MSWI bottom ash are more than those in coal fly ash and granulated blast furnace slag. This raises concerns regarding the durability and leaching risk of construction materials prepared using MSWI bottom ash as raw materials [128].

The mineralogical composition of weathered MSWI bottom ash exhibits significant diversity. However, the mineralogical phases in weathered MSWI bottom ash can be classified into 11 categories: silicon dioxide (SiO_2), iron oxides (FeO_x), silicates, carbonates, sulfates, chloride salts, phosphates, non-ferrous metal oxides, hydroxides, sulfides, and other minerals [128]. A summary of the representative minerals can be found in Table 7. In addition to the crystalline phases, MSWI bottom ashes contain amorphous phases. It is relevant to quantify the amorphous content and its composition as the reactivity of MSWI bottom ashes (and other AAM precursors) is typically governed by it [164]. Based on earlier research, the amorphous phase in MSWI bottom ash can be 30.8–81.3 wt.% [128]. However, the composition of the amorphous material in MSWI bottom ashes has been rarely measured. Thus, there is a lack of comprehensive data on the composition of the amorphous phase in MSWI bottom ash [128].

Table 6 Ranges of the components present in weathered MSWI bottom ash [128], compared to coal fly ash (Class C and Class F) [162] and granulated blast furnace slag [163]

Compound (wt.%)	Weathered MSWI bottom ash	Class C coal fly ash	Class F coal fly ash	Granulated blast furnace slag
SiO_2	10.2–59.3	11.8–46.4	37–62.1	30–40
CaO	13.6–48.1	15.1–54.8	0.5–14	30–50
Al_2O_3	4.2–16.3	2.6–20.5	16.6–35.6	7–20
Fe_2O_3	1.3–20.2	1.4–15.6	2.6–21.2	0–2.5
Na_2O	0.0–8.1	0.2–2.8	0.1–3.6	–
Na_2O_e	0.8–9.0	–	–	–
MgO	1.6–3.3	0.1–6.7	0.3–5.2	0–21
SO_3	0.6–6.8	1.4–12.9	0.2–4.7	–
S	–	–	–	0–2
P_2O_5	0.3–3.5	0.2–0.4	0.1–1.7	–
TiO_2	0.3–2.5	0.6–1.0	0.5–2.6	–
K_2O	0.4–3.7	0.3–9.3	0.1–4.1	–
ZnO	0.2–1.3	–	–	–
CuO	0.1–0.9	–	–	–
Cl	0.1–9.5	–	–	–
MnO	0.1–1.9	0.03–0.2	0.03–0.1	0.2–2.5
PbO	0.2–0.4	–	–	–
LOI	2.7–30	0.3–11.7	0.3–32.8	–

Chen et al. [165] reported that in weathered MSWI bottom ash, 34.2 wt.% SiO_2, 8.8 wt.% CaO, 7.9 wt.% Al_2O_3, and 6.2 wt.% Fe_2O_3 are present in the form of amorphous phase. It is worth noting that weathered MSWI bottom ash contains metallic aluminium (Al). Under alkaline conditions, metallic Al undergoes a redox reaction that results in the release of hydrogen gas. Using MSWI bottom ash containing metallic Al as an AAM precursor will lead to volume expansion and strength reduction of hardened pastes [166, 167]. The metallic Al content in MSWI bottom ash is usually quantified with the water displacement method [168]. Previous researchers found that the metallic Al content is below 2 wt.% in weathered MSWI bottom ash [128].

In contrast to plant-scale treatment, laboratory treatments are referred to as "lab-scale treatments" [128]. While plant-scale treatments are primarily focused on recycling metals and producing aggregates, lab-scale treatments aim to enable the application of MSWI bottom ash in binder production, such as a precursor for AAM. Most of the MSWI bottom ash sent to the laboratory is produced after the plant-scale treatments of fresh MSWI bottom ash [128].

Table 7 Classifications of minerals present in weathered MSWI bottom ash from [128]

Categories			Typical minerals
1	Silicon dioxide (SiO_2)		Quartz, cristobalite
2	Iron oxides (FeO_X)		Magnetite, Hematite, Wustite
3	Silicates	Melilite	Gehlenite and Åkermanite
		Feldspar	Albite and Anorthite
		Pyroxene	Diopside and Wollastonite
		Other silicates	Mullite, Zeolite
4	Carbonates		Calcite and Dolomite
5	Sulfates		Ettringite, Gypsum, and Anhydrite
6	Chloride salts		Halite (NaCl) and Sylvite (KCl)
7	Phosphates		–
8	Non-ferrous metal oxides		Rutile, Corundum, Zincite
9	Hydroxides		Iron hydroxide: Goethite, Lepidocrocite, Ferrihydrite Aluminium hydroxide: gibbsite
10	Sulfides		Copper sulfides, iron sulfides
11	Other minerals		–

According to Chen et al. [128], the lab-scale treatments are designed to solve issues including heterogeneous composition and the presence of hazardous components (such as metal Al, soluble salts, heavy metals, and low reactivity). Lab-scale treatments can be grouped into mechanical, chemical, and thermal treatments (see Fig. 10). Mechanical treatments of MSWI bottom ash aim to decrease particle size, achieve a homogeneous composition, and reduce the metallic Al content. The chemical treatments are mainly about alkaline solution treatment to oxidize metallic Al embedded in MSWI bottom ash. Thermal treatments are usually employed to change the mineralogical composition of MSWI bottom ash. This process helps immobilize the heavy metals, increase the content of reactive phases, and decrease the amount of organic matter in MSWI bottom ash. Depending on the goal, the temperature of thermal treatments can be 500–900 or 1000–1500 °C [128].

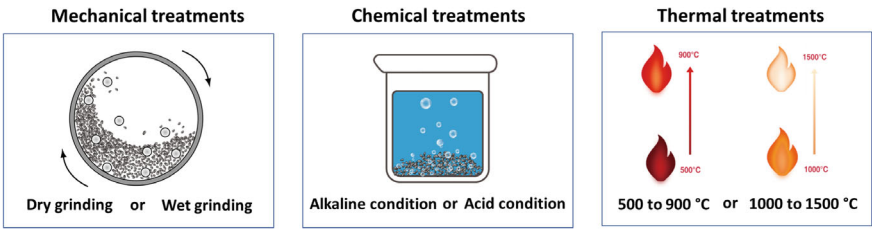


Fig. 10 Illustration of lab-scale treatments proposed to improve the quality of MSWI bottom ash for the application as SCM and AAM precursor [128]

There is very little information regarding the reactivity of MSWI bottom ash as an AAM precursor [128]. In previous research, different methods were used to measure the potential reactivity of MSWI bottom ash for this application, including the modified Chapelle test, which was used by Casanova et al. [169] and Carvalho et al. [170]. They found that MSWI bottom ash's pozzolanic reactivity was lower than that of Class F coal fly ash. Huang et al. [171] assessed the reactivity of MSWI bottom ash produced in China by quantifying the content of reactive SiO_2, CaO, and Al_2O_3. The test results indicated that the reactive SiO_2 content in MSWI bottom ash is much higher than that in blast furnace slag. However, the reactive CaO and Al_2O_3 contents in MSWI bottom ash are lower than those in blast furnace slag. Maldonado-Alameda et al. [172] measured the reactivity of MSWI bottom ash by determining the soluble SiO_2 and Al_2O_3 content in MSWI bottom ash. They found that the molar ratio between dissolved Si and Al was much higher than the optimal value and recommended introducing additional sources of reactive Al_2O_3 and SiO_2 to modify the Si/Al molar ratio when MSWI bottom ash is used to produce alkali-activated materials.

4 Industrial Wastes and By-Products

4.1 Red Mud

Red mud (also known as bauxite residue) is generated as an alkaline industrial by-product during the extraction of alumina from bauxite using Bayer's process. Depending on the bauxite source and extraction procedures used in the plant, approximately 0.7–2 tonnes of red mud is generated per tonne of alumina. It is estimated that nearly 120 million tonnes of red mud are generated annually [173, 174], with a global reserve of 2.7 billion tonnes [175]. The chemical composition of generated red mud depends on the nature of the bauxite ore. The range of chemical compositions typically observed in red mud is shown in Table 8. It is estimated that red mud contains, on average, approximately 30% amorphous content [176]. Iron-containing minerals provide the bauxite residue with its characteristic red colour. Red mud is also intrinsically alkaline, posing significant challenges in its safe disposal. The pH value of the untreated residue liquor of red mud is observed to range between 9.2 and 12.8 [176]. However, this can be beneficial for utilizing red mud as a non-conventional precursor for alkali activation.

The alumina available in red mud depends on the efficiency of the Bayer alumina extraction process. Higher extraction efficiency implies a lower alumina content in the red mud. In most cases, the alumina content in the red mud is reported to be insufficient to produce alkali-activated materials. The variability and complex chemical composition (especially alumina content) suggest that red mud would ideally be suited as a secondary precursor in combination with other conventional precursors. Therefore, studies using red mud as the sole precursor for alkali activation are limited

Table 8 The expected chemical oxide composition range for bauxite residue. From [174]

Chemical oxide	Expected range (wt.%)
Fe_2O_3	5–60
Al_2O_3	5–30
SiO_2	3–50
TiO_2	0.3–15
CaO	2–14
Na_2O	1–10

[177]. Alkali-activated materials have been successfully prepared by combining red mud with fly ash, metakaolin, and blast furnace slag [178–180]. Several studies have successfully produced alkali-activated materials with acceptable mechanical and durability performance using the precursor combination of blast furnace slag and red mud [178, 181–183]. Occhione et al. [177] reported compressive strengths of nearly 12 MPa for geopolymers produced with red mud as the sole precursor. The addition of 20% blast furnace slag resulted in a significant improvement in the strength (nearly 30 MPa). Ai et al. [180] investigated the possibility of utilising red mud as a secondary precursor with metakaolin and fly ash. The combination of red mud and metakaolin was observed to have better mechanical performance due to the higher availability of soluble aluminosilicate from metakaolin. Mechanical activation of the red mud by pulverization has been suggested as a potential strategy to improve the strengths of red mud—fly ash composites [182, 184]. High temperature curing and autoclave curing also appear to show promising results in improving the mechanical properties of red mud geopolymer composites [180, 185].

Pre-treatment of red mud can also increase its reactivity. Calcination of red mud transforms the crystalline phases and improves the solubility of aluminosilicate fractions. Ye et al. [186] suggest an optimum temperature of 800 °C for calcining red mud. Thermally treated red mud has also been used to produce one-part geopolymer systems [15]. The fate of iron-bearing phases in the red mud during alkali activation and its contribution to the development of mechanical properties merit further investigation. Hu et al. [187] suggest that iron (Fe^{3+}) would substitute aluminium (Al^{3+}) in the aluminosilicate structure of the geopolymer. Studies using iron-rich precursors [188] have observed the formation of Fe–O bonds in the geopolymer matrix, with iron occupancies being primarily in the octahedral configuration. The main limitation of utilizing red mud precursor for alkali activation is its complex chemical composition, which depends on the nature of the bauxite ore and alumina extraction efficiency. Activator dosage for red mud must be carefully formulated considering the intrinsic alkalinity to prevent potential efflorescence.

4.2 Metallurgical Slags

This sub-section covers the full range of metallurgical slags, albeit with two exceptions. Firstly, blast furnace slag—this is one of the most widespread and well-understood conventional precursors and has already been covered in Chap. "Conventional Precursors and Activators". Secondly, red mud—this is not classified as a conventional precursor, but its high alkalinity makes it distinct from other metallurgical slags and is covered in a separate sub-section in this chapter. Therefore, this sub-section includes steel slag, lead slag, copper slag, nickel and copper-nickel slag, zinc slag, manganese and silico-manganese slag, and phosphorous slag. There have been several recent reviews on the composition and properties of metallurgical slags [189–191] and their specific use in AAMs [192, 193]. This sub-section will, therefore, give a concise overview of the salient points around quantities available, their composition, activator requirements, and reaction products.

As shown in Fig. 11, there are orders of magnitude in difference between the volumes of material processed in these industries. Primary production of the main non-ferrous metals corresponding to these slags is predicted to continue at similar or increased levels into the twenty-first century [193]. The production of the associated slags can be considered reliable in quantity (even if the absolute quantities are minor compared to conventional precursors).

Collectively, the most common elements in these slags are Si, Fe, Ca, Mg and Al, although there is a wide variety between different types of slags and between different sources [191]. Steel slags (as ferrous slags, distinct from non-ferrous slags) are dominated by Ca and Si, with smaller amounts of Fe, Mg and Al. Crucially, many slags contain trace amounts of hazardous elements (e.g. As, Pb, Cr). Whilst AACs

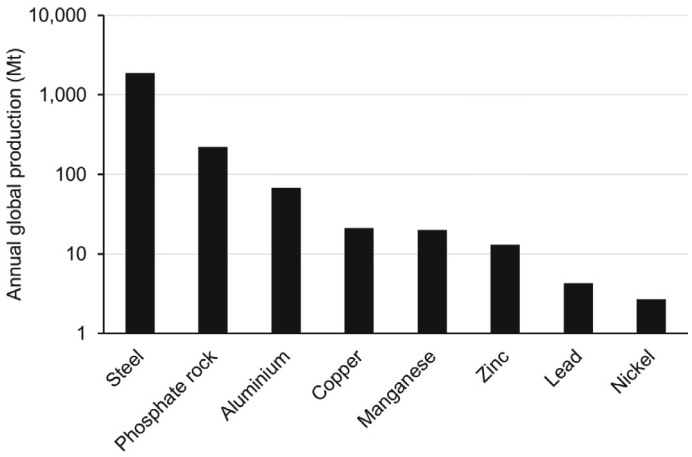


Fig. 11 Annual global production for a range of key non-ferrous metals in 2021. Aluminium values refer to smelter production; Steel values refer to raw steel; all other values refer to mine production. Data from U.S. Geological Survey (2022) [194]

are generally considered an effective route for immobilising hazardous elements, this can be a barrier to their use [192]. In terms of mineralogy, the majority of the phases present are crystalline—olivine group minerals are the most common throughout. In steel slags, the main mineral phases are olivine and merwinite—other phases present in smaller quantities include C_3S, β-C_2S, C_4AF, C_2F, glassy phases, and free lime (CaO) [192, 195]. The presence of small amounts of cementitious phases gives steel slags a small amount of hydraulic reactivity. In non-ferrous slags, olivine (particularly fayalite), spinel (particularly magnetite) and melilite group minerals are the most commonly occurring [191].

A word of caution should be stated regarding the consistency of composition. The chemistry and properties of these slags depend on several factors, including: the quality of ores, extraction technologies, flux additions, smelting conditions, and cooling processes [196]. Recovery of metals from slag is a complementary strategy in a zero-waste strategy for slags [5]. Depending on economic viability, this could become more widespread in future, consequently changing the composition of those slags [193]. Slag composition should, therefore, be thought of as variable not only in space but also in time. The lower hydraulic activity of these slags compared to conventional supplementary cementitious materials makes them more efficient to use as alkali-activated cements and reduces the demands for the aforementioned precursors. They are commonly blended with other precursors because of their low Al content [90]. Given that the Ca content of these slags is typically low, most studies have used sodium silicate activators rather than near-neutral salt activators such as sodium sulfate and sodium carbonate.

Considering the breadth of precursor compositions, blending with other precursors and choice of different activators, giving a detailed overview of reaction product formation is impractical. Binder phases such as C–A–S–H, C–(N)–A–S–H, N–A–S–H, and C–S–H have all been observed in different studies; other commonly occurring reaction products include hydrotalcite type phases and zeolites [192]. As is the case for alkali-activated cements made with other precursors, mechanical strength is strongly affected by the curing regime. Elevated curing temperatures, including hydrothermal curing, can enhance strength development at early ageing times [197, 198]. Another factor influencing strength is the use of pre-treatment on the precursor. Grinding to increase specific surface area has been shown to be effective [199]. A combined process of milling under a carbonating atmosphere has been effective for Cu-Ni slags [200, 201]. Table 9 shows an overview of the curing regime and alkali-activator used to produce AAMs as a function of the slag type, evaluated over the past years.

4.3 Mine Tailings

Mine tailings are the residue generated as a by-product of mineral ore processing and are typically collected in the form of slurry. Mine tailings can be a combination of water, unextracted minerals, chemicals, and heavy metals [213]. Jones and Boger

Table 9 Summary of recent studies using metallurgical slags as precursors for producing AAMs

Slag type	Other constituents	Activator	Curing temp	References
Copper slag	–	Sodium hydroxide and sodium silicate	20 or 65 °C	[197]
Copper slag	Metakaolin	Potassium hydroxide and sodium silicate	20 °C	[202]
Copper slag	Metakaolin or fly ash	Sodium hydroxide and sodium silicate	24 h at 80 °C, then 25 °C	[203]
Copper slag	–	Sodium hydroxide or sodium silicate	20 °C or 12 h in a 80 °C steam atmosphere then 20 °C	[204]
Silico manganese slag	–	Sodium hydroxide	27 °C	[205]
Silico manganese slag	–	Sodium silicate	60 °C	[206]
Silico manganese slag	Fly ash	Sodium hydroxide	27 °C	[207]
Stainless steel slag	–	Sodium hydroxide and sodium silicate or potassium hydroxide and potassium silicate	24 h at 20 °C, 24 h in a 80 °C steam atmosphere, then 20 °C thereafter	[208]
Converter steel slag	–	Sodium silicate	25 °C	[209]
Copper/nickel slag	Fly ash	Sodium hydroxide and sodium silicate	20 °C	[210]
	–	Sodium hydroxide and sodium silicate	24 h at 60 °C, then 23 °C	[211]
Phosphorous slag	–	Sodium hydroxide and sodium carbonate or sodium carbonate and calcium hydroxide	24 °C, or ranges of 50–180 °C for a range of 5–20 h in either hydrothermal or autoclave conditions	[212]

[214] estimated that nearly 14 billion tonnes of tailings (with particle size less than 120 μm) are produced globally every year, necessitating the development of strategies for effectively disposing of these mine tailings. Several studies have demonstrated that mine tailings can be used as a precursor for producing alkali-activated materials [215–218]. However, prior processing, such as drying and grinding, may be necessary before the mine tailings can be used for producing alkali activated materials. The physical and chemical characteristics of the mine tailings will depend on the mineral source, extraction techniques used, and efficiency. X-ray diffraction analyses indicate that phyllosilicates, quartz and carbonates form the significant constituents of mine tailings [215]. The diverse chemical compositions observed in different types of mine

tailings (i.e. gold, iron, bauxite, copper, etc.) have been compiled by Lazorenko et al. [219] in their review on the applicability of utilizing mine tailings for alkali activation. The variations in the chemical compositions also suggest that mine tailings would be suitable as a secondary precursor in combination with other precursors like fly ash, blast furnace slag, and metakaolin. Considering the wide variations in chemical and mineralogical composition of the mine tailings based on their origin, accurate characterisation is critical while developing the mix designs for alkali activation. Since mine tailings mainly contain crystalline low reactive phases in most cases, pre-treatment may be required to increase the reactivity of the mine tailings [220].

Pre-treatment strategies such as mechanochemical activation or heat treatment can improve the reactivity of mine tailings. Mechano-chemical activation can induce structural disorder and increase the reactivity of mine tailings. Niu et al. [221] observed that mechanochemical activation using a vibrator disc mill successfully induced amorphisation in phosphate mine tailings containing nearly 65% phlogopite mica. The activated phosphate mine tailings were then used as a secondary precursor in combination with metakaolin to produce alkali-activated materials [222]. It was also reported that the presence of calcium carbonate in the treated mine tailings accelerated the formation of C–(N)–A–S–H binder. The formation of zeolitic phases like natrolite and cancrinite was also observed [223]. Because calcium carbonate is typically observed in many mine tailings [219], the formation of C–(N)–A–S–H can be expected in alkali-activated systems produced using activated mine tailings.

Mechanochemically activated vanadium mine tailings have also been used in combination with metakaolin in the study by Wei et al. [224] to produce AAMs. The improved particle size packing of mine tailings due to ball milling was attributed as the reason behind the improved mechanical and rheological performance of the geopolymers. Thermal activation has also been reported as an effective route for improving the reactivity of different mine-tailings [225]. The optimal temperature for thermal activation will have to be selected based on the mineralogy of the mine tailings due to the possible recrystallisation of amorphous phases at high temperatures.

The calcination process results in the activation of alumino-silicate minerals present in the mine tailings, such as kaolinite, which transforms into reactive amorphous metakaolin due to thermal treatment. The formation of CaO and MgO from the thermal decomposition of calcite and dolomite (if present) can aid the dissolution of Si and Al, improving the performance of alkali-activated materials [226]. Thermal treatment was reported to be ineffective in increasing the reactivity of Lithium mine tailings [226].

5 Non-kaolinitc Clays

5.1 Clays

Clay minerals are also known as phyllosilicates because they have a silicate layer structure consisting roughly of alternating sheets of tetrahedral silicon-oxygen and octahedral aluminium-oxygen [227]. There are two main classes of clay minerals based on their structure. The first and most common is 1:1 clay, which consists of one sheet of tetrahedral silicon-oxygen and one sheet of octahedral aluminium hydroxide. The other class 2:1 clays have an octahedral sheet of aluminium-oxygen sandwiched by two tetrahedral sheets of silicon-oxygen. The space between layers is filled by a metallic cation and/or water molecules (Fig. 12). Extended literature on the structure and mineralogy of clay minerals can be found in [228]. The structure of the clay minerals and the calcination temperatures are the primary criteria governing their suitability for alkaline activation [229].

The clay-based alkali-activated materials often involve using the 1:1 clay minerals consisting mainly of kaolinite or halloysite [230]. The 2:1 clay minerals are considered non-conventional precursors because of their low reactivity compared to commonly occurring 1:1 clay minerals once calcined. These have limited their utilization in alkali-activated materials. However, works have been reported to understand and alter their reactivity to develop alkali-activated materials with interesting properties. The most common 2:1 clay minerals that have been investigated for geopolymer

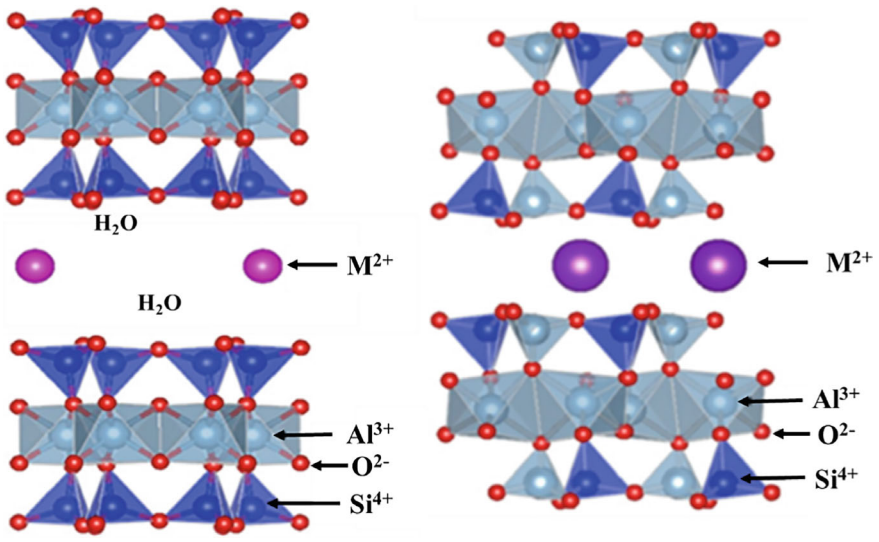


Fig. 12 Three-dimensional visualization of the atomic structure of montmorillonite (left) and illite (right) showing the two layers along with the interlayer containing metallic cation (M) and water molecules. Image obtained using VESTA, adapted from [230]

synthesis involve montmorillonite, $(M^{+y} \cdot H_2O)(Al^{3+}{}_{2-y}Mg^{2+}{}_y)Si^{4+}{}_4O_{10}(OH)_2$ belonging to smectite groups and illite $((K, H_3O)Al_2[(H_2O, OH)_2(Si, Al)_4O_{10}])$ from interlayer-deficient mica group. The atomic structure of these two groups of minerals is depicted in Fig. 12. As observed, 2:1 clays have a layer structure wherein each layer is composed of one octahedral sheet between two tetrahedral sheets. The main difference resides in the composition of the interlayer. Montmorillonite can host various interlayer divalent or monovalent cations (M), including Ca^{2+}, Na^+, Mg^{2+}, K^+, and Sr^{2+}, together with water molecules. The latter gives swelling properties to montmorillonite and justifies its other name as expandable clay. Compared to montmorillonite, illite has only K^+ and lowers exchangeable cation capacity, resulting in a smaller interlayer space [228]. The alkaline activation process on un-calcined montmorillonite and illite demonstrated that the interlayer characteristic also leads to different reactivity in alkaline solution [231]. The latter investigation stressed that alkali-activated montmorillonite leads to good material with phases having polymeric structure and including N–A–S–H or (N, C)–A–S–H. In comparison, illite-based alkali-activated products produce a poor-quality material with no identified geopolymer type phases. Therefore, altering the reactivity of those 2:1 clay is required to develop high-quality materials.

The thermal activation of 2:1 clay minerals has been investigated to alter their reactivity for alkali activation. Here, the mechanism involves the removal of water (dehydration), followed by the elimination of hydroxyl groups of the clay minerals (dehydroxylation), leading to an increase in structural disorder. This is followed by a recrystallization of the amorphous phase as the temperature rises [232]. So, a suitable temperature range must be applied to get the most reactive 2:1 calcined clay. The reactivity in an alkaline medium of thermally activated 2:1 clay containing mainly illite with few smectites at different temperatures has been reported [233]. It was shown that the amount of Al released is optimum at 750 °C and decreases with the rising calcination temperature due to the recrystallization.

Dietel et al. [234] showed that the specific surface area and the solubility rate of Si and Al were also reduced with the increase of the calcination temperature of illite clays from 600 to 925 °C. However, the optimum compressive strength (20 MPa) was achieved with a calcination temperature of 875 °C after 180 days. Further work showed that though the calcination of smectite clay at 750 °C led to partial decomposition of smectite mineral, the resulting alkali-activated materials have developed appealing compressive strength of up to 29 MPa (after 20 days), without the need for high-temperature curing [235]. In addition to the calcination temperature, some authors reported that the calcination of illite and illite-containing smectite is also influenced by the calcination atmosphere [236]. The clays calcined in a reducing atmosphere result in a more intensive dissolution of Si and Al and condensation during alkali activation than in an oxidizing atmosphere at the same temperature. Even after calcination, the reactivity of 2:1 clays remains lower with the limited mechanical performance of their relative alkali-activated products when cured at room temperature (25 °C). Thus, the dissolution and condensation reaction of the calcined illite-smectite rich clay was accelerated by the curing temperature (up to 75 °C) of the binder, which led to almost 80% and 70% improvement of the

dissolution of Si and Al, respectively, within 24 h out of the 168 h of the reaction time [237].

Mechanochemical activation is another method that can be applied to enhance the reactivity of 2:1 clays for its use as precursors for alkaline-activated materials production. It is a high-energy milling process through which structural and chemical changes are triggered by a mechanical impact [238]. The mechanochemical activation of montmorillonite led to a reduced content of Al in six-fold coordination from 100 to 35.4%, while the Al in four-fold coordination increased from zero to 64.6%, compared with the untreated material [239]. Moreover, work demonstrated that mechanochemical activation also increased the specific surface area of montmorillonite, and the extent of the structural change mainly depends on the nature of the interlayer cation [240]. MacKenzie et al. [241] were unsuccessful in producing alkali-activated materials with uncalcined montmorillonite, and showed that even after calcination at 800 °C, the dehydroxylated product could still not give a viable geopolymer. However, applying the mechanochemical process for up to 60 h successfully disrupted the montmorillonite's crystalline 2:1 layer lattice structure and led to a strong geopolymer binder. It was also reported [242] the benefit of the mechanical and thermal activation of carbonate-high illite clay on achieving a binder with a 2-day compressive strength of more than 20 MPa, and 28 days strength of over 30 MPa.

5.2 Low Purity Clays

Low-purity clays consist of the clay minerals that have been altered during weathering of the parent rock with the inclusion of associated minerals [243], therefore containing less than 40% of clay minerals. The most common associated minerals include free iron oxide or iron hydroxide minerals, amorphous silica and alumina, quartz grain, limestone, gypsum, and other more soluble salts [244]. These associated minerals may adversely affect clay reactivity for use in alkali-activated materials. Rahman et al. [245] reported an improvement in the mechanical performance of a low-purity clay after pre-treatment under two calcination methodologies involving low-temperature (120 °C and 5 h) and high-temperature regimes (24 h heating at 750 °C). The clay contained 19.6 wt.% of illite and 21.3 wt.% of kaolinite, whose quantity decreased to 6.3 wt.% and 8.8 wt.%, respectively, after low-temperature calcination. In contrast, all the crystalline clay minerals were seen to transform into amorphous phases after high-temperature calcination except muscovite. The alkali activation of low-grade clay containing 3.4% kaolinite (1:1 clay mineral) and 5.7 wt.% of muscovite (2:1 clays mineral) was carried out in clays pre-treated via mechanical activation. The latter was beneficial for enhancing the amorphous phase content and specific surface area of the clays, enabling production of alkali-activated cements with an optimum 7-d compressive strength of 35 MPa [246].

Another group of low-purity clay includes iron-rich clay, including lateritic soils, which have been extensively investigated (Table 10) [248–253]. Lateritic soils are predominantly distributed in the tropical and sub-tropical regions of the world

(Fig. 13) [254], and therefore, significant efforts have been made in these regions to understand the alkali-activation potential of lateritic soils [254]. The presence of iron results in a characteristic red colour for the alkali-activated materials produced from lateritic soils (Fig. 14).

Lateritic soils consist of clay minerals where aluminium in the octahedral sheet has been partially substituted by iron, modifying the sheet constituting the layers of clay minerals [247]. This leads to a distortion of the crystal structure and significant changes in the mineralogy. Due to the structural change mentioned, the calcination of lateritic soils at temperatures up to 500 °C is sufficient to achieve a chemical reactivity that can be benchmarked to metakaolin [256]. Alkaline activation of lateritic soils containing 34 wt.% of kaolinite and 2 wt.% of illite developed geopolymers with a 28-day compressive strength of 50 MPa [257]. The binder phase is mainly a network of poly-ferro-sialate (N–F(A)–S–H) instead of the polysialate network (N–A–S–H) typically obtained in metakaolin-based geopolymer. It has also been proved that the presence of iron in the reacted product is responsible for the higher compression strength achieved with iron-rich clays [258].

Lemougna et al. [259] used ^{57}Fe Mössbauer spectroscopy to investigate the fate of iron-bearing minerals (augite and ferroan forsterite) in two volcanic ash precursors before and after alkali activation using NaOH (Fig. 15). A decrease in the Fe(II) intensities and a corresponding increase in Fe(III) intensities were observed for both volcanic ashes resulting from the oxidation of Fe(II), indicating the participation of iron in the alkali-activation process. However, only augite was seen to react in these systems, with ferroan forsterite remaining unreactive. This suggests that iron's reactivity could also depend on the type of iron-bearing minerals present in the precursors. A homogenous distribution of iron was also observed throughout the microstructure determined by SEM elemental analysis [259], further indicating the presence of the new ferric sites in the gel phase. Mössbauer spectroscopy [260] on alkali-activated iron-rich slags further confirms the presence of Fe^{2+} and Fe^{3+} in the binder phase, with the first band of Fe^{3+} band forming after 6 h of reaction, with Fe^{3+} in tetrahedral coordination in the silicate framework.

Table 10 reports an overview of the mix designs and curing conditions adopted in the development of alkali-activated lateritic clays. It can be seen the variety of minerals that can be present in such soils and due to relatively low reactivity, high-temperature curing has often been adopted.

5.3 Diatomaceous Earth

Diatomaceous Earth, or diatomite, is a naturally occurring silica source formed from the siliceous skeletal remnants of marine microorganisms (Fig. 16) [267]. Due to its primarily amorphous nature, several studies have investigated the potential of using diatomite as pozzolanic material to partially replace Portland cement [268–271]. In addition to amorphous silica, crystalline phases such as muscovite, quartz, feldspar and kaolinite have been reported in diatomaceous earth [272]. Arbi et al. [273] tried

Table 10 Summary of mix designs used for alkali-activation of lateritic soil

Precursor	Mineralogy	Other additives	Processing	Activator	Curing conditions	References
Laterite	Quartz, Hematite, Ilmenite, Maghemite, Illite, Iron aluminium oxide	Volcanic Ash	Calcined at 700 °C for 4 h	Sodium hydroxide + Sodium Silicate	Room temperature	[261]
Laterite	Kaolinite, Quartz, Hematite, goethite, Ilmenite, Maghemite	–	Calcined at 600 °C for 4 h	Sodium hydroxide + Sodium Silicate	Room temperature	[262]
Laterite	–	–	Calcined at 750 °C for 4 h	Sodium hydroxide + Sodium Silicate	70 °C for 2 h	[263]
Laterite acid leaching residue	Quartz, Willemsite, Lizrdite, Hematite, Goethite, Clinochlore	Metakaolin	Laboratory column leaching test of greek laterite with H_2SO_4	Sodium hydroxide + Sodium Silicate	40, 60, and 80 °C for 24 or 48 h	[264]
Laterite	Kaolinite, Quartz, Hematite, Goethite, Ilmenite, Rutile, Maghemite, Lepidocrocite	–	500, 600, and 700 °C for 4 h	Sodium hydroxide + Sodium Silicate	25 ± 3 °C for 24 h	[256]
Laterite	Kaolinite, Quartz, Hematite, gibbsite	Metakaolin, Basalt powder	700 °C for 4 h	Sodium hydroxide + Rice husk Ash	Room temperature	[265]

(continued)

Table 10 (continued)

Precursor	Mineralogy	Other additives	Processing	Activator	Curing conditions	References
Laterite	Quartz, Kaolinite, Hematite, Sodium Aluminum Silicate hydrate	–	Sodium hydroxide directly mixed with NaOH and cured at different temperatures	Sodium hydroxide	Half of the samples cured 60, 90 °C or 105 °C for 7 days; other half t 250, 450 and 550 °C	[266]
Laterite	Illite, Kaolinite, Goethite, Gibbsite, Hematite, anatase	Sugarcane Bagasse fibre	700 °C for 4 h	Sodium hydroxide + Sodium Silicate	Room temperature	[257]

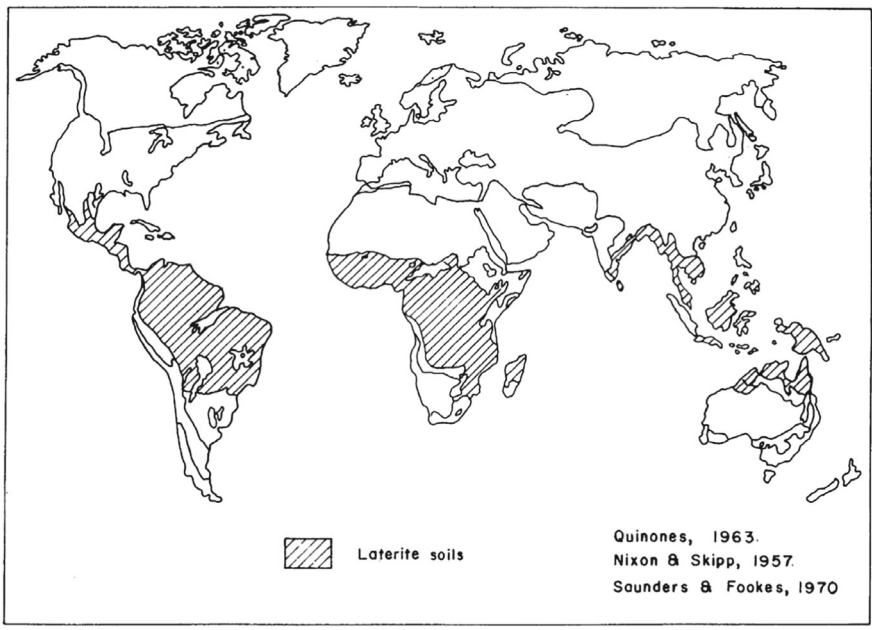


Fig. 13 Distribution of lateritic soil across the world. Fig adapted from [247]

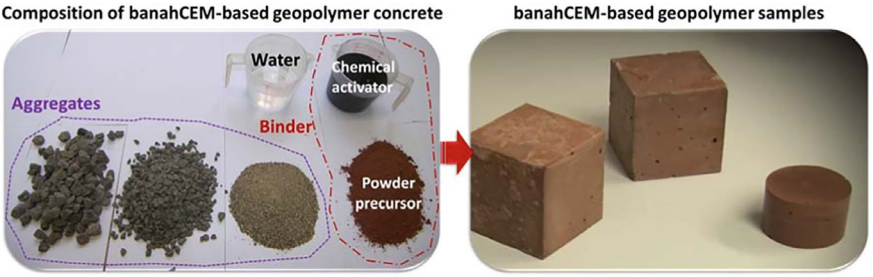


Fig. 14 Alkali-activated concrete produced from lateritic clay precursor [255]. The characteristic red colour is due to the presence of iron-bearing minerals in the precursor

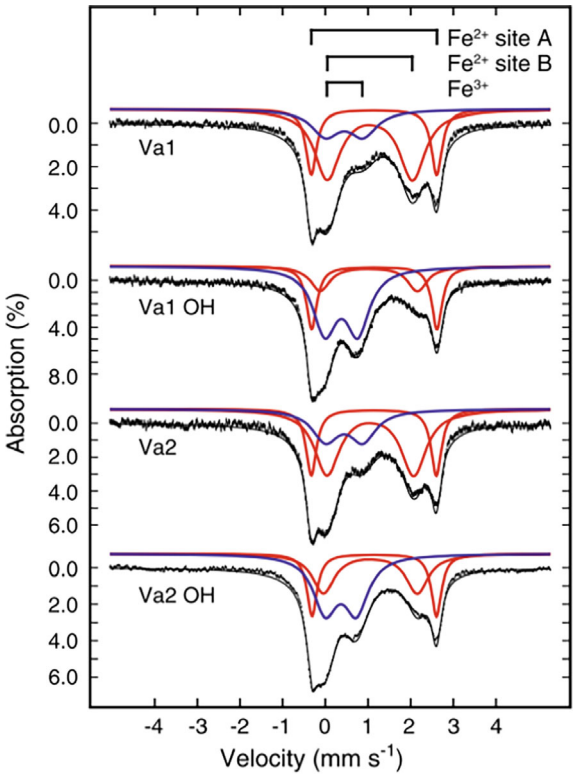


Fig. 15 Mössbauer spectra of the two iron-bearing volcanic-ash precursors before (Va1 and Va2) and after alkali-activation using NaOH (Va1 OH and Va2 OH). Spectra measured at room temperature. Fig from [259]

to combine diatomaceous earth (80%) with calcium aluminate cements (20%) using sodium sulphate and sodium hydroxide as activators with the reactivity of diatomaceous earth seen to increase at higher alkalinity. Chemically, the diatomaceous earth can be considered to be similar to Rice Husk Ash since it does not contain sufficient quantities of reactive alumina to be used as a precursor for producing alkali-activated materials and, therefore, would be more suitable as an alternate source for producing

alkaline activators. Font et al. [274] utilised diatomaceous earth to replace water glass to produce alkali-activated materials from fluid cracking catalysts but observed it to be less reactive when compared to rice husk ash.

Similarly, Adesanya et al. [275] used diatomaceous as a silica source for activating ladle slag. The setting times and compressive strengths of the fly ash/metakaolin alkali-activated cements depended on the nature of the silicate source used as an activator [276]. An increase in setting times and a decrease in the compressive strengths were observed in the presence of diatomaceous earth compared to conventional sodium silicate activator (Fig. 17). The observed variations were attributed to the differences in the rate of silicate dissolution from the diatomaceous earth compared to sodium silicate.

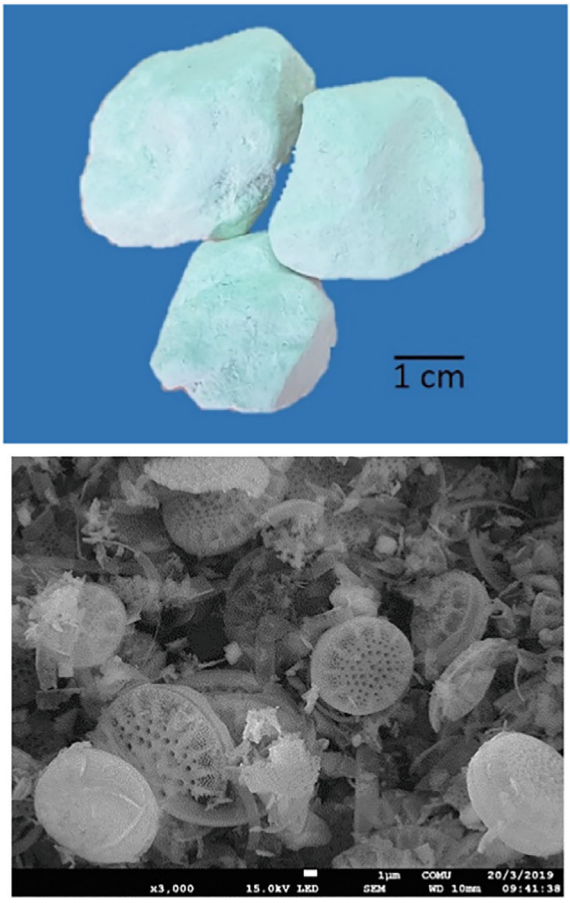


Fig. 16 **a** Photograph of a naturally occurring diatomaceous earth, and **b** Scanning electron micrograph of a diatomaceous earth. Images from [272]

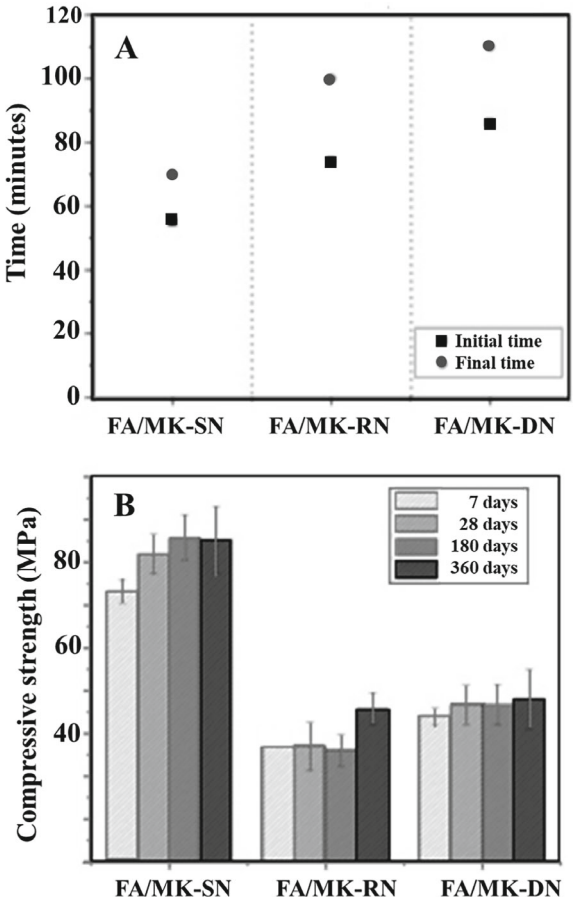


Fig. 17 **a** Setting times of fly ash-metakaolin (70FA/30MK) geopolymers made with diatomaceous earth (DN), sodium silicate (SN) and rice husk ash (RN) as activators and **b** Compressive strength of fly ash-metakaolin (70FA/30MK) geopolymers made with diatomaceous earth (DN), sodium silicate (SN) and rice husk ash (RN) as activators. Data from [276]

5.4 Sewage Sludge Ash

Sewage sludge is a heterogeneous by-product of wastewater treatment plants [277]. It is estimated that nearly 11 million tonnes of sewage sludge is generated annually in Europe [278]. The annual sewage sludge production is expected to increase as more wastewater treatment plants are being set up around the world. Sewage sludge ash is generated by the incineration of dewatered sewage sludge (Fig. 18). During the incineration process, the organic contents present in the sewage sludge are removed, leaving behind the ash residue containing fine granular inorganic minerals. The specific gravity of the SSA depends on the incineration temperature and can range from 1.8 to 2.9 [279]. Additional grinding may be often necessary due to the coarser particle size distribution of the sewage sludge ash [279].

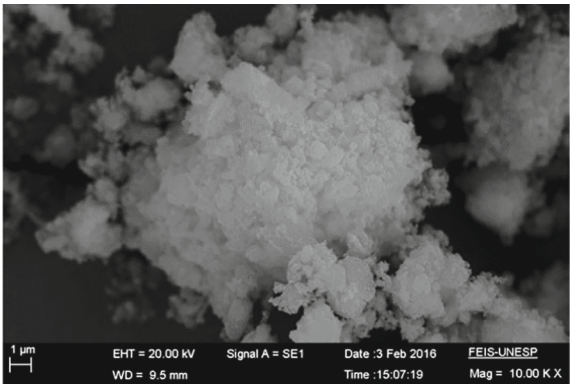


Fig. 18 Scanning electron micrograph of sewage sludge ash. Fig from [288]

Cyr et al. [280] reviewed the chemical and mineralogical compositions of sewage sludge ashes reported in the literature for potential application as a pozzolanic material (Table 11). Silicon, aluminium, calcium, iron and phosphorus are the main elements typically found in sewage sludge ash [281]. Toxic heavy metals like cadmium, zinc, lead, barium and nickel can also be present in the sewage sludge ash [280, 282]. Hence, it is important to consider the potential leaching of these heavy metals when considering potential routes for valorisation. Alkali-activated materials are very effective in waste immobilisation [283], and using SSA as a co-binder with conventional precursor to produce alkali-activated materials can ensure immobilisation of the heavy metals from SSA [284]. Alumina (Al_2O_3) and silica (SiO_2) account for less than 50 wt.% of the chemical composition. The variations in chemical compositions reported for the sewage sludge ash from different sources reiterate the importance of accurately characterising the ashes before they can be used as precursors. The amorphous content in the SSA varied from 0 wt.% (undetected by XRD) [285] to 74 wt.% [286]. Quartz is the main crystalline phase frequently observed in SSA, followed by calcite and hematite [287]. Other minerals like calcium phosphates, feldspars and micas have also been reported [280].

Tashima et al. [288] produced alkali-activated materials cured at room temperature using a combination of blast furnace slag and SSA using sodium hydroxide as the activator. Replacing 20 wt.% of the slag with SSA improved the mechanical properties of the mix. Istuque et al. [289] used SSA to substitute 10% of the metakaolin precursor for producing geopolymers using sodium silicate and sodium hydroxide as activators and cured at 65 °C. Similar compressive strengths (50 MPa) were reported for 0 wt.% SSA, and 10 wt.% SSA mixes after 14 days. However, a delay in the hardening process was observed when SSA was used. Yamaguchi and Ikeda [290] have also reported a similar delay in setting while preparing geopolymers with SSA as a sole precursor. Steam curing at 80 °C was seen to improve the rate of strength development in SSA geopolymers.

Table 11 The mean chemical oxide composition of different sewage sludges reported in the literature and compiled by Cyr et al. [280]

Chemical oxide	Mean (wt.%)	Min (wt.%)	Max (wt. %)
Fe_2O_3	9.2	2.1	30
Al_2O_3	14.2	4.4	34.2
SiO_2	36.1	14.4	65
TiO_2	1.1	0.3	1.9
P_2O_5	11.6	0.3	26.7
CaO	14.8	1.1	40.1
Na_2O	0.9	0.01	6.8
SO_3	2.8	0.01	12.4
K_2O	1.3	0.1	3.1
MgO	2.4	0.02	23.4
MnO	0.3	0.03	0.9
LOI	6.1	0.2	41.8

6 Non-conventional Activators

As discussed in Chap. "Conventional Precursors and Activators", the most widely used activators for producing alkali-activated materials are sodium hydroxide and sodium silicate. The use of such alkaline solution presents several challenges such as handling viscous, corrosive, hazardous substances. This raises concerns of safety and health, and has somehow restricted alkali-activated cement production on an industrial scale [291]. Also, the commonly used activators-sodium hydroxide and sodium silicate are produced via energy-intensive manufacturing processes. Alkali silicates are usually produced from carbonate salts and silica via calcination and then dissolute into the water with a controlled ratio, bringing energy consumption and CO_2 emissions [291]. Heath et al. [292] reported that one kg of sodium silicate production could generate about 300 g of CO_2. Therefore, the application of highly alkaline activators, although promotes the development of high strength, might not be the best option for designing carbon–neutral alkali-activated cements for use on an industrial scale. Hence, the production of alkali activators has been identified as a significant environmental impact contributor of alkali-activated materials when their sustainability is determined via life cycle assessment [293, 294].

Using near-neutral activators has been identified as the most promising way to promote the widespread uptake of alkali-activated cements. Sodium carbonate and sodium sulfate are excellent activator candidates due to their large availability in nature and lower pH value compared with hydroxide or silicate activators [295–297]. The near-neutral pH value of these activators significantly solves the handling issue of corrosive substances. Sodium sulfate (Na_2SO_4) can be obtained from mined mirabilite, by-product during HCl production, or silica pigments [297]. Sodium carbonate (Na_2CO_3) is sourced from mined trona or via the Solvay process [298]. Besides, these neutral salts' costs are very competitive compared to sodium silicate

and sodium hydroxide [295]. Therefore, using near-neutral activators adds extra value to the alkali-activated cement, reaching lower environmental and financial costs than Portland cement and conventional alkali-activated cements.

Most studies using near-neutral salts activators have centred in the production of blast furnace slag cements. There are limited studies evaluating the effect in the microstructure and properties of these cements when adding $Ca(OH)_2$ [299], MgO [300] or by blending near neutral salt activators with sodium silicate or hydroxide [9]. Partially substituting blast furnace slag by fly ashes or silicate fume when using near neutral salt activators have also been investigated [301, 302]. Addition of Portland clinker [303] has also been evaluated, however, this would not be discussed in this Chapter.

Other types of alternative alkali-activators are those derived from wastes. Several reviews have been published in recent years about this topic [304, 305]. In general ashes from different sources, as well as waste glass, clinker dust among others wastes, have been used as SiO_2 source for production of sodium silicate solutions, mainly via an alkaline digestion process. Such alternative activators enabled the production of alkali-activated cement with equal or improved mechanical strengths to those obtained when using commercial products [306, 307]. Therefore, this will not be covered in this chapter. Instead, an overview of the most relevant aspects of near-neutral salt activated slag cements are presented in the following sections.

6.1 Sodium Sulfate Activated Cements

Alkali-activated cement using a sodium sulfate activator has not been extensively explored, this because early reports identified that the early and later strength of these systems were not as high as those obtained when using hydroxide or silicate activators, and in some cases, extended setting times limited their potential application to pre-casting. For example, Wang et al. [303] reported that the sodium sulfate activated slag mortar with a 2 M concentration only developed 20 MPa at 28 days. Rashad et al. [297] found that the setting of sodium sulfate activated slag takes over 50 h when using 3% (Na_2O equivalent) Na_2SO_4. Mobasher et al. [296] reported that the induction period of Na_2SO_4-activated slag using 25 wt.% activator is 80 h, and the time can rise to 110 h by using 5 wt.% solutions.

The low heat released in the sodium sulfate activated slag is considered advantageous for application in nuclear waste cementation, but setting time of this material might take several days [296, 308]. The slag fineness and curing temperature used accelerates the slag reaction in Na_2SO_4-activated slag cements [297]. Tan et al. [309] used wet grinding for decreasing the average slag particle size from 18.12 to 3.87 μm, and found that reaction kinetics of alkali-activated cements is effectively accelerated [309]. Promising results also demonstrated that the replacement of blast furnace slag by 10 wt.% limestone can accelerated the reaction kinetics, independently of the chemical composition of the slag [308]. Limestone addition improved the compressive strength due to the refinement of the pore structure and better space filling.

A similar observation was also found with the slag substitution by 5 wt.% limestone in this system [310]. The filler effect of limestone increases the nucleation of binding gel phases and accelerates the reaction kinetics [311, 312] without modifying the phase assemblage of the cements produced.

The chemical composition of the blast furnace slag used also has a significantly influence in the reaction kinetics of sodium sulfate activated slag cements [295]. It has been reported that a slag with a higher Al_2O_3 content is more reactive [308]. Similar results have been reported for sulpersulfated cements whose main secondary reaction product is also ettringite [313]. This is also consistent with recent results evaluating 16 industrial slags using R^3 test showing that the slag with higher Al_2O_3 contents shows higher kinetics of reaction in the first 7 days [314]. However, the trends observed in the sodium sulfate-activated slag cements [315] differ from what has been reported for sodium hydroxide and sodium silicate systems, where a higher Al_2O_3 and reduced MgO contents can lead to a lower degree of slag reaction. This related to the formation of the secondary reaction products hydrotalcite-type phase [316]. The local chemical environments of Al coordination in the glassy phase is also an important factor affect the reactivity of the slag [308, 317]. More detailed work is needed to understand to what extent of slag reactivity is affected due to Al coordination, regardless to other factors (e.g. chemical composition and fineness).

The majority of studies of sodium sulfate activated slag cements are centred in determining the phase assemblage evolution of a single slag source. It has been reported [296, 297, 308] that the main reaction product formed in these cements is an aluminium substituted calcium silicate hydrate phase, with a tobermorite type structure, with a low Ca/Si ratio. The main secondary reaction product, ettringite ($3CaO \cdot Al_2O_3 \cdot 3CaSO_4 \cdot 32H_2O$), is often reported. It has been hypothesised that a layer double hydroxide (LDH) phase is also forming the Na_2SO_4-activated slag cements, as a low intensity shoulder at $\delta_{iso} = \sim 9$ ppm is reported when samples are analysed by ^{27}Al MAS NMR [296, 308], although no reflection associated with this phase is identifiable when analysed by X-ray diffraction. It has been reported that sulfate-intercalated LDHs are poorly crystalline [318], which might explain these findings.

As a means of increasing slag reactivity and compressive strength development of sodium sulfate activated slag cements, the effect of different additives has been evaluated. Wang et al. [303] reported that the compressive strength of sodium sulfate-activated slag increases significantly by adding 5–10 wt.% Ca $(OH)_2$. He et al. [319] observed addition of 6 wt.% reactive MgO in sodium sulfate-activated slag results in the pH value of the cements to 12, along with improvement of compressive strength. Besides, the addition of 6–8 wt.% reactive MgO also reduces the drying shrinkage of this material due to increased degree of slag reaction with more formation of ettringite [320, 321]. Additionally, Yuan et al. [322] used a blended activator comprising Na_2CO_3 and Na_2SO_4 with the 28-compressive strength slightly increasing with at higher contents of Na_2CO_3 in the activator.

Sodium sulfate solution has also been proved to effectively activate other supplementary cementitious materials (SCMs). Addition of 4 wt.% Na_2SO_4 activator (relative to the mass of the cements) to fly ash/slag blended system led to the production of

binders with enhanced early-stage reactive kinetics, and mechanical properties, associated with a compacted pore structure and reduced drying shrinkage [322]. Similar observations were also reported in sulfate-activated materials with high volume of fly ash blended in mortar [323] and concrete [324]. In 70 wt.% calcined clay/30 wt.% calcium hydroxide system the use of 5 wt.% Na_2SO_4 activator significantly promote the early strength of the paste specimens reaching 13 MPa at 3 days curing, linked to the formation of ettringite. It has also been reported [325] that sodium sulfate can be used to activate construction demolition wastes with 10 times lower heat released than ordinary Portland cement (PC), reaching ~31 MPa strength of the paste sample at 28 days and similar strength at 180 d of curing compared to PC.

6.2 Sodium Carbonate Activated Cements

Sodium carbonate was used as alkali-activator in the early development of AAMs in Ukraine in 1960s [326], with many structures standing, prior to the bombing of Mariupol during the Ukraine-Russian war [327]. Interest in the use of this activator declined over the years due to the extended setting times typically developed by these materials. However, in recent years the interest in the use of this activator has re-emerged. Bernal et al. [328] analysed the kinetics of reaction of sodium carbonate-activated slag binders by isothermal calorimetry. Results revealed that the time to reach the acceleration peak was about 130 h when using 8 wt.% of Na_2CO_3 (relative to the amount of slag) and 0.4 of water to solid ratio. This is somehow consistent with Yuan et al. [329], who also found that the acceleration period in Na_2CO_3-activated slag ranged from 67 to 112 h when varying the water/solid ratio and activator dosage. These results are consistent with a belated setting time typically reported in these systems. However, significant advances in understanding the reaction mechanism of these cements have enable to control the reaction kinetics by selecting slags with specific chemical compositions or by adding smart additives.

Ke et al. [330] controlled the kinetics of reaction for sodium carbonate-activated slag by adding 10 wt.% calcined hydrotalcite-type layer double hydroxide and produced pastes that set within the first 24 h. This was associated with the nucleation sites provide by the nano-additive, accelerating the reaction kinetics and aiding formation of hydrotalcite, particularly in systems produced with slags with high MgO contents. The change in the phase assemblage has implication in the durability of such materials. For example, Ke et al. [331] observed that the addition of CLDH increases the carbonation resistance of these materials and enhanced the CO_2 uptake capacity of these cements, without affecting their mechanical strength. Similar results were identified in specimens exposed to chlorides, where the addition of 5 wt.% CLDH significantly densify the microstructure, reducing the chloride diffusion coefficient [332].

The main reaction products forming in sodium carbonate activated slag cements are C–A–S–H type gels with an Al-substituted tobermorite type structure, layer double hydroxides and $CaCO_3$ polymorphs [329]. The formation of calcite, vaterite

and aragonite has been reported in several studies [328–330, 333]. This is associated with the fact that the CO_3^{2-} supplied by the activator is depleted via formation of calcium carbonates. Once that happens the reaction mechanism of sodium carbonated activated slag cement is like that of sodium hydroxide-activated slag cements [328, 330]. In terms of secondary reaction products, double salt gaylussite ($Na_2Ca(CO_3)_2 \cdot 5H_2O$) and zeolite NaA ($Na_{12}Al_{12}Si_{12}O_{48} \cdot 18H_2O$) were observed in the first curing days [328, 329].

The chemical composition of the slag affects the phase assemblage of sodium carbonate activated slag cements. Two types of LDH phases, calcium hemicarboaluminate and hydrotalcite-type phase, have been identified in these systems. A higher MgO content in the slag favours the formation of MgAl-LDH phases, whereas the slag with high Al_2O_3 and low MgO favour the formation of hemicarbonate instead. A mixture of these two-layer double hydroxide phases was also observed in the NaOH-activated slag cements [334, 335]. The hemicarbonate is stable in the first 28 days, but it gradually decreases with the formation of monocarbonate (C_4AcH_{11}) at 90 days [330]. Myers et al. [336] reported that the monocarbonate is thermodynamically stable with hydroxide-intercalated MgAl-LDH phases.

Depending on the activator and slag fineness, the compressive strength of sodium carbonate activated slag cement paste can reach 30–40 MPa at 7 days and increase to 36–56 MPa at 28 days, when mixes are used with 0.4 water/binder ratio, by varying activator dosage from 3 to 5% (equivalent Na_2O by mass of slag) [333]. A similar strength development was also observed in the mortar by Bernal et al. [328] where the compressive strength of Na_2CO_3-activated slag mortar increased dramatically from 10 MPa in 7 days to 30 MPa and then achieved 44 MPa at 56 days, when using 8 wt.% of activator (relative to the mass of slag) and 2:75 of sand: binder ratio [328]. In the concrete level, Abdalqader et al. [300] prepared Na_2CO_3-activated concrete with 1:0.4:1.5:3 of the binder: water: sand: gravel ratio and 10 wt.% of activator (relative to the weight of binder) and found that the compressive strength achieved 35 MPa, 50 MPa, 68 MPa at 7 days, 28 days, and 90 days, respectively.

Other strategies for improving strength development have been considered for sodium carbonate activated slag cements. For example, Shi et al. [337] reported that the strength increases with reduced particle size at an optimum of 400 m^2/kg and then the strength decreases. The 10% replacement of slag by reactive MgO and 0.5% substitution of hydromagnesite particles in sodium carbonate activated slag concrete significantly enhanced the compressive strength reaching about 39 MPa at 28 days of curing compared to the plain sodium carbonate slag concrete with 14 MPa [338]. This was explained by the fact that the addition of MgO promotes the additional consumption of carbonate ions from the activator, increasing alkalinity in the pore solution [338]. The hydromagnesite provides extra nucleation sites, which increase the consumption of carbonate ions leading to increase amount of $CaCO_3$ polymorphs and hydrotalcite-type phases [338].

Sodium carbonate is also an effective activator when using other precursors, beyond blast furnace slag. 5 wt. % Na_2CO_3 activator (relative to total solid mass) addition to a $Ca(OH)_2$-fly ash system led to the development of cements with ~35 MPa at 28 days, which is significantly higher than the sample without adding Na_2CO_3

activator (~10 MPa) or when using 5% NaOH activator (5 MPa) for the same precursors [339]. The use of Na_2CO_3 activator increased the Al substitution in C–A–S–H gel and dissolution rate of the fly ash, producing denser pore structures [339]. The use of Na_2CO_3 also accelerated the reaction kinetics of 75 wt.% slag/25 wt.% fly ash systems, resulting in a compressive strength of ~60 MPa at 28 days with higher Al substitution in C–A–S–H gel compared to using 5% activator dosage (~50 MPa) [302, 340]. Also, 30% replacement of calcined recycled concrete fine in Na_2CO_3-activated slag cements was reported lead to compressive strengths of ~30 MPa at 28 days, and increased activator dosage enhanced the compressive strength and refined pore structure [341].

7 Concluding Remarks

It is clear that alkali-activation offers an important route for the use of several industrial by products, as alkali activated materials can be produced from a variety of precursors beyond blast furnace slag or fly ashes. Therefore, this might be a preferred route for utilization and valorisation of by-products in the near future, as approaches with greater circularity continue being developed and adopted.

The majority of studies in using alternative precursors have centred in optimizing pre-conditioning treatment of such materials to enhance their chemical reactivity, or in optimizing mix designs to control their reaction kinetics. This with the aim to demonstrate that these novel cement formulations can be used as construction materials. So far, the majority of studies have centred in the evaluation of the factors influencing phase assemblage formation. This in an effort to identify the factors that might influence their performance and consequently develop strategies for their property's optimisation. However, general knowledge about different precursor types is rather limited. Studies often are limited to evaluating a single by-product source with specific properties, which makes it difficult to draw general conclusions for other precursors from a similar category of by-product. This because slight changes in physical or chemical properties of such by products can lead to the development of completely different properties. This is a major challenge associated with the nature of alternative precursors.

Given the opportunities and challenges described for the wide variety of non-conventional precursors under investigation, it is reasonable to consider the systems for which research efforts may have most impact. In addition to the scientific aspects of phase assemblage formation, mechanical properties and durability performance, the logistical aspects of material sourcing must also be a key consideration. Alkali-activated material products will most likely be technically and commercially feasible for by-products or wastes which are produced in high volumes at a consistent rate, in centralized (rather than dispersed) industrial processes, and have a relatively consistent or predictable composition. Whilst the design and manufacture of alkali-activated materials from a wide range of non-conventional precursors is a desirable long-term objective, industrial by-products and mining tailings may offer the best opportunity

for a 'breakthrough' into the roster of conventional precursors. There is a limited understanding about the mechanical strength evolution of alkali-activated materials based on alternative precursors with almost no studies evaluating performance of concretes, or their longer-term durability. Therefore, there is great opportunity for continuing the research in these materials to elucidate their suitability in different applications, without being limited to the production of concretes.

Regarding alternative activators, although different combinations are being tested to tailor the chemical composition of alkali-activated materials, near-neutral salts are the most effective alternative to conventional alkali hydroxide and alkali silicate activators. There is significant knowledge in the factors controlling reaction kinetics and properties developed by alkali-activated produced with these activators, to the point that binders with desirable properties can now be effectively designed. However, such knowledge is limited to blast furnace slag-based alkali-activated materials. Effectiveness of such activators when using different precursors remains largely unexplored.

References

1. Scrivener, K.L., John, V.M., Gartner, E.M.: Eco-efficient cements: potential economically viable solutions for a low-CO_2 cement-based materials industry. Cem. Concr. Res. **114**, 2–26 (2018). https://doi.org/10.1016/j.cemconres.2018.03.015
2. Shah, I.H., Miller, S.A., Jiang, D., Myers, R.J.: Cement substitution with secondary materials can reduce annual global CO_2 emissions by up to 1.3 gigatons. Nat. Commun. **30**, **13**(1), 5758 (2022). https://doi.org/10.1038/s41467-022-33289-7
3. Shen, H., Forssberg, E.: An overview of recovery of metals from slags. Waste Manag. **23**, 933–949 (2003). https://doi.org/10.1016/S0956-053X(02)00164-2
4. Marsh, A.T.M., Velenturf, A.P.M., Bernal, S.A.: Circular Economy strategies for concrete: implementation and integration. J. Clean. Prod. **362**, 132486 (2022). https://doi.org/10.1016/j.jclepro.2022.132486
5. Binnemans, K., Jones, P.T., Blanpain, B., Van Gerven, T., Pontikes, Y.: Towards zero-waste valorisation of rare-earth-containing industrial process residues: a critical review. J. Clean. Prod. **99**, 17–38 (2015). https://doi.org/10.1016/j.jclepro.2015.02.089
6. Balomenos, E., Davris, P., Pontikes, Y., Panias, D.: Mud2Metal: lessons learned on the path for complete utilization of bauxite residue through industrial symbiosis. J. Sustain. Metall. **3**, 551–560 (2017). https://doi.org/10.1007/s40831-016-0110-4
7. Van Deventer, J.S.J., Provis, J.L., Duxson, P.: Technical and commercial progress in the adoption of geopolymer cement. Miner. Eng. **29**, 89–104 (2012). https://doi.org/10.1016/j.mineng.2011.09.009
8. Wesseling, J.H., Van der Vooren, A.: Lock-in of mature innovation systems: the transformation toward clean concrete in the Netherlands. J. Clean. Prod. **155**, 114–124 (2017). https://doi.org/10.1016/j.jclepro.2016.08.115
9. Gorgolewski, M.: Designing with reused building components: some challenges. Build. Res. Inf. **36**, 175–188 (2008). https://doi.org/10.1080/09613210701559499
10. Gálvez-Martos, J.L., Styles, D., Schoenberger, H., Zeschmar-Lahl, B.: Construction and demolition waste best management practice in Europe. Resour. Conserv. Recycl. **136**, 166–178 (2018). https://doi.org/10.1016/J.RESCONREC.2018.04.016
11. Cai, G., Waldmann, D.: A material and component bank to facilitate material recycling and component reuse for a sustainable construction: concept and preliminary study. Clean Technol. Environ. Policy **21**, 2015–2032 (2019). https://doi.org/10.1007/S10098-019-01758-1

12. Marinković, S., Josa, I., Braymand, S., Tošić, N.: Sustainability assessment of recycled aggregate concrete structures: a critical view on the current state-of-knowledge and practice. Struct. Concr. **24**, 1956–1979 (2023). https://doi.org/10.1002/suco.202201245
13. Monier, V., Hestin, M., Impériale, A.-C., Prat, L., Hobbs, G., Adams, K., Pairon, M., Roberti de Winghe, M., Wiaux, F., Wahlström, M., Gaillot, O., Ramos, M.: Resource efficient use of mixed wastes: improving management of construction and demolition waste. Final Report (2017). http://ec.europa.eu/environment/waste/studies/pdf/construction/Minutes.pdf
14. Nedeljković, M., Visser, J., Šavija, B., Valcke, S., Schlangen, E.: Use of fine recycled concrete aggregates in concrete: a critical review. J. Build. Eng. **38** (2021). https://doi.org/10.1016/j.jobe.2021.102196
15. Florea, M.V.A., Ning, Z., Brouwers, H.J.H.: Activation of liberated concrete fines and their application in mortars. Constr. Build. Mater. **50**, 1–12 (2014). https://doi.org/10.1016/j.conbuildmat.2013.09.012
16. Braga, M., De Brito, J., Veiga, R.: Reduction of the cement content in mortars made with fine concrete aggregates. Mater. Struct. **47**, 171–182 (2014). https://doi.org/10.1617/s11527-013-0053-1
17. Angulo, S.C., Ulsen, C., John, V.M., Kahn, H., Cincotto, M.A.: Chemical-mineralogical characterization of C&D waste recycled aggregates from São Paulo, Brazil. Waste Manage. **29**, 721–730 (2009). https://doi.org/10.1016/j.wasman.2008.07.009
18. Oksri-Nelfia, L., Mahieux, P.Y., Amiri, O., Turcry, P., Lux, J.: Reuse of recycled crushed concrete fines as mineral addition in cementitious materials. Mater. Struct. **49**, 3239–3251 (2016). https://doi.org/10.1617/s11527-015-0716-1
19. Schoon, J., De Buysser, K., Van Driessche, I., De Belie, N.: Fines extracted from recycled concrete as alternative raw material for Portland cement clinker production. Cem. Concr. Compos. **58**, 70–80 (2015). https://doi.org/10.1016/j.cemconcomp.2015.01.003
20. Kwon, E., Ahn, J., Cho, B., Park, D.: A study on development of recycled cement made from waste cementitious powder. Constr. Build. Mater. **83**, 174–180 (2015). https://doi.org/10.1016/j.conbuildmat.2015.02.086
21. Bordy, A., Younsi, A., Aggoun, S., Fiorio, B.: Cement substitution by a recycled cement paste fine: role of the residual anhydrous clinker. Constr. Build. Mater. **132**, 1–8 (2017). https://doi.org/10.1016/j.conbuildmat.2016.11.080
22. Kalinowska-Wichrowska, K., Kosior-Kazberuk, M., Pawluczuk, E.: The properties of composites with recycled cement mortar used as a supplementary cementitious material. Materials **13**, 64 (2020). https://doi.org/10.3390/ma13010064
23. Nedeljković, M., Visser, J., Nijland, T.G., Valcke, S., Schlangen, E.: Physical, chemical and mineralogical characterization of Dutch fine recycled concrete aggregates: a comparative study. Constr. Build. Mater. **270** (2021). https://doi.org/10.1016/j.conbuildmat.2020.121475
24. Robayo-Salazar, R.A., Rivera, J.F., Mejía de Gutiérrez, R.: Alkali-activated building materials made with recycled construction and demolition wastes. Constr. Build. Mater. **149**, 130–138 (2017). https://doi.org/10.1016/j.conbuildmat.2017.05.122
25. Bassani, M., Tefa, L., Russo, A., Palmero, P.: Alkali-activation of recycled construction and demolition waste aggregate with no added binder. Constr. Build. Mater. **205**, 398–413 (2019). https://doi.org/10.1016/j.conbuildmat.2019.02.031
26. Villaquirán-Caicedo, M.A., Mejía de Gutiérrez, R.: Comparison of different activators for alkaline activation of construction and demolition wastes. Constr. Build. Mater. **281** (2021). https://doi.org/10.1016/j.conbuildmat.2021.122599
27. Borrachero, M.V., Payá, J., Brito, S., Segura, Y.P., Soriano, L., Tashima, M.M., Monzó, J.M.: Reusing construction and demolition waste to prepare alkali-activated cement. Materials **15**,(2022). https://doi.org/10.3390/ma15103437
28. Allahverdi, A., Kani, E.N.: Use of construction and demolition waste (CDW) for alkali-activated or geopolymer cements. In: Handbook of Recycled Concrete and Demolition Waste, pp. 439–475 Elsevier (2013)
29. Komnitsas, K., Zaharaki, D., Vlachou, A., Bartzas, G., Galetakis, M.: Effect of synthesis parameters on the quality of construction and demolition wastes (CDW) geopolymers. Adv. Powder Technol. **26**, 368–376 (2015). https://doi.org/10.1016/j.apt.2014.11.012

30. Tefa, L., Bassani, M., Coppola, B., Palmero, P.: Strength development and environmental assessment of alkali-activated construction and demolition waste fines as stabilizer for recycled road materials. Constr. Build. Mater. **289**, 123017 (2021). https://doi.org/10.1016/j.conbuildmat.2021.123017
31. Sun, C., Chen, L., Xiao, J., Singh, A., Zeng, J.: Compound utilization of construction and industrial waste as cementitious recycled powder in mortar. Resour. Conserv. Recycl. **170**, 105561 (2021). https://doi.org/10.1016/j.resconrec.2021.105561
32. Mahmoodi, O., Siad, H., Lachemi, M., Dadsetan, S., Sahmaran, M.: Development of normal and very high strength geopolymer binders based on concrete waste at ambient environment. J. Clean. Prod. **279**, 123436 (2021). https://doi.org/10.1016/j.jclepro.2020.123436
33. Ahmari, S., Ren, X., Toufigh, V., Zhang, L.: Production of geopolymeric binder from blended waste concrete powder and fly ash. Constr. Build. Mater. **35**, 718–729 (2012). https://doi.org/10.1016/j.conbuildmat.2012.04.044
34. Alhawat, M., Ashour, A., Yildirim, G., Aldemir, A., Sahmaran, M.: Properties of geopolymers sourced from construction and demolition waste: a review. J. Build. Eng. **50**, 104104 (2022). https://doi.org/10.1016/j.jobe.2022.104104
35. Wong, C.L., Mo, K.H., Alengaram, U.J., Yap, S.P.: Mechanical strength and permeation properties of high calcium fly ash-based geopolymer containing recycled brick powder. J. Build. Eng. **32**, 101655 (2020). https://doi.org/10.1016/j.jobe.2020.101655
36. Huo, W., Zhu, Z., Chen, W., Zhang, J., Kang, Z., Pu, S., Wan, Y.: Effect of synthesis parameters on the development of unconfined compressive strength of recycled waste concrete powder-based geopolymers. Constr. Build. Mater. **292**, 123264 (2021). https://doi.org/10.1016/j.conbuildmat.2021.123264
37. Mahmoodi, O., Siad, H., Lachemi, M., et al.: Development of ceramic tile waste geopolymer binders based on pre-targeted chemical ratios and ambient curing. Constr. Build. Mater. **258**, 120297 (2020). https://doi.org/10.1016/j.conbuildmat.2020.120297
38. Ahmari, S., Zhang, L.: Production of eco-friendly bricks from copper mine tailings through geopolymerization. Constr. Build. Mater. **29**, 323–331 (2012). https://doi.org/10.1016/j.conbuildmat.2011.10.048
39. Tuyan, M., Andiç-Çakir, Ö., Ramyar, K.: Effect of alkali activator concentration and curing condition on strength and microstructure of waste clay brick powder-based geopolymer. Compos. B Eng. **135**, 242–252 (2018). https://doi.org/10.1016/j.compositesb.2017.10.013
40. Vásquez, A., Cárdenas, V., Robayo, R.A., Mejia de Gutiérrez, R.: Geopolymer based on concrete demolition waste. Adv. Powder Technol. **27**, 1173–1179 (2016). https://doi.org/10.1016/j.apt.2016.03.029
41. Hwang, C.L., Yehualaw, M.D., Vo, D.H., Huynh, T.P., Largo, A.: Performance evaluation of alkali activated mortar containing high volume of waste brick powder blended with ground granulated blast furnace slag cured at ambient temperature. Constr. Build. Mater. **223**, 657–667 (2019). https://doi.org/10.1016/j.conbuildmat.2019.07.062
42. Vafaei, M., Allahverdi, A.: Strength development and acid resistance of geopolymer based on waste clay brick powder and phosphorous slag. Struct. Concr. **20**, 1596–1606 (2019). https://doi.org/10.1002/suco.201800138
43. Sun, Z., Cui, H., An, H., Tao, D., Xu, Y., Zhai, J., Li, Q.: Synthesis and thermal behavior of geopolymer-type material from waste ceramic. Constr. Build. Mater. **49**, 281–287 (2013). https://doi.org/10.1016/j.conbuildmat.2013.08.063
44. Part, W.K., Ramli, M., Cheah, C.B.: An overview on the influence of various factors on the properties of geopolymer concrete derived from industrial by-products. Constr. Build. Mater. **77**, 370–395 (2015). https://doi.org/10.1016/j.conbuildmat.2014.12.065
45. Akduman, Ş, Kocaer, O., Aldemir, A., Şahmaran, M., Yıldırım, G., Almahmood, H., Ashour, A.: Experimental investigations on the structural behaviour of reinforced geopolymer beams produced from recycled construction materials. J. Build. Eng. **41**, 102776 (2021). https://doi.org/10.1016/j.jobe.2021.102776
46. Aldemir, A., Akduman, S., Kocaer, O., Aktepe, R., Sahmaran, M., Yildirim, G., Almahmood, H., Ashour, A.: Shear behaviour of reinforced construction and demolition waste-based

geopolymer concrete beams. J. Build. Eng. **47**, 103861 (2022). https://doi.org/10.1016/j.jobe.2021.103861
47. HM Revenue and Customs.: Slag wool, rock wool and similar mineral wools and mixtures—Including intermixtures thereof, in bulk, sheets or rolls (2020). https://www.uktradeinfo.com/commodities/68061000
48. Huuhka, S.: Demolished buildings: empirical evidence on types, ages and construction materials. In: Proceeding of CESB 2016—Central Europe Towards Sustainable Building 2016: Innovations for Sustainable Future, pp. 1105–1112. Czech Technical University, Prague (2016)
49. Yliniemi, J., Ramaswamy, R., Luukkonen, T., Laitinen, O., de Sousa, Á.N., Huuhtanen, M., Illikainen, M.: Characterization of mineral wool waste chemical composition, organic resin content and fiber dimensions: aspects for valorization. Waste Manag. **131**, 323–330 (2021). https://doi.org/10.1016/j.wasman.2021.06.022
50. Sattler, T., Sartori, M., Galler, R., Pomberger, R., Krainz, J., Schimek, J., Vollprecht, D.: Effects of cement addition and briquetting of rock wool on its geomechanical stability in landfills. Waste Manag. Res. **38**, 408–414 (2020). https://doi.org/10.1177/0734242X20906876
51. Kowatsch, S.: Mineral wool insulation binders. In: Phenolic Resins: a Century of Progress, pp. 209–242. Springer, Berlin Heidelberg (2010)
52. Yliniemi, J., Laitinen, O., Kinnunen, P., Illikainen, M.: Pulverization of fibrous mineral wool waste. J. Mater. Cycles Waste Manag. **20**, 1248–1256 (2018). https://doi.org/10.1007/s10163-017-0692-3
53. Yliniemi, J., Walkley, B., Provis, J.L., Kinnunen, P., Illikainen, M.: Influence of activator type on reaction kinetics, setting time, and compressive strength of alkali-activated mineral wools. J. Therm. Anal. Calorim. **144**, 1129–1138 (2021). https://doi.org/10.1007/s10973-020-09651-6
54. Yliniemi, J., Walkley, B., Provis, J.L., Kinnunen, P., Illikainen, M.: Nanostructural evolution of alkali-activated mineral wools. Cem. Concr. Compos. **106**, 103472 (2020). https://doi.org/10.1016/j.cemconcomp.2019.103472
55. Lemougna, P.N., Adediran, A., Yliniemi, J., et al.: Effect of organic resin in glass wool waste and curing temperature on the synthesis and properties of alkali-activated pastes. Mater. Des. **212**, 110287 (2021). https://doi.org/10.1016/j.matdes.2021.110287
56. Pavlin, M., Horvat, B., Češnovar, M., Ducman, V.: The preparation and characterization of low-temperature foams based on the alkali activation of waste stone wool. Ceram. Int. **48**, 17668–17681 (2022). https://doi.org/10.1016/j.ceramint.2022.03.037
57. Mastali, M., Zahra, A., Hugo, K., Faraz, R.: Utilization of mineral wools in production of alkali activated materials. Constr. Build. Mater. **283**, 122790 (2021). https://doi.org/10.1016/j.conbuildmat.2021.122790
58. Li, Z., Beltran, I.A., Chen, Y., Šavija, B., Ye, G.: Early-age properties of alkali-activated slag and glass wool paste. Constr. Build. Mater. **291**, 123326 (2021). https://doi.org/10.1016/j.conbuildmat.2021.123326
59. Sgarlata, C., Dal Poggetto, G., Piccolo, F., Catauro, M., Traven, K., Češnovar, M., Nguyen, H., Yliniemi, J., Barbieri, L., Ducman, V., Lancellotti, I.: Antibacterial properties and cytotoxicity of 100% waste derived alkali activated materials: slags and stone wool-based binders. Front. Mater. **8**, 1–15 (2021). https://doi.org/10.3389/fmats.2021.689290
60. Pavlin, M., Horvat, B., Ducman, V.: Preparation of façade panels based on alkali-activated waste mineral wool, their characterization, and durability aspects. Int. J. Appl. Ceram. Technol. **19**, 1227–1234 (2022). https://doi.org/10.1111/ijac.13998
61. Łaźniewska-Piekarczyk, B., Czop, M., Smyczek, D.: The comparison of the environmental impact of waste mineral wool and mineral in wool-based geopolymer. Materials **15**, 2050 (2022). https://doi.org/10.3390/ma15062050
62. König, K., Traven, K., Pavlin, M., Ducman, V.: Evaluation of locally available amorphous waste materials as a source for alternative alkali activators. Ceram. Int. **47**, 4864–4873 (2021). https://doi.org/10.1016/j.ceramint.2020.10.059

63. Kinnunen, P., Yliniemi, J., Talling, B., Illikainen, M.: Rockwool waste in fly ash geopolymer composites. J. Mater. Cycles Waste Manag. **19**, 1220–1227 (2017). https://doi.org/10.1007/s10163-016-0514-z
64. Yliniemi, J., Kinnunen, P., Karinkanta, P., Illikainen, M.: Utilization of mineral wools as alkali-activated material precursor. Materials **9**, 312 (2016). https://doi.org/10.3390/ma9050312
65. Erofeev, V.T., Rodin, A.I., Yakunin, V.V., Bogatov, A.D., Bochkin, V.S., Chegodajkin, A.M.: Alkali-activated slag binders from rock-wool production wastes. Mag. Civil Eng. **82**, 219–227 (2018). https://doi.org/10.18720/MCE.82.20
66. Alzaza, A., Mastali, M., Kinnunen, P., et al.: Production of lightweight alkali activated mortars using mineral wools. Materials **12**(10), 1695 (2019). https://doi.org/10.3390/MA12101695
67. Yliniemi, J., Luukkonen, T., Kaiser, A., Illikainen, M.: Mineral wool waste-based geopolymers. IOP Conf. Ser.: Earth Environ. Sci. **297**, 012006 (2019). https://doi.org/10.1088/1755-1315/297/1/012006
68. Nguyen, H., Kaas, A., Kinnunen, P., Carvelli, V., Monticelli, C., Yliniemi, J., Illikainen, M.: Fiber reinforced alkali-activated stone wool composites fabricated by hot-pressing technique. Mater. Des. **186**, 108315 (2020). https://doi.org/10.1016/j.matdes.2019.108315
69. Pavlin, M., Frankovič, A., Horvat, B., Ducman, V.: Optimization of alkali-activated mineral wool mixture for panel production. In: Proceedings of the 3rd RILEM Spring Convention and Conference (RSCC 2020) Volume 4: Shift to a Circular Economy 3, pp. 143–153. Springer International Publishing (2021)
70. Pavlin, M., Horvat, B., Frankovič, A., Ducman, V.: Mechanical, microstructural and mineralogical evaluation of alkali-activated waste glass and stone wool. Ceram. Int. **47**, 15102–15113 (2021). https://doi.org/10.1016/j.ceramint.2021.02.068
71. Martirena, F., Monzó, J.: Vegetable ashes as supplementary cementitious materials. Cem. Concr. Res. **114**, 57–64 (2018). https://doi.org/10.1016/j.cemconres.2017.08.015
72. Freire, A.L., Moura-Nickel, C.D., Scaratti, G., De Rossi, A., Araújo, M.H., Júnior, A.D., Rodrigues, A.E., Castellón, E.R., Moreira, R.D.: Geopolymers produced with fly ash and rice husk ash applied to CO_2 capture. J. Clean. Prod. **273** (2020). https://doi.org/10.1016/j.jclepro.2020.122917
73. Sousa, L.N., Figueiredo, P.F., França, S., de Moura Solar Silva, M.V., Borges, P.H., Bezerra, A.C.: Effect of non-calcined sugarcane bagasse ash as an alternative precursor on the properties of alkali-activated pastes. Molecules **27**, 1–18 (2022). https://doi.org/10.3390/molecules27041185
74. Nadziri, N., Ismail, I., Hamdan, S.: Binding gel characterization of alkali-activated binders based on palm oil fuel ash (POFA) and fly ash. J. Sustain. Cem.-Based Mater. **7**, 1–14 (2018). https://doi.org/10.1080/21650373.2017.1299054
75. Deepika, S., Anand, G., Bahurudeen, A., Santhanam, M.: Construction products with sugarcane bagasse ash binder. J. Mater. Civ. Eng. **29**, 04017189 (2017). https://doi.org/10.1061/(asce)mt.1943-5533.0001999
76. Matalkah, F., Soroushian, P., Balchandra, A., Peyvandi, A.: Characterization of alkali-activated nonwood biomass ash-based geopolymer concrete. J. Mater. Civ. Eng. **29**, 04016270 (2017). https://doi.org/10.1061/(asce)mt.1943-5533.0001801
77. Van Tuan, N., Ye, G., Van Breugel, K., Copuroglu, O.: Hydration and microstructure of ultra high performance concrete incorporating rice husk ash. Cem. Concr. Res. **41**, 1104–1111 (2011). https://doi.org/10.1016/j.cemconres.2011.06.009
78. Zareei, S.A., Ameri, F., Bahrami, N.: Microstructure, strength, and durability of eco-friendly concretes containing sugarcane bagasse ash. Constr. Build. Mater. **184**, 258–268 (2018). https://doi.org/10.1016/j.conbuildmat.2018.06.153
79. Sata, V., Jaturapitakkul, C., Kiattikomol, K.: Influence of pozzolan from various by-product materials on mechanical properties of high-strength concrete. Constr. Build. Mater. **21**, 1589–1598 (2007). https://doi.org/10.1016/j.conbuildmat.2005.09.011
80. Athira, V.S., Charitha, V., Athira, G., Bahurudeen, A.: Agro-waste ash based alkali-activated binder: cleaner production of zero cement concrete for construction. J. Clean. Prod. **286**, 125429 (2021). https://doi.org/10.1016/j.jclepro.2020.125429

81. Batra, V.S., Urbonaite, S., Svensson, G.: Characterization of unburned carbon in bagasse fly ash. Fuel **87**, 2972–2976 (2008). https://doi.org/10.1016/j.fuel.2008.04.010
82. Islam, A., Alengaram, U.J., Jumaat, M.Z., Bashar, I.I.: The development of compressive strength of ground granulated blast furnace slag-palm oil fuel ash-fly ash based geopolymer mortar. Mater. Des. **56**, 833–841 (2014). https://doi.org/10.1016/j.matdes.2013.11.080
83. Castaldelli, V.N., Akasaki, J.L., Melges, J.L., Tashima, M.M., Soriano, L., Borrachero, M.V., Monzó, J., Payá, J.: Use of slag/sugar cane bagasse ash (SCBA) blends in the production of alkali-activated materials. Materials **6**, 3108–3127 (2013). https://doi.org/10.3390/ma6083108
84. Zabihi, S.M., Tavakoli, H., Mohseni, E.: Engineering and microstructural properties of fiber-reinforced rice husk-ash based geopolymer concrete. J. Mater. Civ. Eng. **30**, 04018183 (2018). https://doi.org/10.1061/(asce)mt.1943-5533.0002379
85. Salih, M.A., Farzadnia, N., Abang Ali, A.A., Demirboga, R.: Effect of different curing temperatures on alkali activated palm oil fuel ash paste. Constr. Build. Mater. **94**, 116–125 (2015). https://doi.org/10.1016/j.conbuildmat.2015.06.052
86. Soriano Martinez, L., Font, A., Tashima, M.M., Monzó Balbuena, J.M., Borrachero Rosado, M.V., Bonifacio, T., Paya Bernabeu, J.J.: Almond-shell biomass ash (ABA): a greener alternative to the use of commercial alkaline reagents in alkali-activated cement. Constr. Build. Mater. **290**, 123251 (2021). https://doi.org/10.1016/j.conbuildmat.2021.123251
87. Moraes, J.C., Tashima, M.M., Akasaki, J.L., Melges, J.L., Monzó, J., Borrachero, M.V., Soriano, L., Payá, J.: Increasing the sustainability of alkali-activated binders: the use of sugar cane straw ash (SCSA). Constr. Build. Mater. **124**, 148–154 (2016). https://doi.org/10.1016/j.conbuildmat.2016.07.090
88. Tong, K.T., Vinai, R., Soutsos, M.N.: Use of Vietnamese rice husk ash for the production of sodium silicate as the activator for alkali-activated binders. J. Clean. Prod. **201**, 272–286 (2018). https://doi.org/10.1016/j.jclepro.2018.08.025
89. Vinai, R., Ntimugura, F., Cutbill, W., Evans, R., Zhao, Y.: Bio-derived sodium silicate for the manufacture of alkali-activated binders: use of bamboo leaf ash as silicate source. Int. J. Appl. Ceram. Technol. (2022). https://doi.org/10.1111/ijac.14004
90. Bernal, S.A., Rodríguez, E.D., Kirchheim, A.P., Provis, J.L.: Management and valorisation of wastes through use in producing alkali-activated cement materials. J. Chem. Technol. Biotechnol. **91**, 2365–2388 (2016). https://doi.org/10.1002/jctb.4927
91. Kamseu, E., Beleuk à Moungam, L., Cannio, M., Billong, N., Chaysuwan, D., Melo, U.C., Leonelli, C.: Substitution of sodium silicate with rice husk ash-NaOH solution in metakaolin based geopolymer cement concerning reduction in global warming. J. Clean. Prod. **142**, 3050–3060 (2017). https://doi.org/10.1016/j.jclepro.2016.10.164
92. Suksiripattanapong, C., Kua, T.A., Arulrajah, A., Maghool, F., Horpibulsuk, S.: Strength and microstructure properties of spent coffee grounds stabilized with rice husk ash and slag geopolymers. Constr. Build. Mater. **146**, 312–320 (2017). https://doi.org/10.1016/j.conbuildmat.2017.04.103
93. Hwang, C.L., Huynh, T.P.: Effect of alkali-activator and rice husk ash content on strength development of fly ash and residual rice husk ash-based geopolymers. Constr. Build. Mater. **101**, 1–9 (2015). https://doi.org/10.1016/j.conbuildmat.2015.10.025
94. Karim, M.R., Zain, M.F.M., Jamil, M., Lai, F.C.: Fabrication of a non-cement binder using slag, palm oil fuel ash and rice husk ash with sodium hydroxide. Constr. Build. Mater. **49**, 894–902 (2013). https://doi.org/10.1016/j.conbuildmat.2013.08.077
95. Detphan, S., Chindaprasirt, P.: Preparation of fly ash and rice husk ash geopolymer. Int. J. Miner. Metall. Mater. **16**, 720–726 (2009). https://doi.org/10.1016/S1674-4799(10)60019-2
96. Alomayri, T., Adesina, A., Das, S.: Influence of amorphous raw rice husk ash as precursor and curing condition on the performance of alkali activated concrete. Case Stud. Constr. Mater. **15**, e00777 (2021). https://doi.org/10.1016/j.cscm.2021.e00777
97. Castaldelli, V.N., Moraes, J.C., Akasaki, J.L., Melges, J.L., Monzó, J., Borrachero, M.V., Soriano, L., Payá, J., Tashima, M.M.: Study of the binary system fly ash/sugarcane bagasse ash (FA/SCBA) in SiO_2/K_2O alkali-activated binders. Fuel **174**, 307–316 (2016). https://doi.org/10.1016/j.fuel.2016.02.020

98. Yadav, A.L., Sairam, V., Srinivasan, K., Muruganandam, L.: Synthesis and characterization of geopolymer from metakaolin and sugarcane bagasse ash. Constr. Build. Mater. **258**, 119231 (2020). https://doi.org/10.1016/j.conbuildmat.2020.119231
99. Emdadi, Z., Asim, N., Amin, M.H., Ambar Yarmo, M., Maleki, A., Azizi, M., Sopian, K.: Development of green geopolymer using agricultural and industrialwaste materials with high water absorbency. Appl. Sci. **7**(5), 514 (2017). https://doi.org/10.3390/app7050514
100. Salih, M.A., Abang Ali, A.A., Farzadnia, N.: Characterization of mechanical and microstructural properties of palm oil fuel ash geopolymer cement paste. Constr. Build. Mater. **65**, 592–603 (2014). https://doi.org/10.1016/j.conbuildmat.2014.05.031
101. Pera, J., Amrouz, A.: Development of highly reactive metakaolin from paper sludge. Adv. Cem. Based Mater. **7**, 49–56 (1998). https://doi.org/10.1016/S1065-7355(97)00016-3
102. Adesanya, E., Ohenoja, K., Luukkonen, T., Kinnunen, P., Illikainen, M.: One-part geopolymer cement from slag and pretreated paper sludge. J. Clean. Prod. **185**, 168–175 (2018). https://doi.org/10.1016/j.jclepro.2018.03.007
103. García, R., de la Villa, R.V., Vegas, I., Frías, M., de Rojas, M.S.: The pozzolanic properties of paper sludge waste. Constr. Build. Mater. **22**, 1484–1490 (2008). https://doi.org/10.1016/j.conbuildmat.2007.03.033
104. Ingale, S.D., Nemade, P.D.: Effect of paper sludge ash on properties of cement concrete: a review. Mater. Today: Proc. (2023). https://doi.org/10.1016/j.matpr.2023.03.492
105. Bernal, S.A., Ball, R.J., Hussein, O., Heath, A., Provis, J.L.: Paper sludge ash as a precursor for production of alkali-activated materials. In: Proceedings of Advances in Chemically-Activated Materials Conference (CAM'2014), pp. 140–149 (2014)
106. Gluth, G.J.G., Lehmann, C., Rübner, K., Kühne, H.C.: Reaction products and strength development of wastepaper sludge ash and the influence of alkalis. Cem. Concr. Compos. **45**, 82–88 (2014). https://doi.org/10.1016/j.cemconcomp.2013.09.009
107. Kinuthia, J.: Wastepaper sludge ash. In: Waste and Supplementary Cementitious Materials in Concrete, pp. 289–321. Woodhead Publishing (2018)
108. Segui, P., Aubert, J.E., Husson, B., Measson, M.: Characterization of wastepaper sludge ash for its valorization as a component of hydraulic binders. Appl. Clay Sci. **57**, 79–85 (2012). https://doi.org/10.1016/j.clay.2012.01.007
109. Senthamilselvi, P., Thangaraju, P.: Effect of incinerated paper sludge ash on fly ash–based geopolymer concrete. J. Croat. Assoc. Civil Eng. **69**, 851–859 (2017). https://doi.org/10.14256/JCE.1864.2016
110. Li, Z., Ohnuki, T., Ikeda, K.: Development of paper sludge ash-based geopolymer and application to treatment of hazardous water contaminated with radioisotopes. Materials **9**(8), 633 (2016). https://doi.org/10.3390/ma9080633
111. Antunes Boca Santa, R.A., Bernardin, A.M., Riella, H.G., Kuhnen, N.C.: Geopolymer synthetized from bottom coal ash and calcined paper sludge. J. Clean. Prod. **57**, 302–307 (2013). https://doi.org/10.1016/j.jclepro.2013.05.017
112. Mengasini, L., Mavroulidou, M., Gunn, M.J.: Alkali-activated concrete mixes with ground granulated blast furnace slag and paper sludge ash in seawater environments. Sustain. Chem. Pharm. **20**, 100380 (2021). https://doi.org/10.1016/j.scp.2021.100380
113. Mavroulidou, M., Shah, S.: Alkali-activated slag concrete with paper industry waste. Waste Manag. Res. **39**, 466–472 (2021). https://doi.org/10.1177/0734242X20983890
114. Martynkova, R., Mavroulidou, M.: Properties of alkali-activated concrete based on industrial wastes or by-products. In: Proceedings of the 14th International Conference on Environmental Science and Technology Athens, pp. 3–5, Greece (2015)
115. Mavroulidou, M.: Use of waste paper sludge ash as a calcium-based stabiliser for clay soils. Waste Manag. Res.: J. Sustain. Circ. Econ. **36**, 1066–1072 (2018). https://doi.org/10.1177/0734242X18804043
116. Yan, S., Sagoe-Crentsil, K.: Evaluation of fly ash geopolymer mortar incorporating calcined wastepaper sludge. J. Sustain. Cem.-Based Mater. **5**, 370–380 (2016). https://doi.org/10.1080/21650373.2016.1174962

117. Yan, S., Sagoe-Crentsil, K.: Properties of wastepaper sludge in geopolymer mortars for masonry applications. J. Environ. Manag. **112**, 27–32 (2012). https://doi.org/10.1016/j.jenvman.2012.07.008
118. Kaza, S., Yao, L., Bhada-Tata, P., Van Woerden, F.: What a Waste 2.0: a Global Snapshot of Solid Waste Management to 2050. World Bank Publications (2018)
119. Tozlu, A., Özahi, E., Abuşoılu, A.: Waste to energy technologies for municipal solid waste management in Gaziantep. Renew. Sustain. Energy Rev. **54**, 809–815 (2016). https://doi.org/10.1016/J.RSER.2015.10.097
120. Bunge, R.: Recovery of metals from waste incinerator bottom ash. In: Holm, O., Thome-Kozmiensky, E. (eds.) Removal, Treatment and Utilisation of Waste Incineration Bottom Ash, pp. 63–143 (2015)
121. Kim, J., Nam, B.H., Al Muhit, B.A., Tasneem, K.M., An, J.: Effect of chemical treatment of MSWI bottom ash for its use in concrete. Mag. Concr. Res. **67**, 179–186 (2015). https://doi.org/10.1680/macr.14.00170
122. Li, M., Xiang, J., Hu, S., Sun, L.S., Su, S., Li, P.S., Sun, X.X.: Characterization of solid residues from municipal solid waste incinerator. Fuel **83**, 1397–1405 (2004). https://doi.org/10.1016/j.fuel.2004.01.005
123. Sabbas, T., Polettini, A., Pomi, R., Astrup, T., Hjelmar, O., Mostbauer, P., Cappai, G., Magel, G., Salhofer, S., Speiser, C., Heuss-Assbichler, S.: Management of municipal solid waste incineration residues. Waste Manag. **23**(1), 61–88 (2003). https://doi.org/10.1016/S0956-053X(02)00161-7
124. Phua, Z., Giannis, A., Dong, Z.L., Lisak, G., Ng, W.J.: Characteristics of incineration ash for sustainable treatment and reutilization. Environ. Sci. Pollut. Res. **26**, 16974–16997 (2019). https://doi.org/10.1007/s11356-019-05217-8
125. Chimenos, J.M., Segarra, M., Fernandez, M.A., Espiell, F.: Characterization of the bottom ash in municipal solid waste incinerator. J. Hazard. Mater. A **64**, 211–222 (1999). https://doi.org/10.1016/S0304-3894(98)00246-5
126. Lin, K.L., Lin, D.F.: Hydration characteristics of municipal solid waste incinerator bottom ash slag as a pozzolanic material for use in cement. Cem. Concr. Compos. **28**, 817–823 (2006). https://doi.org/10.1016/j.cemconcomp.2006.03.003
127. Alderete, N.M., Joseph, A.M., Van den Heede, P., Matthys, S., De Belie, N.: Effective and sustainable use of municipal solid waste incineration bottom ash in concrete regarding strength and durability. Resour. Conserv. Recycl. **167**, 105356 (2021). https://doi.org/10.1016/j.resconrec.2020.105356
128. Chen, B., Perumal, P., Illikainen, M., Ye, G.: A review on the utilization of municipal solid waste incineration (MSWI) bottom ash as a mineral resource for construction materials. J. Build. Eng. 106386 (2023). https://doi.org/10.1016/j.jobe.2023.106386
129. Li, Y.M., Wu, X.Q., Wang, L.J., et al.: Comparative study on utilization of different types of municipal solid waste incineration bottom ash for clinker sintering. J. Mater. Cycles Waste Manag. **22**, 1828–1843 (2020). https://doi.org/10.1007/s10163-020-01067-6
130. Zhang, Z., Wang, J., Liu, L., Ma, J., Shen, B.: Preparation of additive-free glass-ceramics from MSW incineration bottom ash and coal fly ash. Constr. Build. Mater. **254**, 119345 (2020). https://doi.org/10.1016/j.conbuildmat.2020.119345
131. Appendino, P., Ferraris, M., Matekovits, I., Salvo, M.: Production of glass-ceramic bodies from the bottom ashes of municipal solid waste incinerators. J. Eur. Ceram. Soc. **24**, 803–810 (2004). https://doi.org/10.1016/S0955-2219(03)00264-4
132. Monteiro, R.C., Alendouro, S.J., Figueiredo, F.M., Ferro, M.C., Fernandes, M.H.: Development and properties of a glass made from MSWI bottom ash. J. Non-Cryst. Solids **352**(2), 130–135 (2006)
133. Rambaldi, E., Esposito, L., Andreola, F., Barbieri, L., Lancellotti, I., Vassura, I.: The recycling of MSWI bottom ash in silicate based ceramic. Ceram. Int. **36**, 2469–2476 (2010). https://doi.org/10.1016/J.CERAMINT.2010.08.005
134. Taurino, R., Karamanov, A., Rosa, R., Karamanova, E., Barbieri, L., Atanasova-Vladimirova, S., Avdeev, G., Leonelli, C.: New ceramic materials from MSWI bottom ash obtained by an

innovative microwave-assisted sintering process. J. Eur. Ceram. Soc. **37**(1), 323–331 (2017). https://doi.org/10.1016/j.jeurceramsoc.2016.08.011
135. Vegas, I., Ibañez, J.A., José, J.T.S., Urzelai, A.: Construction demolition wastes, Waelz slag and MSWI bottom ash: a comparative technical analysis as material for road construction. Waste Manag. **28**, 565–574 (2008). https://doi.org/10.1016/j.wasman.2007.01.016
136. Pera, J., Coutaz, L., Ambroise, J., Chababbet, M.: Use of incinerator bottom ash in concrete. Cem. Concr. Res. **27**(1), 1–5 (1997). https://doi.org/10.1016/S0008-8846(96)00193-7
137. Li, X.G., Lv, Y., Ma, B.G., Chen, Q.B., Yin, X.B., Jian, S.W.: Utilization of municipal solid waste incineration bottom ash in blended cement. J. Clean. Prod. **32**, 96–100 (2012). https://doi.org/10.1016/j.jclepro.2012.03.038
138. Tang, P., Chen, W., Xuan, D., Zuo, Y., Poon, C.S.: Investigation of cementitious properties of different constituents in municipal solid waste incineration bottom ash as supplementary cementitious materials. J. Clean. Prod. **258**, 120675 (2020). https://doi.org/10.1016/j.jclepro.2020.120675
139. Maldonado-Alameda, À., Giro-Paloma, J., Alfocea-Roig, A., Formosa, J., Chimenos, J.M.: Municipal solid waste incineration bottom ash as sole precursor in the alkali-activated binder formulation. Appl. Sci. **10**(12), 4129 (2020). https://doi.org/10.3390/APP10124129
140. Bertolini, L., Carsana, M., Cassago, D., Curzio, A.Q., Collepardi, M.: MSWI ashes as mineral additions in concrete. Cem. Concr. Res. **34**, 1899–1906 (2004). https://doi.org/10.1016/j.cemconres.2004.02.001
141. Clavier, K.A., Watts, B., Liu, Y., Ferraro, C.C., Townsend, T.G.: Risk and performance assessment of cement made using municipal solid waste incinerator bottom ash as a cement kiln feed. Resour. Conserv. Recycl. **146**, 270–279 (2019). https://doi.org/10.1016/j.resconrec.2019.03.047
142. Oehmig, W.N., Roessler, J.G., Blaisi, N.I., Townsend, T.G.: Contemporary practices and findings essential to the development of effective MSWI ash reuse policy in the United States. Environ. Sci. Policy **51**, 304–312 (2015). https://doi.org/10.1016/j.envsci.2015.04.024
143. Alam, Q., Florea, M.V.A., Schollbach, K., Brouwers, H.J.H.: A two-stage treatment for Municipal Solid Waste Incineration (MSWI) bottom ash to remove agglomerated fine particles and leachable contaminants. Waste Manag. **67**, 181–192 (2017). https://doi.org/10.1016/j.wasman.2017.05.029
144. Alam, Q., Lazaro, A., Schollbach, K., Brouwers, H.J.H.: Chemical speciation, distribution and leaching behavior of chlorides from municipal solid waste incineration bottom ash. Chemosphere **241**, 124985 (2020). https://doi.org/10.1016/j.chemosphere.2019.124985
145. Flesoura, G., Garcia-Banos, B., Catala-Civera, J.M., Vleugels, J., Pontikes, Y.: In-situ measurements of high-temperature dielectric properties of municipal solid waste incinerator bottom ash. Ceram. Int. **45**, 18751–18759 (2019). https://doi.org/10.1016/j.ceramint.2019.06.101
146. De Windt, L., Dabo, D., Lidelöw, S., Badreddine, R., Lagerkvist, A.: MSWI bottom ash used as basement at two pilot-scale roads: comparison of leachate chemistry and reactive transport modeling. Waste Manag. **31**, 267–280 (2011). https://doi.org/10.1016/j.wasman.2010.06.002
147. Le, N.H., Razakamanantsoa, A., Nguyen, M.L., Phan, V.T., Dao, P.L., Nguyen, D.H.: Evaluation of physicochemical and hydromechanical properties of MSWI bottom ash for road construction. Waste Manag. **80**, 168–174 (2018). https://doi.org/10.1016/j.wasman.2018.09.007
148. Cheeseman, C.R., Da Rocha, S.M., Sollars, C., Bethanis, S., Boccaccini, A.R.: Ceramic processing of incinerator bottom ash. Waste Manag. **23**, 907–916 (2003). https://doi.org/10.1016/S0956-053X(03)00039-4
149. Ferraris, M., Salvo, M., Ventrella, A., Buzzi, L., Veglia, M.: Use of vitrified MSWI bottom ashes for concrete production. Waste Manag. **29**(3), 1041–1047 (2009). https://doi.org/10.1016/j.wasman.2008.07.014
150. Bethanis, S., Cheeseman, C.R., Sollars, C.J.: Effect of sintering temperature on the properties and leaching of incinerator bottom ash. Waste Manag. Res. **22**, 255–264 (2004). https://doi.org/10.1177/0734242X04045426

151. Qiao, X.C., Tyrer, M., Poon, C.S., Cheeseman, C.R.: Characterization of alkali-activated thermally treated incinerator bottom ash. Waste Manag. **28**, 1955–1962 (2008). https://doi.org/10.1016/j.wasman.2007.09.007
152. Qiao, X.C., Tyrer, M., Poon, C.S., Cheeseman, C.R.: Novel cementitious materials produced from incinerator bottom ash. Resour. Conserv. Recycl. **52**, 496–510 (2008). https://doi.org/10.1016/j.resconrec.2007.06.003
153. Biganzoli, L., Ilyas, A., van Praagh, M., Persson, K.M., Grosso, M.: Aluminium recovery versus hydrogen production as resource recovery options for fine MSWI bottom ash fraction. Waste Manag. **33**, 1174–1181 (2013). https://doi.org/10.1016/j.wasman.2013.01.037
154. Rübner, K., Haamkens, F., Linde, O.: Use of municipal solid waste incinerator bottom ash as aggregate in concrete. Q. J. Eng. Geol. Hydrogeol. **41**, 459–464 (2008). https://doi.org/10.1144/1470-9236/07-036
155. Giro-Paloma, J., Maldonado-Alameda, A., Formosa, J., Barbieri, L., Chimenos, J.M., Lancellotti, I.: Geopolymers based on the valorization of Municipal Solid Waste Incineration residues. IOP Conf. Ser.: Mater. Sci. Eng. **251**, 012125 (2017). https://doi.org/10.1088/1757-899X/251/1/012125
156. Izquierdo, M., López-Soler, Á., Vazquez Ramonich, E., Barra, M., Querol, X.: Characterisation of bottom ash from municipal solid waste incineration in Catalonia. J. Chem. Technol. Biotechnol. **77**, 576–583 (2002). https://doi.org/10.1002/jctb.605
157. Chen, B., Perumal, P., Aghabeyk, F., Adediran, A., Illikainen, M., Ye, G.: Advances in using municipal solid waste incineration (MSWI) bottom ash as precursor for alkali-activation materials: a critical review. Resour. Conserv. Recycl. **204**, 107516 (2024). https://doi.org/10.1016/j.resconrec.2024.107516
158. Santos, R.M., Mertens, G., Salman, M., Cizer, Ö., Van Gerven, T.: Comparative study of ageing, heat treatment and accelerated carbonation for stabilization of municipal solid waste incineration bottom ash in view of reducing regulated heavy metal/metalloid leaching. J. Environ. Manag. **128**, 807–821 (2013). https://doi.org/10.1016/j.jenvman.2013.06.033
159. Alam, Q., Hendrix, Y., Thijs, L., Lazaro, A., Schollbach, K., Brouwers, H.J.: Novel low temperature synthesis of sodium silicate and ordered mesoporous silica from incineration bottom ash. J. Clean. Prod. **211**, 874–883 (2019). https://doi.org/10.1016/j.jclepro.2018.11.173
160. Antiohos, S., Maganari, K., Tsimas, S.: Evaluation of blends of high and low calcium fly ashes for use as supplementary cementing materials. Cem. Concr. Compos. **27**(3), 349–356 (2005). https://doi.org/10.1016/j.cemconcomp.2004.05.001
161. Hooton, R.D.: Canadian use of ground granulated blast-furnace slag as a supplementary cementing material for enhanced performance of concrete. Can. J. Civ. Eng. **27**(4), 754–760 (2000). https://doi.org/10.1139/l00-014
162. Hemalatha, T., Ramaswamy, A.: A review on fly ash characteristics—Towards promoting high volume utilization in developing sustainable concrete. J. Clean. Prod. **147**, 546–559 (2017). https://doi.org/10.1016/j.jclepro.2017.01.114
163. Özbay, E., Erdemir, M., Durmuş, H.İ.: Utilization and efficiency of ground granulated blast furnace slag on concrete properties—A review. Constr. Build. Mater. **105**, 423–434 (2016). https://doi.org/10.1016/j.conbuildmat.2015.12.153
164. Chen, B.: Utilization of MSWI bottom ash as a mineral resource for low-carbon construction materials: quality-upgrade treatments, mix design method, and microstructure analysis. Ph.D. thesis. Delft University of Technology, The Netherlands (2023)
165. Chen, B., Ye, G.: The role of water-treated municipal solid waste incineration (MSWI) bottom ash in microstructure formation and strength development of blended cement pastes. Cem. Concr. Res. **1**(178), 107440 (2024). https://doi.org/10.1016/j.cemconres.2024.107440
166. Tang, P., Florea, M.V.A., Spiesz, P., Brouwers, H.J.H.: Application of thermally activated municipal solid waste incineration (MSWI) bottom ash fines as binder substitute. Cem. Concr. Compos. **70**, 194–205 (2016). https://doi.org/10.1016/j.cemconcomp.2016.03.015
167. Chen, B., van Zijl, M.B., Keulen, A., Ye, G.: Thermal treatment on MSWI bottom ash for the utilisation in alkali activated materials. KnE Eng. (2020). https://doi.org/10.18502/keg.v5i4.6792

168. Qiao, X.C., Ng, B.R., Tyrer, M., Poon, C.S., Cheeseman, C.R.: Production of lightweight concrete using incinerator bottom ash. Constr. Build. Mater. **22**, 473–480 (2008). https://doi.org/10.1016/j.conbuildmat.2006.11.013
169. Casanova, S., Silva, R.V., de Brito, J., Pereira, M.F.C.: Mortars with alkali-activated municipal solid waste incinerator bottom ash and fine recycled aggregates. J. Clean. Prod. **289** (2021). https://doi.org/10.1016/j.jclepro.2020.125707
170. Carvalho, R., Silva, R.V., de Brito, J., Pereira, M.F.C.: Alkali activation of bottom ash from municipal solid waste incineration: optimization of NaOH- and Na_2SiO_3-based activators. J. Clean. Prod. **291** (2021). https://doi.org/10.1016/j.jclepro.2021.125930
171. Huang, G., Ji, Y., Li, J., Zhang, L., Liu, X., Liu, B.: Effect of activated silica on polymerization mechanism and strength development of MSWI bottom ash alkali-activated mortars. Constr. Build. Mater. **201**, 90–99 (2019). https://doi.org/10.1016/j.conbuildmat.2018.12.125
172. Maldonado-Alameda, A., Giro-Paloma, J., Svobodova-Sedlackova, A., Formosa, J., Chimenos, J.M.: Municipal solid waste incineration bottom ash as alkali-activated cement precursor depending on particle size. J. Clean. Prod. **242**, 118443 (2020). https://doi.org/10.1016/j.jclepro.2019.118443
173. Evans, K., Nordheim, E., Tsesmelis, K.: Bauxite residue management. In: Light Metals, pp. 63–66. Springer International Publishing, Cham (2012)
174. Evans, K.: The history, challenges, and new developments in the management and use of bauxite residue. J. Sustain. Metall. **2**, 316–331 (2016). https://doi.org/10.1007/s40831-016-0060-x
175. Klauber, C., Gräfe, M., Power, G.: Bauxite residue issues: II. Options for residue utilization. Hydrometallurgy **108**, 11–32 (2011). https://doi.org/10.1016/j.hydromet.2011.02.007
176. Gräfe, M., Power, G., Klauber, C.: Bauxite residue issues: III. Alkalinity and associated chemistry. Hydrometallurgy **108**, 60–79 (2011). https://doi.org/10.1016/j.hydromet.2011.02.004
177. Occhicone, A., Vukčević, M., Bosković, I., Ferone, C.: Red mud-blast furnace slag-based alkali-activated materials. Sustainability **13**(20), 11298 (2021). https://doi.org/10.3390/su132011298
178. Liang, X., Ji, Y.: Mechanical properties and permeability of red mud-blast furnace slag-based geopolymer concrete. SN Appl. Sci. **3**, 1–10 (2021). https://doi.org/10.1007/s42452-020-03985-4
179. Liang, X., Ji, Y.: Preparation sequences and pretreatment optimization of alkali-activated red mud and blast furnace slag-based materials. J. Mater. Cycles Waste Manag. **23**, 259–271 (2020). https://doi.org/10.1007/s10163-020-01126-y
180. Ai, T., Zhong, D., Zhang, Y., Zong, J., Yan, X., Niu, Y.: The effect of red mud content on the compressive strength of geopolymers under different curing systems. Buildings **11**(7), 298 (2021). https://doi.org/10.3390/buildings11070298
181. Lemougna, P.N., Wang, K.T., Tang, Q., Cui, X.M.: Study on the development of inorganic polymers from red mud and slag system: application in mortar and lightweight materials. Constr. Build. Mater. **156**, 486–495 (2017). https://doi.org/10.1016/j.conbuildmat.2017.09.015
182. Bayat, A., Hassani, A., Yousefi, A.A.: Effects of red mud on the properties of fresh and hardened alkali-activated slag paste and mortar. Constr. Build. Mater. **167**, 775–790 (2018). https://doi.org/10.1016/j.conbuildmat.2018.02.105
183. Liang, X., Ji, Y.: Experimental study on durability of red mud-blast furnace slag geopolymer mortar. Constr. Build. Mater. **267**, 120942 (2021). https://doi.org/10.1016/j.conbuildmat.2020.120942
184. Singh, S., Aswath, M.U., Ranganath, R.V.: Effect of mechanical activation of red mud on the strength of geopolymer binder. Constr. Build. Mater. **177**, 91–101 (2018). https://doi.org/10.1016/j.conbuildmat.2018.05.096
185. Hoang, M.D., Do, Q.M., Le, V.Q.: Effect of curing regime on properties of red mud based alkali activated materials. Constr. Build. Mater. **259**, 119779 (2020). https://doi.org/10.1016/j.conbuildmat.2020.119779

186. Ye, N., Yang, J., Ke, X., Zhu, J., Li, Y., Xiang, C., Wang, H., Li, L., Xiao, B.: Synthesis and characterization of geopolymer from bayer red mud with thermal pretreatment. J. Am. Ceram. Soc. **97**, 1652–1660 (2014). https://doi.org/10.1111/jace.12840
187. Hu, Y., Liang, S., Yang, J., Chen, Y., Ye, N., Ke, Y., Tao, S., Xiao, K., Hu, J., Hou, H., Fan, W.: Role of Fe species in geopolymer synthesized from alkali-thermal pretreated Fe-rich Bayer red mud. Constr. Build. Mater. **200**, 398–407 (2019). https://doi.org/10.1016/j.conbuildmat.2018.12.122
188. Gomes, K.C., Lima, G.S., Torres, S.M., de Barros, S.R., Vasconcelos, I.F., Barbosa, N.P.: Iron distribution in geopolymer with ferromagnetic rich precursor. Mater. Sci. Forum **643**, 131–138 (2010). https://doi.org/10.4028/www.scientific.net/MSF.643.131
189. Jin, F.: Sustainable utilization of slags. In: Low Carbon Stabilization and Solidification of Hazardous Wastes, pp. 321–341. Elsevier (2022)
190. Piatak, N.M., Ettler, V. (eds.): Metallurgical Slags: environmental Geochemistry and Resource Potential. Royal Society of Chemistry, Cambridge (2021)
191. Piatak, N.M., Parsons, M.B., Seal, R.R.: Characteristics and environmental aspects of slag: a review. Appl. Geochem. **57**, 236–266 (2015). https://doi.org/10.1016/j.apgeochem.2014.04.009
192. Criado, M., Ke, X., Provis, J.L., Bernal, S.A.: Alternative inorganic binders based on alkali-activated metallurgical slags. In: Sustainable and Nonconventional Construction Materials Using Inorganic Bonded Fiber Composites, pp. 185–220. Woodhead Publishing (2017)
193. Marsh, A.T.M., Yang, T., Adu-Amankwah, S., Bernal, S.A.: Utilization of metallurgical wastes as raw materials for manufacturing alkali-activated cements. In: Waste and Byproducts in Cement-Based Materials, pp. 335–383. Woodhead Publishing (2021)
194. US Geological Survey.: Mineral commodity summaries 2022. Reston, VA (2022)
195. Shi, C., Qian, J.: High performance cementing materials from industrial slags—A review. Resour. Conserv. Recycl. **29**, 195–207 (2000). https://doi.org/10.1016/S0921-3449(99)00060-9
196. Piatak, N.M.: Environmental characteristics and utilization potential of metallurgical slag. In: Environmental Geochemistry, 2nd edn, pp. 487–519. Elsevier B.V. (2018)
197. Nazer, A., Payá, J., Borrachero, M.V., Monzó, J.: Use of ancient copper slags in Portland cement and alkali activated cement matrices. J. Environ. Manag. **167**, 115–123 (2016). https://doi.org/10.1016/j.jenvman.2015.11.024
198. Salman, M., Cizer, Ö., Pontikes, Y., Vandewalle, L., Blanpain, B., Van Balen, K.: Effect of curing temperatures on the alkali activation of crystalline continuous casting stainless steel slag. Comput. Chem. Eng. **71**, 308–316 (2014). https://doi.org/10.1016/j.conbuildmat.2014.08.067
199. Zhang, Z., Zhu, Y., Yang, T., Li, L., Zhu, H., Wang, H.: Conversion of local industrial wastes into greener cement through geopolymer technology: a case study of high-magnesium nickel slag. J. Clean. Prod. **141**, 463–471 (2017). https://doi.org/10.1016/j.jclepro.2016.09.147
200. Kalinkin, A.M., Kumar, S., Gurevich, B.I., et al.: Geopolymerization behavior of Cu–Ni slag mechanically activated in air and in CO_2 atmosphere. Int. J. Miner. Process. **112–113**, 101–106 (2012). https://doi.org/10.1016/j.minpro.2012.05.001
201. Kalinkin, A.M., Kumar, S., Gurevich, B.I., et al.: Synthesis of geopolymer materials based on slags of nonferrous metallurgy with the use of mechanoactivation. Glass Phys. Chem **40**, 26–30 (2014). https://doi.org/10.1134/S1087659614010088
202. Nikolov, A., Karamanov, A.: Thermal properties of geopolymer based on fayalite waste from copper production and metakaolin. Materials **15** (2022). https://doi.org/10.3390/ma15072666
203. Singh, J., Singh, S.P.: Development of alkali-activated cementitious material using copper slag. Constr. Build. Mater. **211**, 73–79 (2019). https://doi.org/10.1016/j.conbuildmat.2019.03.233
204. Yan, Z., Sun, Z., Yang, J., Yang, H., Ji, Y., Hu, K.: Mechanical performance and reaction mechanism of copper slag activated with sodium silicate or sodium hydroxide. Constr. Build. Mater. **266**, 120900 (2021). https://doi.org/10.1016/j.conbuildmat.2020.120900

205. Kumar, S., García-Triñanes, P., Teixeira-Pinto, A., Bao, M.: Development of alkali activated cement from mechanically activated silico-manganese (SiMn) slag. Cem. Concr. Compos. **40**, 7–13 (2013). https://doi.org/10.1016/j.cemconcomp.2013.03.026
206. Su, Z., Liu, Z., Wang, H., Xu, S., Wang, D., Han, F.: Reaction kinetics, microstructure and phase evolution of alkali-activated Si–Mn slag during early age. Constr. Build. Mater. **333**, 127437 (2022). https://doi.org/10.1016/j.conbuildmat.2022.127437
207. Nath, S.K., Kumar, S.: Influence of granulated silico-manganese slag on compressive strength and microstructure of ambient cured alkali-activated fly ash binder. Waste Biomass Valoriz. **10**, 2045–2055 (2019). https://doi.org/10.1007/s12649-018-0213-1
208. Salman, M., Cizer, Ö., Pontikes, Y., Snellings, R., Vandewalle, L., Blanpain, B., Van Balen, K.: Cementitious binders from activated stainless steel refining slag and the effect of alkali solutions. J. Hazard. Mater. **286**, 211–219 (2015). https://doi.org/10.1016/j.jhazmat.2014.12.046
209. Sun, J., Chen, Z.: Effect of silicate modulus of water glass on the hydration of alkali-activated converter steel slag. J. Therm. Anal. Calorim. **138**, 47–56 (2019). https://doi.org/10.1007/s10973-019-08146-3
210. Yang, T., Yao, X., Zhang, Z.: Geopolymer prepared with high-magnesium nickel slag: characterization of properties and microstructure. Constr. Build. Mater. **59**, 188–194 (2014). https://doi.org/10.1016/j.conbuildmat.2014.01.038
211. Adediran, A., Yliniemi, J., Illikainen, M.: Mineralogy and glass content of Fe-rich fayalite slag size fractions and their effect on alkali activation and leaching of heavy metals. Int. J. Ceram. Eng. Sci. **3**, 287–300 (2021). https://doi.org/10.1002/ces2.10107
212. Maghsoodloorad, H., Khalili, H., Allahverdi, A.: Alkali-activated phosphorous slag performance under different curing conditions: compressive strength, hydration products, and microstructure. J. Mater. Civ. Eng. **30**, 1–12 (2018). https://doi.org/10.1061/(asce)mt.1943-5533.0002101
213. Rao, F., Liu, Q.: Geopolymerization and its potential application in mine tailings consolidation: a review. Miner. Process. Extr. Metall. Rev. **36**, 399–409 (2015). https://doi.org/10.1080/08827508.2015.1055625
214. Jones, H., Boger, D.V.: Sustainability and waste management in the resource industries. Ind. Eng. Chem. Res. **51**, 10057–10065 (2012). https://doi.org/10.1021/ie202963z
215. He, X., Yuhua, Z., Qaidi, S., Isleem, H.F., Zaid, O., Althoey, F., Ahmad, J.: Mine tailings-based geopolymers: a comprehensive review. Ceram. Int. **48**(17), 24192–24212 (2022). https://doi.org/10.1016/j.ceramint.2022.05.345
216. Mabroum, S., Moukannaa, S., El Machi, A., Taha, Y., Benzaazoua, M., Hakkou, R.: Mine wastes based geopolymers: a critical review. Clean. Eng. Technol. **1**, 100014 (2020). https://doi.org/10.1016/j.clet.2020.100014
217. Simonsen, A.M.T., Solismaa, S., Hansen, H.K., Jensen, P.E.: Evaluation of mine tailings' potential as supplementary cementitious materials based on chemical, mineralogical and physical characteristics. Waste Manag. **102**, 710–721 (2020). https://doi.org/10.1016/j.wasman.2019.11.037
218. Xiaolong, Z., Shiyu, Z., Hui, L., Yingliang, Z.: Disposal of mine tailings via geopolymerization. J. Clean. Prod. **284**, 124756 (2021). https://doi.org/10.1016/j.jclepro.2020.124756
219. Lazorenko, G., Kasprzhitskii, A., Shaikh, F., Krishna, R.S., Mishra, J.: Utilization potential of mine tailings in geopolymers: physicochemical and environmental aspects. Process Saf. Environ. Prot. **147**, 559–577 (2021). https://doi.org/10.1016/j.psep.2020.12.028
220. Kinnunen, P., Ismailov, A., Solismaa, S., Sreenivasan, H., Räisänen, M.L., Levänen, E., Illikainen, M.: Recycling mine tailings in chemically bonded ceramics—A review. J. Clean. Prod. **174**, 634–649 (2018). https://doi.org/10.1016/j.jclepro.2017.10.280
221. Niu, H., Kinnunen, P., Sreenivasan, H., Adesanya, E., Illikainen, M.: Structural collapse in phlogopite mica-rich mine tailings induced by mechanochemical treatment and implications to alkali activation potential. Miner. Eng. **151**, 106331 (2020). https://doi.org/10.1016/j.mineng.2020.106331

222. Qaidi, S.M., Tayeh, B.A., Zeyad, A.M., de Azevedo, A.R., Ahmed, H.U., Emad, W.: Recycling of mine tailings for the geopolymers production: a systematic review. Case Stud. Constr. Mater. **16**, e00933 (2022). https://doi.org/10.1016/j.cscm.2022.e00933
223. Niu, H., Abdulkareem, M., Sreenivasan, H., Kantola, A.M., Havukainen, J., Horttanainen, M., Telkki, V.V., Kinnunen, P., Illikainen, M.: Recycling mica and carbonate-rich mine tailings in alkali-activated composites: a synergy with metakaolin. Miner. Eng. **157**, 106535 (2020). https://doi.org/10.1016/j.mineng.2020.106535
224. Wei, B., Zhang, Y., Bao, S.: Preparation of geopolymers from vanadium tailings by mechanical activation. Constr. Build. Mater. **145**, 236–242 (2017). https://doi.org/10.1016/j.conbuildmat.2017.03.234
225. Kiventerä, J., Perumal, P., Yliniemi, J., Illikainen, M.: Mine tailings as a raw material in alkali activation: a review. Int. J. Miner. Metall. Mater. **27**, 1009–1020 (2020). https://doi.org/10.1007/s12613-020-2129-6
226. Perumal, P., Piekkari, K., Sreenivasan, H., Kinnunen, P., Illikainen, M.: One-part geopolymers from mining residues—Effect of thermal treatment on three different tailings. Miner. Eng. **144**, 106026 (2019). https://doi.org/10.1016/j.mineng.2019.106026
227. Bergala, F., Lagaly, G.: Chapter 1 General introduction: clays, clay minerals, and clay science. In: Bergaya, F., Lagaly, G. (eds.) Developments in Clay Science, Handbook, pp. 1–18. Elsevier (2006)
228. Brigatti, M.F., Galan, E., Theng, B.K.G.: Chapter 2 Structures and mineralogy of clay minerals. In: Bergaya, F., Lagaly, G. (eds.) Developments in Clay Science, Handbook, pp. 19–86. Elsevier (2006)
229. Liew, Y.M., Heah, C.Y., Mohd Mustafa, A.B., Kamarudin, H.: Structure and properties of clay-based geopolymer cements: a review. Prog. Mater. Sci. **83**, 595–629 (2016). https://doi.org/10.1016/j.pmatsci.2016.08.002
230. Khalifa, A.Z., Cizer, Ö., Pontikes, Y., Heath, A., Patureau, P., Bernal, S.A., Marsh, A.T.M.: Advances in alkali-activation of clay minerals. Cem. Concr. Res. **132**, 106050 (2020). https://doi.org/10.1016/j.cemconres.2020.106050
231. Marsh, A.T.M., Heath, A., Patureau, P., Evernden, M., Walker, P.: Alkali activation behaviour of un-calcined montmorillonite and illite clay minerals. Appl. Clay Sci. **166**, 250–261 (2018). https://doi.org/10.1016/j.clay.2018.09.011
232. Hanein, T., Thienel, K.C., Zunino, F., Marsh, A.T., Maier, M., Wang, B., Canut, M., Juenger, M.C., Ben Haha, M., Avet, F., Parashar, A., Al-Jaberi, L.A., Almenares-Reyes, S., Alujas-Diaz, A., Scrivener, K.L., Bernal, S.A., Provis, J.L., Sui, T., Bishnoi, S., Martirena-Hernández, F.: Clay calcination technology : state-of-the-art review by the RILEM TC 282. Mater. Struct. **55**, 1–29 (2022). https://doi.org/10.1617/s11527-021-01807-6
233. Buchwald, A., Hohmann, M., Posern, K., Brendler, E.: The suitability of thermally activated illite/smectite clay as raw material for geopolymer binders. Appl. Clay Sci. **46**, 300–304 (2009). https://doi.org/10.1016/j.clay.2009.08.026
234. Dietel, J., Warr, L.N., Bertmer, M., Steudel, A., Grathoff, G.H., Emmerich, K.: The importance of specific surface area in the geopolymerization of heated illitic clay. Appl. Clay Sci. **139**, 99–107 (2017). https://doi.org/10.1016/j.clay.2017.01.001
235. Valentini, L., Contessi, S., Dalconi, M.C., Zorzi, F., Garbin, E.: Alkali-activated calcined smectite clay blended with waste calcium carbonate as a low-carbon binder. J. Clean. Prod. **184**, 41–49 (2018). https://doi.org/10.1016/j.jclepro.2018.02.249
236. Seiffarth, T., Hohmann, M., Posern, K., Kaps, C.: Effect of thermal pre-treatment conditions of common clays on the performance of clay-based geopolymeric binders. Appl. Clay Sci. **73**, 35–41 (2013). https://doi.org/10.1016/j.clay.2012.09.010
237. Hu, N., Bernsmeier, D., Grathoff, G.H., Warr, L.N.: The influence of alkali activator type, curing temperature and gibbsite on the geopolymerization of an interstratified illite-smectite rich clay from Friedland. Appl. Clay Sci. **135**, 386–393 (2017). https://doi.org/10.1016/j.clay.2016.10.021
238. Djobo, J.N.Y., Elimbi, A., Tchakouté, H.K., Kumar, S.: Mechanical activation of volcanic ash for geopolymer synthesis: effect on reaction kinetics, gel characteristics, physical and

mechanical properties. RSC Adv. **6**, 39106–39117 (2016). https://doi.org/10.1039/c6ra03667h
239. Borges, R., Dutra, L.M., Barison, A., Wypych, F.: MAS NMR and EPR study of structural changes in talc and montmorillonite induced by grinding. Clay Miner. **51**, 69–80 (2016). https://doi.org/10.1180/claymin.2016.051.1.06
240. Fernández, M., Alba, M.D., Torres Sánchez, R.M.: Effects of thermal and mechanical treatments on montmorillonite homoionized with mono- and polyvalent cations: insight into the surface and structural changes. Colloids Surf. A **423**, 1–10 (2013). https://doi.org/10.1016/j.colsurfa.2013.01.040
241. MacKenzie, K.J.D., Komphanchai, S., Vagana, R.: Formation of inorganic polymers (geopolymers) from 2:1 layer lattice aluminosilicates. J. Eur. Ceram. Soc. **28**, 177–181 (2008). https://doi.org/10.1016/j.jeurceramsoc.2007.06.004
242. D'Elia, A., Pinto, D., Eramo, G., Laviano, R., Palomo, A., Fernández-Jiménez, A.: Effect of alkali concentration on the activation of carbonate-high illite clay. Appl. Sci. **10**, 55–68 (2020)
243. Galán, E., Ferrell, R.E.: Genesis of clay minerals. In: Bergaya, F., Lagaly, G. (eds.) Developments in Clay Science, Handbook, pp. 83–126. Elsevier (2013)
244. Mostafa, N.Y., Mohsen, Q., El-Maghraby, A.: Characterization of low-purity clays for geopolymer binder formulation. Int. J. Miner. Metall. Mater. **21**(6), 609–619 (2014). https://doi.org/10.1007/S12613-014-0949-Y
245. Rahman, M.M., Law, D.W., Patnaikuni, I., Gunasekara, C., Tahmasebi Yamchelou, M.: Low-grade clay as an alkali-activated material. Appl. Sci. **11**, 1–17 (2021). https://doi.org/10.3390/app11041648
246. Yamchelou, M.T., Law, D.W., Patnaikuni, I., Li, J.: Alkali activation of mechanically activated low-grade clay. J. Sustain. Cem.-Based Mater. **10**, 272–288 (2021). https://doi.org/10.1080/21650373.2020.1838355
247. Gidigasu, M.D.: Laterite Soil Engineering Pedogenesis and Engineering Principles, 1st edn. Elsevier (1976)
248. Al-Rkaby, A.H.J., Odeh, N.A., Sabih, A., Odah, H.: Geotechnical characterization of sustainable geopolymer improved soil. J. Mech. Behav. Mater. **31**, 484–491 (2022). https://doi.org/10.1515/jmbm-2022-0044
249. Lassinantti Gualtieri, M., Romagnoli, M., Pollastri, S., Gualtieri, A.F.: Inorganic polymers from laterite using activation with phosphoric acid and alkaline sodium silicate solution: mechanical and microstructural properties. Cem. Concr. Res. **67**, 259–270 (2015). https://doi.org/10.1016/j.cemconres.2014.08.010
250. Cong, P., Cheng, Y.: Advances in geopolymer materials: a comprehensive review. J. Traff. Transp. Eng. (English Ed.) **8**, 283–314 (2021). https://doi.org/10.1016/j.jtte.2021.03.004
251. Kaze, C.R., Adesina, A., Lecomte-Nana, G.L., Alomayri, T., Kamseu, E., Melo, U.C.: Alkali-activated laterite binders: influence of silica modulus on setting time, rheological behaviour and strength development. Clean. Eng. Technol. **4** (2021). https://doi.org/10.1016/j.clet.2021.100175
252. McIntosh, A., Lawther, S.E., Kwasny, J., Soutsos, M.N., Cleland, D., Nanukuttan, S.: Selection and characterisation of geological materials for use as geopolymer precursors. Adv. Appl. Ceram. **114**, 378–385 (2015). https://doi.org/10.1179/1743676115Y.0000000055
253. Mathew, G., Issac, B.M.: Effect of molarity of sodium hydroxide on the aluminosilicate content in laterite aggregate of laterised geopolymer concrete. J. Build. Eng. **32**, 101486 (2020). https://doi.org/10.1016/j.jobe.2020.101486
254. Kaze, R.C., Naghizadeh, A., Tchadjie, L., Adesina, A., Djobo, J.N., Nemaleu, J.G., Kamseu, E., Melo, U.C., Tayeh, B.A.: Lateritic soils based geopolymer materials: a review. Constr. Build. Mater. **344**, 128157 (2022). https://doi.org/10.1016/j.conbuildmat.2022.128157
255. Kwasny, J., Soutsos, M., McIntosh, J.A., Cleland, D.J.: banahCEM–comparison of properties of a laterite-based geopolymer with conventional concrete. In: Proceedings of 9th International Concrete Conference 2016: environment, Efficiency and Economic Challenges for Concrete, pp. 383–394. University of Dundee, Scotland (2016)

256. Kaze, R.C., à Moungam, L.B., Djouka, M.F., Nana, A., Kamseu, E., Melo, U.C., Leonelli, C.: The corrosion of kaolinite by iron minerals and the effects on geopolymerization. Appl. Clay Sci. **138**, 48–62 (2017). https://doi.org/10.1016/j.clay.2016.12.040
257. Nkwaju, R.Y., Djobo, J.N., Nouping, J.N., Huisken, P.W., Deutou, J.G., Courard, L.J.: Iron-rich laterite-bagasse fibers based geopolymer composite : mechanical, durability and insulating properties. Appl. Clay Sci. **183**, 105333 (2019). https://doi.org/10.1016/j.clay.2019.105333
258. Kaze, R.C., Beleuk à Moungam, L.M., Cannio, M., Rosa, R., Kamseu, E., Melo, U.C., Leonelli, C.: Microstructure and engineering properties of Fe_2O_3 (FeO)–Al_2O_3–SiO_2 based geopolymer composites. J. Clean. Prod. **199**, 849–859 (2018). https://doi.org/10.1016/j.jclepro.2018.07.171
259. Lemougna, P.N., MacKenzie, K.J., Jameson, G.N., Rahier, H., Chinje Melo, U.F.: The role of iron in the formation of inorganic polymers (geopolymers) from volcanic ash: a ^{57}Fe Mössbauer spectroscopy study. J. Mater. Sci. **48**, 5280–5286 (2013). https://doi.org/10.1007/s10853-013-7319-4
260. Peys, A., Douvalis, A.P., Hallet, V., Rahier, H., Blanpain, B., Pontikes, Y.: Inorganic polymers from CaO–FeO_x–SiO_2 slag: the start of oxidation of Fe and the formation of a mixed valence binder. Front. Mater. **6**, 1–10 (2019). https://doi.org/10.3389/fmats.2019.00212
261. Metekong, J.V., Kaze, C.R., Deutou, J.G., Venyite, P., Nana, A., Kamseu, E., Melo, U.C., Tatietse, T.T.: Evaluation of performances of volcanic-ash-laterite based blended geopolymer concretes: mechanical properties and durability. J. Build. Eng. **34** (2021). https://doi.org/10.1016/j.jobe.2020.101935
262. Kaze, R.C., Nemaleu, J.G., Kamseu, E., Chinje, F.U., Andreola, F., Leonelli, C.: Towards optimization of mechanical and microstructural performances of Fe-rich laterite geopolymer binders cured at room temperature by varying the activating solution. RSC Adv. **12**, 33737–33750 (2022). https://doi.org/10.1039/d2ra05365a
263. Haris, A., Irhamsyah, A., Akifah, N., Amalia, N.S.: Physico-mechanical properties of geopolymer based on laterite deposit Sidrap, South Sulawesi. J. Phys: Conf. Ser. **1244**, 12037 (2019). https://doi.org/10.1088/1742-6596/1244/1/012037
264. Komnitsas, K., Bartzas, G., Karmali, V., Petrakis, E.: Factors affecting alkali activation of laterite acid leaching residues. Environments **8**, 1–21 (2021). https://doi.org/10.3390/environments8010004
265. Venyite, P., Makone, E.C., Kaze, R.C., Nana, A., Nemaleu, J.G., Kamseu, E., Chinje Melo, U., Leonelli, C.: Effect of combined metakaolin and basalt powder additions to laterite-based geopolymers activated by rice husk ash (RHA)/NaOH solution. Silicon **14**, 1643–1662 (2022). https://doi.org/10.1007/s12633-021-00950-7
266. Lemougna, P.N., Madi, A.B., Kamseu, E., Melo, U.C., Delplancke, M.P., Rahier, H.: Influence of the processing temperature on the compressive strength of Na activated lateritic soil for building applications. Constr. Build. Mater. **65**, 60–66 (2014). https://doi.org/10.1016/j.conbuildmat.2014.04.100
267. Patterson, H.B.W.: Chapter 6 Filtration and filters. In: Bleaching and Purifying Fats and Oils: theory and Practice, 2nd edn., pp. 159–188. Elsevier (2009)
268. Yilmaz, B., Ediz, N.: The use of raw and calcined diatomite in cement production. Cem. Concr. Compos. **30**, 202–211 (2008). https://doi.org/10.1016/j.cemconcomp.2007.08.003
269. Degirmenci, N., Yilmaz, A.: Use of diatomite as partial replacement for Portland cement in cement mortars. Constr. Build. Mater. **23**, 284–288 (2009). https://doi.org/10.1016/j.conbuildmat.2007.12.008
270. Pavlíková, M., Rovnaníková, P., Záleská, M., Pavlík, Z.: Diatomaceous earth—Lightweight pozzolanic admixtures for repair mortars—Complex chemical and physical assessment. Materials **15** (2022). https://doi.org/10.3390/ma15196881
271. Jud Sierra, E., Miller, S.A., Sakulich, A.R., MacKenzie, K., Barsoum, M.W.: Pozzolanic activity of diatomaceous earth. J. Am. Ceram. Soc. **93**, 3406–3410 (2010). https://doi.org/10.1111/j.1551-2916.2010.03886.x

272. Reka, A.A., Pavlovski, B., Fazlija, E., et al.: Diatomaceous earth: characterization, thermal modification, and application. Open Chem. **19**, 451–461 (2021). https://doi.org/10.1515/chem-2020-0049
273. Arbi, K., Palomo, A., Fernández-Jiménez, A.: Alkali-activated blends of calcium aluminate cement and slag/diatomite. Ceram. Int. **39**, 9237–9245 (2013). https://doi.org/10.1016/j.ceramint.2013.05.031
274. Font, A., Soriano, L., Reig, L., et al.: Use of residual diatomaceous earth as a silica source in geopolymer production. Mater. Lett. **223**, 10–13 (2018). https://doi.org/10.1016/j.matlet.2018.04.010
275. Adesanya, E., Ohenoja, K., Kinnunen, P., Illikainen, M.: Alkali activation of ladle slag from steel-making process. J. Sustain. Metall. **3**, 300–310 (2017). https://doi.org/10.1007/s40831-016-0089-x
276. Mejía, J.M., Mejía De Gutiérrez, R., Montes, C.: Rice husk ash and spent diatomaceous earth as a source of silica to fabricate a geopolymeric binary binder. J. Clean. Prod. **118**, 133–139 (2016). https://doi.org/10.1016/j.jclepro.2016.01.057
277. Payá, J., Monzó, J., Borrachero, M.V., Soriano, L.: Sewage sludge ash. In: New Trends in Eco-Efficient and Recycled Concrete, pp. 121–152. Woodhead Publishing (2019)
278. Krüger, O., Grabner, A., Adam, C.: Complete survey of german sewage sludge ash. Environ. Sci. Technol. **48**, 11811–11818 (2014). https://doi.org/10.1021/es502766x
279. Lynn, C.J., Dhir, R.K., Ghataora, G.S., West, R.P.: Sewage sludge ash characteristics and potential for use in concrete. Constr. Build. Mater. **98**, 767–779 (2015). https://doi.org/10.1016/j.conbuildmat.2015.08.122
280. Cyr, M., Coutand, M., Clastres, P.: Technological and environmental behavior of sewage sludge ash (SSA) in cement-based materials. Cem. Concr. Res. **37**, 1278–1289 (2007). https://doi.org/10.1016/j.cemconres.2007.04.003
281. Kappel, A., Ottosen, L.M., Kirkelund, G.M.: Colour, compressive strength and workability of mortars with an iron rich sewage sludge ash. Constr. Build. Mater. **157**, 1199–1205 (2017). https://doi.org/10.1016/j.conbuildmat.2017.09.157
282. Ottosen, L.M., Jensen, P.E., Kirkelund, G.M.: Electrodialytic separation of phosphorus and heavy metals from two types of sewage sludge ash. Sep. Sci. Technol. (Philadelphia) **49**, 1910–1920 (2014). https://doi.org/10.1080/01496395.2014.904347
283. Komljenović, M., Tanasijević, G., Džunuzović, N., Provis, J.L.: Immobilization of cesium with alkali-activated blast furnace slag. J. Hazard. Mater. **388**, 121765 (2020). https://doi.org/10.1016/j.jhazmat.2019.121765
284. Sitarz, M., Zdeb, T., Castro Gomes, J., Grünhäuser Soares, E., Hager, I.: The immobilisation of heavy metals from sewage sludge ash in geopolymer mortars. MATEC Web Conf. **322**, 01026 (2020). https://doi.org/10.1051/matecconf/202032201026
285. Pan, S.C., Tseng, D.H.: Sewage sludge ash characteristics and its potential applications. Water Sci. Technol. **44**, 261–267 (2001). https://doi.org/10.2166/wst.2001.0636
286. Dyer, T.D., Halliday, J.E., Dhir, R.K.: Hydration reaction of sewage sludge ash for use as a cement component in concrete production. In: Recycling and Reuse of Sewage Sludge, pp. 226–238. Thomas Telford Publishing (2001)
287. Lynn, C.J., Dhir, R.K., Ghataora, G.S.: Environmental impacts of sewage sludge ash in construction: leaching assessment. Resour. Conserv. Recycl. **136**, 306–314 (2018). https://doi.org/10.1016/j.resconrec.2018.04.029
288. Tashima, M.M., Reig, L., Santini, M.A., Moraes, J.C.B., Akasaki, J.L., Payá, J.O., Borrachero, M.V., Soriano, L.: Compressive strength and microstructure of alkali-activated blast furnace slag/sewage sludge ash (GGBS/SSA) blends cured at room temperature. Waste Biomass Valoriz. **8**, 1441–1451 (2017). https://doi.org/10.1007/s12649-016-9659-1
289. Istuque, D.B., Soriano, L., Akasaki, J.L., Melges, J.L., Borrachero, M.V., Monzó, J., Payá, J., Tashima, M.M.: Effect of sewage sludge ash on mechanical and microstructural properties of geopolymers based on metakaolin. Constr. Build. Mater. **203**, 95–103 (2019). https://doi.org/10.1016/j.conbuildmat.2019.01.093

290. Yamaguchi, N., Ikeda, K.: Preparation of geopolymeric materials from sewage sludge slag with special emphasis to the matrix compositions. J. Ceram. Soc. Jpn. **118**, 107–112 (2010). https://doi.org/10.2109/jcersj2.118.107
291. Luukkonen, T., Abdollahnejad, Z., Yliniemi, J., Kinnunen, P., Illikainen, M.: One-part alkali-activated materials: a review. Cem. Concr. Res. **103**, 21–34 (2018). https://doi.org/10.1016/j.cemconres.2017.10.001
292. Heath, A., Paine, K., McManus, M.: Minimising the global warming potential of clay based geopolymers. J. Clean. Prod. **78**, 75–83 (2014). https://doi.org/10.1016/j.jclepro.2014.04.046
293. Habert, G., D'Espinose De Lacaillerie, J.B., Roussel, N.: An environmental evaluation of geopolymer based concrete production: reviewing current research trends. J. Clean. Prod. **19**, 1229–1238 (2011). https://doi.org/10.1016/j.jclepro.2011.03.012
294. Habert, G., Ouellet-Plamondon, C.: Recent update on the environmental impact of geopolymers. RILEM Tech. Lett. **1**, 17 (2016). https://doi.org/10.21809/rilemtechlett.v1.6
295. Bernal, S.A.: Advances in near-neutral salts activation of blast furnace slags. RILEM Tech. Lett. **1**, 39 (2016). https://doi.org/10.21809/rilemtechlett.v1.8
296. Mobasher, N., Bernal, S.A., Provis, J.L.: Structural evolution of an alkali sulfate activated slag cement. J. Nucl. Mater. **468**, 97–104 (2016). https://doi.org/10.1016/j.jnucmat.2015.11.016
297. Rashad, A.M., Bai, Y., Basheer, P.A., Milestone, N.B., Collier, N.C.: Hydration and properties of sodium sulfate activated slag. Cement Concr. Compos. **37**, 20–29 (2013). https://doi.org/10.1016/j.cemconcomp.2012.12.010
298. Steinhauser, G.: Cleaner production in the Solvay Process: general strategies and recent developments. J. Clean. Prod. **16**, 833–841 (2008). https://doi.org/10.1016/j.jclepro.2007.04.005
299. Douglas, E., Brandstetr, J.: A preliminary study on the alkali activation of ground granulated blast-furnace slag. Cem. Concr. Res. **20**, 746–756 (1990). https://doi.org/10.1016/0008-8846(90)90008-L
300. Abdalqader, A., Jin, F., Al-Tabbaa, A.: Performance of magnesia-modified sodium carbonate-activated slag/fly ash concrete. Cement Concr. Compos. **103**, 160–174 (2019). https://doi.org/10.1016/j.cemconcomp.2019.05.007
301. Cheah, C.B., Tan, L.E., Ramli, M.: The engineering properties and microstructure of sodium carbonate activated fly ash/slag blended mortars with silica fume. Compos. B Eng. **160**, 558–572 (2019). https://doi.org/10.1016/j.compositesb.2018.12.056
302. Abdalqader, A.F., Jin, F., Al-Tabbaa, A.: Development of greener alkali-activated cement: utilisation of sodium carbonate for activating slag and fly ash mixtures. J. Clean. Prod. **113**, 66–75 (2016). https://doi.org/10.1016/j.jclepro.2015.12.010
303. Wang, S.D., Scrivener, K.L., Pratt, P.L.: Factors affecting the strength of alkali-activated slag. Cem. Concr. Res. **24**, 1033–1043 (1994). https://doi.org/10.1016/0008-8846(94)90026-4
304. Adesanya, E., Perumal, P., Luukkonen, T., Yliniemi, J., Ohenoja, K., Kinnunen, P., Illikainen, M.: Opportunities to improve sustainability of alkali-activated materials: a review of side-stream based activators. J. Clean. Prod. **286**, 125558 (2021). https://doi.org/10.1016/j.jclepro.2020.125558
305. Mendes, B.C., Pedroti, L.G., Vieira, C.M., Marvila, M., Azevedo, A.R., De Carvalho, J.M., Ribeiro, J.C.: Application of eco-friendly alternative activators in alkali-activated materials: a review. J. Build. Eng. **35**, 102010 (2021). https://doi.org/10.1016/j.jobe.2020.102010
306. Puertas, F., Torres-Carrasco, M.: Use of glass waste as an activator in the preparation of alkali-activated slag. Mechanical strength and paste characterisation. Cem. Concr. Res. **57**, 95–104 (2014). https://doi.org/10.1016/j.cemconres.2013.12.005
307. Kalina, L., Bílek, V., Jr., Kiripolský, T., Novotný, R., Másilko, J.: Cement kiln by-pass dust: an effective alkaline activator for pozzolanic materials. Materials **11**(9), 1770 (2018). https://doi.org/10.3390/ma11091770
308. Marsh, A.T., Yue, Z., Dhandapani, Y., Button, K., Adu-Amankwah, S., Bernal, S.A.: Influence of limestone addition on sodium sulphate activated blast furnace slag cements. Constr. Build. Mater. **360**, 129527 (2022). https://doi.org/10.1016/j.conbuildmat.2022.129527

309. Tan, H., Deng, X., He, X., Zhang, J., Zhang, X., Su, Y., Yang, J.: Compressive strength and hydration process of wet-grinded granulated blast-furnace slag activated by sodium sulfate and sodium carbonate. Cem. Concr. Compos. **97**, 387–398 (2019). https://doi.org/10.1016/j.cemconcomp.2019.01.012
310. Rashad, A.M.: Influence of different additives on the properties of sodium sulfate activated slag. Constr. Build. Mater. **79**, 379–389 (2015). https://doi.org/10.1016/j.conbuildmat.2015.01.022
311. Dhandapani, Y., Santhanam, M., Kaladharan, G., Ramanathan, S.: Towards ternary binders involving limestone additions—A review. Cem. Concr. Res. **143**, 106396 (2021). https://doi.org/10.1016/j.cemconres.2021.106396
312. Oey, T., Kumar, A., Bullard, J.W., Neithalath, N., Sant, G.: The filler effect: The influence of filler content and surface area on cementitious reaction rates. J. Am. Ceram. Soc. **96**, 1978–1990 (2013). https://doi.org/10.1111/jace.12264
313. Gruskovnjak, A., Lothenbach, B., Winnefeld, F., et al.: Hydration mechanisms of super sulphated slag cement. Cem. Concr. Res. **38**, 983–992 (2008). https://doi.org/10.1016/j.cemconres.2008.03.004
314. Blotevogel, S., Ehrenberg, A., Steger, L., Doussang, L., Kaknics, J., Patapy, C., Cyr, M.: Ability of the R^3 test to evaluate differences in early age reactivity of 16 industrial ground granulated blast furnace slags (GGBS). Cem. Concr. Res. **130**, 105998 (2020). https://doi.org/10.1016/j.cemconres.2020.105998
315. Adesina, A., Rodrigue Kaze, C.: Physico-mechanical and microstructural properties of sodium sulfate activated materials: a review. Constr. Build. Mater. **295**, 123668 (2021). https://doi.org/10.1016/j.conbuildmat.2021.123668
316. Ben Haha, M., Lothenbach, B., Le Saout, G., Winnefeld, F.: Influence of slag chemistry on the hydration of alkali-activated blast-furnace slag—Part II: effect of Al_2O_3. Cem. Concr. Res. **42**, 74–83 (2012). https://doi.org/10.1016/j.cemconres.2011.08.005
317. Kucharczyk, S., Zajac, M., Stabler, C., Thomsen, R.M., Haha, M.B., Skibsted, J., Deja, J.: Structure and reactivity of synthetic $CaO–Al_2O_3–SiO_2$ glasses. Cem. Concr. Res. **120**, 77–91 (2019). https://doi.org/10.1016/j.cemconres.2019.03.004
318. Bernard, E., Zucha, W.J., Lothenbach, B., Mäder, U.: Stability of hydrotalcite (Mg–Al layered double hydroxide) in presence of different anions. Cem. Concr. Res. **152**, 106674 (2022). https://doi.org/10.1016/j.cemconres.2021.106674
319. He, J., Zheng, W., Bai, W., Hu, T., He, J., Song, X.: Effect of reactive MgO on hydration and properties of alkali-activated slag pastes with different activators. Constr. Build. Mater. **271**, 121608 (2021). https://doi.org/10.1016/j.conbuildmat.2020.121608
320. Al-kroom, H., Arif, M.A., Saleh, A.A., Shalaby, H.M., Abd Elrahman, M., Abdel-Gawwad, H.A.: The role of nano magnesia in accelerating the early hydration rate of sodium sulfate activated slag. Constr. Build. Mater. **373**, 130863 (2023). https://doi.org/10.1016/j.conbuildmat.2023.130863
321. Zheng, W., He, J., Tong, Y., He, J., Song, X., Sang, G.: Investigation of effects of reactive MgO on autogenous and drying shrinkage of near-neutral salt activated slag cement. Ceram. Int. **48**, 5518–5526 (2022). https://doi.org/10.1016/j.ceramint.2021.11.096
322. Yuan, B., Yu, Q.L., Brouwers, H.J.H.: Phase modification induced drying shrinkage reduction on Na_2CO_3 activated slag by incorporating Na_2SO_4. Mater. Struct. **50**, 1–11 (2017). https://doi.org/10.1617/s11527-017-1088-5
323. Wu, M., Zhang, Y., Jia, Y., She, W., Liu, G., Yang, Z., Zhang, Y., Zhang, W., Sun, W.: Effects of sodium sulfate on the hydration and properties of lime-based low carbon cementitious materials. J. Clean. Prod. **220**, 677–687 (2019). https://doi.org/10.1016/j.jclepro.2019.02.186
324. Joseph, S., Snellings, R., Cizer, Ö.: Activation of Portland cement blended with high volume of fly ash using Na_2SO_4. Cem. Concr. Compos. **104**, 103417 (2019). https://doi.org/10.1016/j.cemconcomp.2019.103417
325. Mei, J., Tan, H., Li, H., Ma, B., Liu, X., Jiang, W., Zhang, T., Li, X.: Effect of sodium sulfate and nano-SiO_2 on hydration and microstructure of cementitious materials containing high volume fly ash under steam curing. Constr. Build. Mater. **163**, 812–825 (2018). https://doi.org/10.1016/j.conbuildmat.2017.12.159

326. Xu, H., Provis, J.L., van Deventer, J.S.J., Krivenko, P.V.: Characterization of aged slag concretes. ACI Mater. J. **105**(2), 131 (2008). https://doi.org/10.14359/19753
327. Conway, E.: The key to fixing climate change was hiding in Mariupol's concrete. In: The Times (2022). https://www.thetimes.co.uk/article/key-fixing-climate-change-mariupol-concrete-ukraine-shelling-fvm5vmpm. Accessed 5 Aug. 2023
328. Bernal, S.A., Provis, J.L., Myers, R.J., San Nicolas, R., van Deventer, J.S.J.: Role of carbonates in the chemical evolution of sodium carbonate-activated slag binders. Mater. Struct. **48**, 517–529 (2014). https://doi.org/10.1617/s11527-014-0412-6
329. Yuan, B., Yu, Q.L., Brouwers, H.J.H.: Time-dependent characterization of Na_2CO_3 activated slag. Cem. Concr. Compos. **84**, 188–197 (2017). https://doi.org/10.1016/j.cemconcomp.2017.09.005
330. Ke, X., Bernal, S.A., Provis, J.L.: Controlling the reaction kinetics of sodium carbonate-activated slag cements using calcined layered double hydroxides. Cem. Concr. Res. **81**, 24–37 (2016). https://doi.org/10.1016/j.cemconres.2015.11.012
331. Ke, X., Criado, M., Provis, J.L., Bernal, S.A.: Slag-based cements that resist damage induced by carbon dioxide. ACS Sustain. Chem. Eng. **6**, 5067–5075 (2018). https://doi.org/10.1021/acssuschemeng.7b04730
332. Ke, X., Bernal, S.A., Hussein, O.H., Provis, J.L.: Chloride binding and mobility in sodium carbonate-activated slag pastes and mortars. Mater. Struct. **50**, 1–13 (2017). https://doi.org/10.1617/s11527-017-1121-8
333. Yuan, B., Yu, Q.L., Brouwers, H.J.H.: Evaluation of slag characteristics on the reaction kinetics and mechanical properties of Na_2CO_3 activated slag. Constr. Build. Mater. **131**, 334–346 (2017). https://doi.org/10.1016/j.conbuildmat.2016.11.074
334. Escalante-García, J.I., Fuentes, A.F., Gorokhovsky, A., et al.: Hydration products and reactivity of blast-furnace slag activated by various alkalis. J. Am. Ceram. Soc. **86**, 2148–2153 (2003). https://doi.org/10.1111/j.1151-2916.2003.tb03623.x
335. Wang, S.D., Scrivener, K.L.: Hydration products of alkali activated slag cement. Cem. Concr. Res. **25**, 561–571 (1995). https://doi.org/10.1016/0008-8846(95)00045-E
336. Myers, R.J., Lothenbach, B., Bernal, S.A., Provis, J.L.: Thermodynamic modelling of alkali-activated slag cements. Appl. Geochem. **61**, 233–247 (2015). https://doi.org/10.1016/j.apgeochem.2015.06.006
337. Shi, C., Li, Y.: Investigation on some factors affecting the characteristics of alkali-phosphorus slag cement. Cem. Concr. Res. **19**, 527–533 (1989). https://doi.org/10.1016/0008-8846(89)90004-5
338. Dung, N.T., Hooper, T.J.N., Unluer, C.: Improving the carbonation resistance of Na_2CO_3-activated slag mixes via the use of reactive MgO and nucleation seeding. Cem. Concr. Compos. **115**, 103832 (2021). https://doi.org/10.1016/j.cemconcomp.2020.103832
339. Jeon, D., Jun, Y., Jeong, Y., Oh, J.E.: Microstructural and strength improvements through the use of Na_2CO_3 in a cementless $Ca(OH)_2$-activated Class F fly ash system. Cem. Concr. Res. **67**, 215–225 (2015). https://doi.org/10.1016/j.cemconres.2014.10.001
340. Abdalqader, A.F., Jin, F., Al-Tabbaa, A.: Characterisation of reactive magnesia and sodium carbonate-activated fly ash/slag paste blends. Constr. Build. Mater. **93**, 506–513 (2015). https://doi.org/10.1016/j.conbuildmat.2015.06.015
341. Wang, H., Wang, L., Xu, Y., Cao, K., Ge, Y., Wang, X., Li, Q.: Accelerating the reaction kinetics of Na_2CO_3-activated slag mortars by calcined recycled concrete fines. Materials **15**, 1–17 (2022). https://doi.org/10.3390/ma15155375